Characterising Vegetation Structure Using MODIS Multi-Angular Data

The impact of variations in the size of pixels' ground IFOV on MODIS BRDF modelling

A thesis submitted in fulfilment of the requirements for the degree of Doctor of Philosophy in Applied Science

Geoffrey William McCamley
B. App. Science (Mathematics)
B. App Science (Surveying) with Honours 1st Class

School of Mathematics and Geospatial Science
College of Science, Engineering and Health
RMIT University
January 2014

Declaration

I certify that except where due acknowledgement has been made, the work is of the author alone; the work has not been submitted previously, in whole or in part, to qualify for any other academic award; the content of the thesis is the result of work which has been carried out since the official commencement date of the author's candidature; any editorial work, paid or unpaid, carried out by a third party is acknowledged; and, ethics procedures and guidelines have been followed.

Signature   …………………………………………………..

Name   Geoffrey McCamley

Date   /   /

Abstract

Bi-directional Reflectance Distribution Functions (BRDF) seek to characterise changes in a surface's reflectance associated with variations in view and illumination angles, i.e. reflected light is not scattered uniformly in all directions from the Earth's surface. BRDF effects provide a source of information that can be used to assist in the characterisation of land surface features when viewed from sensors on board Earth observing satellites. For example, structural information derived from BRDF effects could be used to distinguish vegetated surfaces that otherwise exhibit the same spectral response or be used to describe the vertical structure of vegetation.

The Moderate Resolution Imaging Spectroradiometer (MODIS) sensor on board NASA's Terra and Aqua Earth orbiting satellites has a wide field of view and, based on MODIS observations, a suite of BRDF products has been developed by MODIS science teams, i.e. the MCD43 product suite. The MODIS BRDF product is based on the RossThick-LiSparse-Reciprocal model. Weights for the isotropic, volumetric and geometric kernels of the RossThick-LiSparse-Reciprocal model are derived from MODIS observations for each of seven reflective bands, in eight day intervals, at the pixel level. The MODIS BRDF product has been validated, has worldwide coverage and a 12 year history. The MODIS BRDF product represents an operational, readily available, "off the shelf" BRDF dataset, whereby any additional information that can be extracted from it will have maximum benefit towards understanding how BRDF effects can assist with the characterisation of vegetation.

The aim of this research was to discover how BRDF effects could be used to assist with the characterisation of vegetation at the pixel level. Past studies considering BRDF effects to assist with the characterisation of vegetation have found BRDF parameters to be noisy and interpretation of vegetation structure at a pixel level problematic. This thesis seeks to develop new techniques that can be used to assist with the characterisation of land surfaces at the pixel level. Motivated by this research objective, land surfaces with particular characteristics are considered and a re-expression of the MODIS BRDF model is developed within this thesis to analyse changes in the Normalised Difference Vegetation Index (NDVI) associated with variations in view zenith angle. This represents a semi-empirical approach to replacing the isotropic, volumetric and geometric parameters within the MODIS BRDF model with the alternate parameter set: namely NDVI and a height-to-width ratio of vegetation surface components. The model has been applied to a 10 year temporal transect of single species crop fields, a spatial transect

between Melbourne and Darwin (Australia) and to regions on the Australian continent which allows the spatial relationship of BRDF effects to be investigated.

The results identified that the directional scattering of reflected electromagnetic radiation (EMR) is not the principal cause of variation in the MODIS BRDF product. The model developed in this thesis unexpectedly reveals that reflectance variations associated with enlargement of a pixel's ground instantaneous field of view (that is, a pixel's footprint on the ground) with increasing view zenith angle is the principal source of variation in the MODIS BRDF product. Variations in pixels' ground instantaneous field of view is a well known effect associated with wide field of view sensors such as MODIS but is not specifically considered in the derivation of the MODIS BRDF product.

The finding of this artefact within the MODIS BRDF product means that the original research aims cannot be addressed using MODIS BRDF data. However and perhaps more importantly, the identification of this artefact raises significant issues for the validity, use and interpretation of all land surface products based directly or indirectly on MODIS BRDF modelling. For example, it may be necessary to reconsider the interpretation applied to MODIS's Nadir BRDF Adjusted Reflectance (NBAR) product and surface albedo product, which is considered an important factor in climate modelling. Furthermore, the MODIS BRDF product is used as the basis for atmospheric and BRDF corrections of Landsat images for Australia and the MODIS BRDF product is also used in the development of the foliage clumping indices. Downstream products and applications based on MODIS BRDF modelling may also require reassessment based on the findings contained in this thesis.

Acknowledgements

Table of Contents

1 Introduction

1.1 Background

Bi-directional Reflectance Distribution Functions (BRDF) seek to characterise changes in a surface's reflectance associated with variations in view and illumination angles, i.e. reflected light is not scattered uniformly in all directions from the Earth's surface (Schaaf, 2012, Diner et al., 1999). For passive remote sensing instruments on Earth observing satellites (EOS) the illumination angle is usually associated with the position of the Sun, i.e. time of day, season and latitude. The view angle variations arise with either sensors that have a wide field of view or the degree to which the sensor is tilted by design to realise a non nadir view angle.

BRDF cannot be directly measured (Schaepman-Strub et al., 2006), but rather surface reflectance is sampled at different illumination and view geometries and modelled. Samples may be taken in-situ, from aircraft or from sensors on board EOS. BRDF modelling is usually based upon the consideration that surfaces are not smooth and flat, but contain three-dimensional objects that cast shadows and obscure other features that result in non isotropic reflectance. BRDF model parameters may be derived by 'best fitting' multiple observations from different illumination and view geometries to a mathematical (BRDF) model. This process may be performed independently for each pixel and separately for individual reflectance bands/wavelengths of light (Lucht et al., 2000).

There are three main uses of BRDF. Traditionally, remote sensing approaches using wide field of view scanners have often considered the view and solar angle dependences to be a problematic source of noise or error requiring a correction or normalisation to a 'standard' geometry (Diner et al., 1999). BRDF effects are used to standardise image features to a common illumination and view geometry that better enables the comparison of features within and between images. This is particularly important with time series analysis of imagery. Secondly, BRDF can be angularly integrated to derived surface albedo which is considered an important factor in climate modelling (Asner et al., 1998); the more reflective the Earth the less incident radiation is absorbed and re-emitted at longer (e.g. thermal) wavelengths. The third application of BRDF is to assist

in the characterisation of land surface features, for example combining the spectral and directional aspects of reflected light in order to describe surface features (Schaepman, 2006). This thesis is focused on this third use of BRDF, i.e. to assist with the characterisation of land surface features when viewed from sensors on board EOS.

1.2   Rationale

Canopy structure is defined as the vertical and horizontal spatial distribution, orientation and density of foliage and its supporting structures (Chopping, 2006). BRDF theoretical models are derived with consideration of these factors and have the potential to provide additional new information about vegetation structure that is not apparent in spectral signatures alone. For example, structural information derived from BRDF effects could be used to distinguish vegetated land surfaces that have the same spectral response or provide a measure of the vertical height of vegetation.

1.3   Thesis Aim

The Moderate Resolution Imaging Spectroradiometer (MODIS) sensor on board NASA's Terra and Aqua Earth orbiting satellites has a wide field of view that generates view angle effects. Using MODIS data, science teams have developed BRDF modelling for seven MODIS bands. The MODIS BRDF model is based on the RossThick-LiSparse-Reciprocal model (Lucht et al., 2000). MODIS BRDF modelling has been validated (Schaaf et al., 2002), the model used is ubiquitous (Armston et al., 2006), has been applied over the 12 year MODIS archive history, has worldwide coverage and is the principal dataset used in this thesis. The MODIS BRDF product represents an operational, readily available, "off the shelf" BRDF dataset, whereby any additional information that can be extracted from it will have the maximum benefit towards understanding how BRDF effects can assist in the characterisation of vegetation.

Past studies considering BRDF effects to assist with the characterisation of vegetation (including the use of MODIS BRDF modelling and studies focused on the Australian landscape) have found BRDF parameters to be noisy and interpretation of vegetation structure at a pixel level has been problematic. Studies have tended to focus on vegetated study areas at regional and continental scales through which issues of noise

and surface homogeneity have been generalised or dealt with statistically (Armston et al., 2006, Grant, 2000, Lovell and Graetz, 2001, Hill et al., 2008). This thesis seeks to develop new techniques that can be used to assist in the characterisation of land surfaces at the pixel level using the MODIS BRDF product.

1.3.1   Research Questions

The research questions addressed in this thesis are:

1. How do MODIS BRDF effects vary between bare soil and vegetation, and can variations be quantified with consideration to the density of vegetation cover?
2. In which wavelengths (MODIS bands) do BRDF effects vary between soil and vegetation, and how do these variations relate to reflectance characteristics in respective bands?
3. How do MODIS BRDF effects relate to vegetation indices which may be considered a pseudo measure of bio-mass?
4. Are MODIS BRDF effects able to reveal additional information about the structure of vegetation or the height of vegetation?

1.4   Thesis Structure

The motivation for this thesis was to discover how Bidirectional Reflectance Distribution Functions (BRDF) could assist with the characterisation of vegetation, e.g. describe the structure of vegetation from imagery acquired by the MODIS space borne sensor which provides multi-angular views. An unexpected finding is described in chapter 6, i.e. MODIS BRDF modelling is less the consequence of directional scattering of reflected light, but is predominantly due to variations in reflectance observations associated with enlargement of pixels' ground instantaneous field of view (IFOV).

Whilst chapter 6 includes the key finding of this thesis, the structure of this thesis is aligned to the processes that were developed in pursuit of the original research questions, although reinterpretation of results from earlier chapters is made in light of the finding contained in chapter 6. The inclusion of earlier research chapters is considered necessary to fully explain the derivation of this finding and may also be indicative of useful approaches to study how BRDF effects can be used to assist with the

characterisation of vegetation where changes in the ground IFOV have a less significant impact on BRDF modelling.

1.4.1 Outline of Chapters

A literature review is contained in **chapter 2**, which concludes by identifying gaps and opportunities from prior research. **Chapter 3** introduces the principal dataset used. The research questions are addressed in three principal chapters:

Chapter 4 considers a 10 year temporal transect of single species cropped fields. This approach seeks to minimise noise and homogeneity issues which have been identified in past studies as impacting the use of BRDF effects to assist with the characterisation of vegetation. This chapter asks if the MODIS BRDF parameter weights vary between soil and vegetation, i.e. research questions 1 - 3. This chapter introduces a simple geometric optical model for re-expressing MODIS BRDF in terms of an alternative set of parameters with the objective of determining if MODIS BRDF effects can be used to describe a measure for the height of vegetation, i.e. research question 4.

Chapter 5 broadens the applicability of the model described in chapter 4. The modified model is applied to pixels along a transect line between Melbourne and Darwin, Australia, that samples a large range of land cover types and vegetation densities. The results are compared to vegetation indices and identifiable surface features along the transect line in order to address research questions 3 and 4.

Chapter 6 applies the model from the previous chapters to an arid region in central Australia. This allows the spatial relationship of BRDF effects to be investigated in the context of research questions 3 and 4. The thesis conclusions are formulated in this chapter and the results from chapters 4 and 5 are reconsidered in light of the conclusions drawn in chapter 6.

Chapter 7 summaries the results and discusses their implications (that go beyond the scope of this thesis), and identifies further research that may be undertaken.

2 Literature Review

2.1 Introduction

Earth observing satellites (EOS) carrying sensors that measure electromagnetic radiation (EMR) reflected from the Earth's surface have been in use for more than 40 years and offer many benefits over close range or in situ observation techniques in understanding and monitoring surface features. "Earth observation from airborne or space borne platforms is the only observational approach capable of providing data at the relevant scales and resolution needed to extrapolate findings of in situ (field) studies to larger areas, to document the heterogeneity of the landscape at regional scales and to connect these findings into a global view." (Schaepman, 2006) (page 209).

Many countries have developed their own networks of EOS with numerous satellites currently in operation and more planned for the future. EOSs carry multiple sensors that target specific issues related to oceanographic, terrestrial and atmospheric domains. The data that sensors' produce is complex in nature and the accumulated archive of this data is extensive in volume.

Noise is always a problem in any field of satellite measurement (Gao et al., 2003). There are many sources of noise within remotely sensed satellite data. If the objective is to use remotely sensed image data to identify surface features and the condition of those features, then understanding sources of noise and variability within the acquired image data is a critical component. Sources of variability will compromise analysis of features within an image or inter-comparison between images taken at different temporal periods or comparisons from different sensors. Pre-analysis typically requires identification of the sources of variance within the data and its address, so as to leave the strongest possible signal that is representative of the specific features of interest on the Earth's surface being investigated. Typically these sources of variability involve radiometric, temporal, spatial and spectral attributes associated with the sensor and acquired images. Also considered may be the influence of the Earth's atmosphere through which the EMR signal passes before detection by the sensor. All of these aspects of remote sensing are extensive areas requiring on-going monitoring and calibration.

An additional source of variance in the EMR signal received by EOS sensors is derived from angular effects. Variations in reflectance are associated with the angle that the

source of incident radiation makes with the surface (usually this being the Sun and its position in the sky) and the viewing angle that the sensor forms with the (Earth's) surface when an image is acquired. There is always an angle of incidence associated with the incoming energy that illuminates the terrain and an angle of existence from the terrain to the sensor system. The *bidirectional* nature of remote sensing data collection is known to influence the spectral and polarization characteristics of reflectance data (Jensen, 2007). Due to its three dimensional structure, the Earth's surface scatters radiation anisotropically, especially at the shorter wavelengths that characterize solar irradiance. The Bidirectional Reflectance Distribution Function (BRDF) specifies the behaviour of surface scattering as a function of illumination angle and view angle at a particular wavelength (Schaaf, 2012).
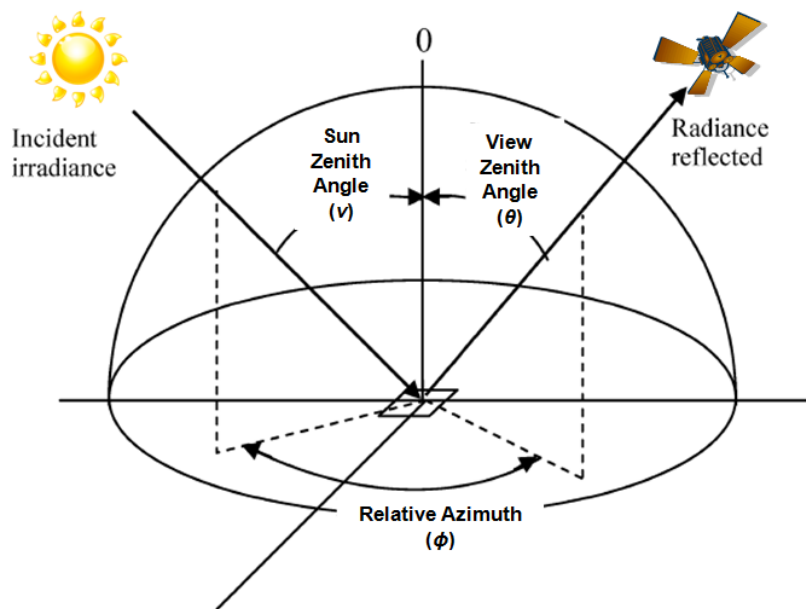
Figure 2.1 (Su et al., 2009) depicts illumination and view angles

Shown in Figure 2.1 is a typical consideration of angular effects which are expressed in terms of three angles, i.e. Sun zenith angle (v), sensor/view zenith angle (θ) and the relative azimuth angle (Φ).

The literature review chapter of this thesis considers variability in EOS sensor reflectance data due to view and illumination angles, with a specific focus on vegetated surfaces. This chapter also reviews angular variability, definition of terminology used and the results of past vegetation studies using angular effects to assist with the characterisation of vegetation. Finally, issues, gaps and opportunities identified within the literature review are discussed.

2.2 EOS sensors that generate wide view angle geometries

In laboratory experiments both the illumination and view angles can be controlled, however for passive sensors on board EOS this is not the case. The illumination angle will be determined by the location of the Sun. This in turn will be associated with the time of day, season and latitude when an image is acquired.

There are generally two means by which sensors on EOS generate view angle geometries. The view direction will be associated with either the point location on the ground (i.e. the pixel) within the sensor's field of view, or as a consequence of the sensor being specifically tilted in order to realise a viewing angle with respect to the Earth's surface. Satellite sensors that are not specifically tilted by design and have a narrow field of view will generate minimal view angle effects. If the size of the view angle is sufficiently small, it may be disregarded and/or the angle not captured and recorded in derived data products. For example, the Landsat series of satellites have a small field of view with a relatively high spatial resolution and generate view angles of only +/- 7° off nadir (Li et al., 2010). Even though view angle effects are minimal for Landsat, illumination angle effects will still be exist due to the time of day, season and latitude of acquired images. Traditionally, remote sensing approaches using wide field of view scanners have often considered the view and solar zenith angle dependence of reflected radiation to be a problematic source of noise or error requiring a correction or normalisation to a "standard" direction (Diner et al., 1999).
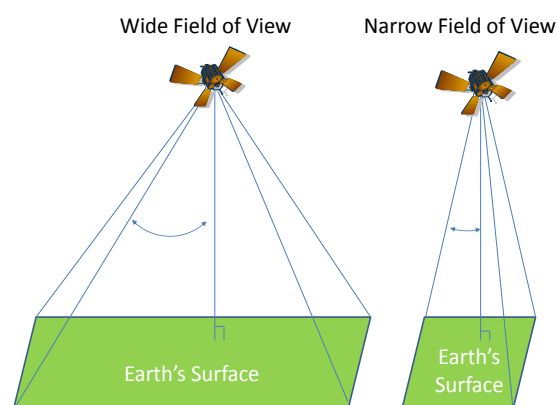
Figure 2.2 – Diagrammatic depiction of sensors with a wide field of view and a narrow field of view

Figure 2.2 shows how a wide field of view sensor (left) acquires a larger area of the Earth's surface and in doing so generates larger view angles for pixels acquired towards the edge of the image, where a narrow field of view sensor (right) generates smaller view angles.
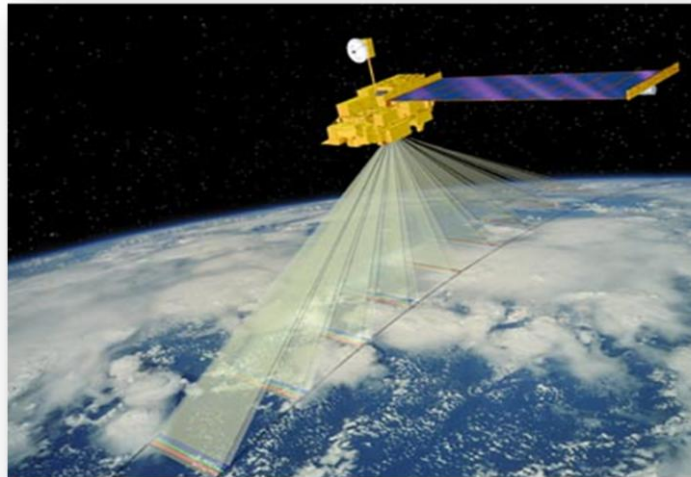
Figure 2.3 - Multi-angle Imaging Spectro-Radiometer (MISR) on board NASA's Terra EOS. Source : http://www-misr.jpl.nasa.gov/mission/miview1.html.

The MISR sensor on board NASA's Terra EOS shown in Figure 2.3, is specifically designed to view the Earth's surface obliquely. The forward motion of the space craft causes points on the ground to be observed in turn by the nine push-broom cameras that are orientated at fixed along track view angles (Diner et al., 1999).

There are numerous sensors on board EOSs that yield view angle effects, i.e. variable view angles that substantially diverge from nadir. Schaepman identifies the British Compact High Resolution Imaging Spectroradiometer (CHRIS) launched in 1999 on board the Belgium PROBA platform as the first fully spectro-directional space-borne instrument, but MISR which was also launched in 1999 is generally considered the most important (Schaepman, 2006). Four EOS sensors with multiple view angle abilities are discussed below with consideration to the range of view angles they generate, the spectral bands employed and their spatial resolution. Studies using multi-angle reflectance data derived from these sensors are discussed in section 2.8.

Table 2.4 – Summary Comparison of Key Multi-View Angle Sensors

Sensor	Launch	Bands	View Angle	Spatial Resolution (at nadir)
AVHRR	1991	1 visible 1 near IR	+/- 55°	1.1km
POLDER	1997	8 visible 8 near IR	+/- 42°	6 x7 km
MISR	1999 on board Terra	3 visible 1 near IR	0° +/- 26.1° +/- 45.6° +/- 60.0° +/- 70.5°	275m
MODIS	1999 (Terra) 2002 (Aqua)	36 Bands from 0.4um to 14.5um	+/- 55	2 x 250m 5 x 500m 29 x 1km

The Advanced Very High Resolution Radiometer (AVHRR) has been carried on board a series of US National Oceanographic and Atmospheric Agency (NOAA) EOSs. The platform(s) on which AVHRR is carried has a sun-synchronous polar orbit at 833 km. AVHRR has two bands particularly useful for measurement of vegetation, i.e. one in the visible (0.58 – 0.68um) and one in the near infrared (0.725 – 1.10um). AVHRR is an across track scanner and the view angle range of +/- 55° is derived from the sensors wide field of view which is necessary to achieve Earth-wide coverage twice daily with its 2,700km swath (Jensen, 2007).

Polarisation and Directionality of Earth's Reflectance (POLDER) developed by the French space agency CNES, flew on ADEOS (ADvanced Earth Observation Satellite), developed by the Japanese space agency, JAXA for a period of 9 months between 1996 and 1997. A second, identical instrument flew on the successor to ADEOS (i.e. ADEOS-2), between December 2002 and October 2003. POLDER is a wide field of view imaging radiometer that provided the first global, systematic measurements of spectral, directional and polarized characteristics of the solar radiation reflected by the Earth/atmosphere system. The POLDER instrument is a camera composed of a two-dimensional CCD detector array, wide field of view telecentric optics and a rotating wheel carrying spectral and polarized filters. This provided a 43° field of view along track and a 51° across track (POLDER, 2013, Lovell and Graetz, 2001).

Multi-angle Imaging Spectro-Radiometer (MISR) is one of five instruments on NASA's Terra EOS. MISR is a push-broom scanner with look angles that are spread in the forward and aft directions along the line of flight so that over a period of 7 minutes a

360km wide swath of Earth comes onto view at all nine angles. Each MISR camera sees instantaneously a single row of pixels at right angles to the ground track in a push-broom format. The forward and aft cameras for each view angle are the same and arranged symmetrically around the nadir. MISR records data in red, green, blue and near infrared wavelengths at 275m resolution (MISR, 2013, Jensen, 2007).

NASA's Moderate Resolution Imaging Spectroradiometer (MODIS), which is flown on the same platform as MISR (i.e. Terra) is similar to AVHRR in that the angular effects are derived from the sensor's wide-field of view (Barnsley et al., 1994). There are two MODIS sensors, one is flown on NASA's Terra EOS in a descending orbit (10:28 am equatorial crossing time) and the other on Aqua EOS in an ascending orbit (1:28 pm equatorial crossing time). Terra was launched 18th December 1999 and Aqua launched 4th May 2002. Both Terra and Aqua are in a 705-km Sun-synchronous orbit and each sensor views the entire surface of the earth every one to two days. It has a field of view of +/- 55° off-nadir and a swath width of 2,328km. The curvature of the Earth makes the view zenith angle larger than the scan angle, i.e. making the view zenith angle as large as 65° (Tan et al., 2006). MODIS is a whiskbroom scanning imaging radiometer consisting of an across-track scan mirror. It collects data in 36 spectral bands from 0.4um to 14.5um. MODIS spatial resolution ranges from 250 x 250m (bands 1 and 2), 500 x 500m (bands 3 through 7) and 1 x 1 km (bands 8 through 36) (Masuoka et al., 1998, Jensen, 2007).

MODIS bands 1 through 7, (refer table 2.5) are used to derive the MODIS BRDF product and sub-products.

Table 2.5 – MODIS Bands

Band	Spectral Passband	Spatial Resolution
R_1 (red)	0.620 – 0.670um	250 x 250m
R_2 (NIR)	0.841 – 0.876um	250 x 250m
R_3 (blue)	0.459 – 0.470um	500 x 500m
R_4 (green)	0.545 – 0.565um	500 x 500m
R_5	1.228 – 1.250um	500 x 500m
R_6	1.627 – 1.652um	500 x 500m
R_7	2.105 – 2.155um	500 x 500m

2.3 Definition of Bidirectional Reflectance Distribution Function (BRDF)

EMR incident on a surface may be considered to be reflected in a continuum between Lambertian through to Specular which represent the extreme cases with regards to the reflected EMR. Lambertian reflectance is where incident EMR is reflected equally in all directions, i.e. isotropic. Specular reflectance is the opposite, where EMR is reflected away from the surface with the same angle (to the surface normal) as the incidence radiation and is most commonly seen as the bright reflectance off a body of still water (Jensen, 2007). With the exception of mirror like surfaces such as an absolutely calm body of water, all terrestrial surfaces reflect light diffusely, scattering shortwave radiation into an angular reflectance pattern or Bidirectional Reflectance Distribution Function (BRDF) (Diner et al., 1999). BRDF is formally defined as the ratio of radiance (W m^{-2} sr^{-1} nm^{-1}) reflected in one direction (θ, Φ_r) to the Sun's incident irradiance (W m^{-2} nm^{-1}) from direction (v, Φ_i) (Jensen, 2007). Schaepman (2006) states that physical definitions of BRDF appeared in the mid-20th century and standardisation of the nomenclature in the early 1970's was coined by F. Nicodemus at the same time as BRDF found its way into computer science and particularly photorealistic rendering.

Schaepman-Strub (Schaepman-Strub et al., 2006) citing Nicodemus (Nicodemus et al., 1977) states that BRDF, as a ratio of infinitesimals, is a derivative with "instantaneous" values and can never be measured directly. BRDF is approximated by measurements over finite solid angles and subsequent atmospheric correction and angular modelling. BRDF facilitates the derivation of many other quantities, e.g. conical and hemispherical quantities are derived by integration over corresponding finite solid angles. Schaepman-Strub identifies nine "cases", based upon incident and reflected radiation which may be considered as directional, conical (i.e. solid angle measured in steradians) or hemispherical. These nine cases are shown in Figure 2.6. Only cases 5 and 8 provide directly measurable quantities, i.e. one cannot measure reflectance at an infinitesimal point nor can it be measured across an entire hemisphere. The seven other cases can be derived by integration of the BRDF over finite solid angles.

BRDF and the related entity Bidirectional Reflectance Factor (BRF) which is defined as the ratio of reflected radiant flux from a surface area to the reflected radiant flux from an ideal and diffuse surface of the same area under identical view geometry and single

11

direction illumination are shown in Figure 2.6 as Case 1. BRF equates to π x BRDF
(Schaepman-Strub et al., 2006)
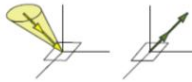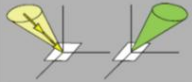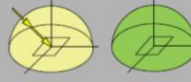
Figure 2.6 (Schaepman-Strub et al., 2006) considered nine cases based upon incident
and reflected radiation.

2.4   Models for representing BRDF

BRDF cannot be directly measured; as measurements must be of finite solid angles (i.e.
not continuous infinitesimal measurements). Representations of BRDF are based on
'sampling' (reflectance observed at different illumination and view angles) and modelled
with mathematical functions. Therefore, there is not a singular BRDF model, but rather
multiple BRDF models have been developed that seek to best represent variations in
reflectance based on view and illumination angles. The magnitude and angular shape is
governed by the composition, density and geometric structure of the reflecting medium.
It is widely accepted that the assumption of Lambertian or directionally isotropic BRDF is
generally not valid (Diner et al., 1999).

BRDF representations may be considered to be physically based or empirically based.
These differ in the detail with which they describe the physical processes responsible for
EMR scattering, the degree of a priori knowledge and the number of observations
needed to derive model parameters. While physical models describe the scattering of
EMR explicitly, empirical models do not attempt to explain it but rather describe the

12

BRDF by any empirically suitable mathematical function. Physical models are more complex than their empirical counterparts and semi-empirical models are between the two in terms of complexity (Wanner et al., 1995).

A list of kernel and other semi-empirical BRDF models has been compiled by Jupp (Jupp, 1998). Jupp groups BRDF models as kernel or non-kernel models. Kernel models based on a linear combination of kernel functions which seek to represent some physical surface characteristics. Kernel models may be applied individually or in combination. Kernels functions listed by Jupp include:

- Ross-thin (Wanner et al., 1995),
- Ross-thick (Wanner et al., 1995),
- Li-Sparse (Wanner et al., 1995),
- Li-Dense (Wanner et al., 1995),
- Roujean (Wanner et al., 1995) (Roujean et al., 1992),
- Cox-Munk (Cox and Munk, 1954), and
- Walthall model (Walthall et al., 1985).

Non-kernel models listed by Jupp include:

- Rahman-Pinty-Verstraete (RPV) (Rahman et al., 1993),
- Staylor & Suttles (Staylor and Suttles, 1986),
- Shibayama &Weigand (Shibayama and Weigand, 1985),
- Dymond & Qi (Dymond and Qi, 1998),
- Chen modifications to Roujean (Chen and Cihlar, 1997),
- Pickup & Chewings (Pickup et al., 1995a, Pickup et al., 1995b),
- Otterman (Otterman and Weiss, 1984),
- Verstraete-Pinty & Dickingson (VPD) (Dickinson et al., 1990),
- Hapke BRDF model for soils (Hapke, 1981), and
- Minnaert's model (Minnaert, 1941).

All models have similarity in their form, i.e. being trigonometric functions of view angle (θ), illumination angle (v) and the relative azimuth (Φ). Zenith angles are measured from the normal to the surface. Use of the relative azimuth, means that modelling is

derived without considering the absolute azimuth of illumination and view geometries and also reduces the number of variables to three angular parameters.

If the relative azimuth is 0° (or 180°), then the illumination source and the viewer/sensor lie in the same plane and the geometry created is referred to as the principal plane. If the relative azimuth is 90° (or 270°), then the illumination source and the viewer/sensor are orthogonal to one another and the geometry created is referred to as the cross plane.

| + 75 ° | + 45 ° | 0 ° | - 45 ° | - 75 ° |

Backward scattering   nadir   Forward scattering
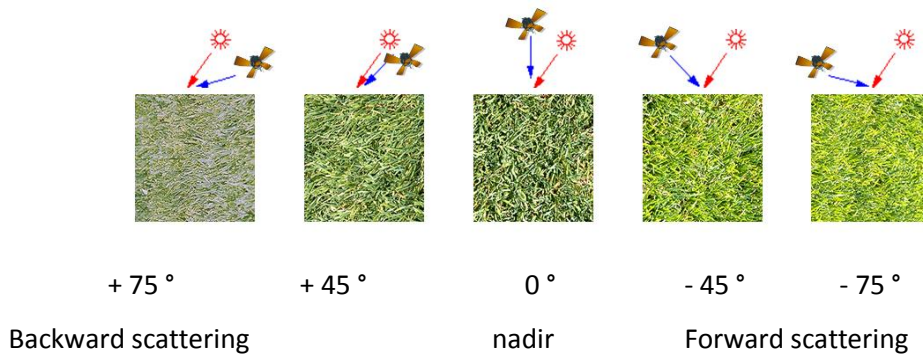
Figure 2.7 (Jensen, 2007)

Figure 2.7 shows bidirectional reflectance effects upon a field of ryegrass in the principal plane with a solar zenith angle of 35°. The convention of defining backward scatter as when the illumination source and sensor are in the same quadrant and forward scatter when they are in opposite quadrants is shown in Figure 2.7.

From studies prior to the 1980's some general observations about the nature of vegetation canopy reflectance associated with view and illumination angles had been made: (a) reflectance generally increases with the zenith view angle for all azimuth angles, (b) greatest increases were in the principal plane due to backscatter in the direction of the sun and (c) increased solar angles tend to generally increase reflectance (Walthall et al., 1985). Walthall developed one of the earliest models for representing BRDF (Walthall et al., 1985):

$$R(\theta, v, \phi) = a\,\theta^2 + b\,\theta\cos(\phi - v) + c \tag{1}$$

Where: θ, v, and ϕ are the view angle, illumination angle and relative azimuth. The parameters a, b and c are numerical values derived from least squares fitting to observations.

These general observations about the nature of vegetation canopy give rise to the "bowl shape" of reflectance and the hot spot which are depicted in Figures 2.8 and 2.9. The hot spot is the enhancement of surface reflectance observed when the direction from which a remote sensing instrument views the surface is close to coincidence with the Sun direction (Grant et al., 2003). The widely accepted explanation for the hot spot effect is shadow hiding, in which particles at the surface (leaves, soil grains) cast shadows on adjacent particles. Those shadows are visible at large phase angles (the angle between the sun and view directions), but at zero phase angle they are hidden by the particles that cast them (Breon et al., 2002). The angular width and amplitude of the hot spot at different wavelengths of light is potentially a source of additional information that may be used to assist with the characterisation of vegetation (Lacaze and Roujean, 2000).
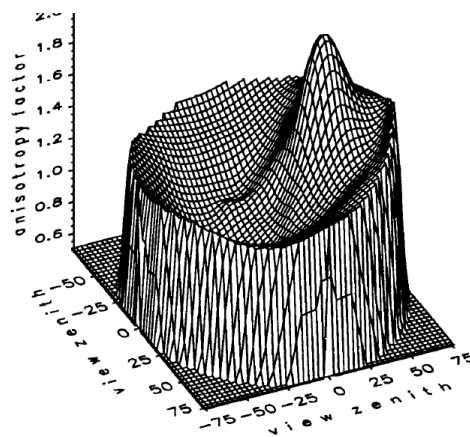
Figure 2.8 – shows the characteristic bowl shape reflectance from vegetation with the hot spot (Sandmeier et al., 1998).

Figure 2.9 – Depicts visually the hot spot at the centre of the picture where no shadowing is apparent. (Source: http://www.atoptics.co.uk/opod.htm)

15

Two particular models frequently referenced in literature are the linear combination of kernel functions in the form of the RossThick-Li Sparse model and the Rahman-Pinty-Verstraete model. These BRDF representations are discussed in more detail below.

2.4.1   Rahman-Pinty-Verstraete Model

The Rahman-Pinty-Verstraete Model (Rahman et al., 1993) splits a BRDF field into its amplitude component and an associated angular field describing the anistropic behaviour of the surface. The model has three free parameters (r_0, k and b), where r_0 gives the overall reflectance level, k is representative of the bowl or bell shape of the surface anisotropy and b described the predominance of forward or backward scattering. The function '*h*' is a factor to account for the hot spot. The function '*p*' (equation 5) is assumed to depend only on the scattering angle Ω (Su et al., 2009). The RPV model is defined by equations 2 – 5.

$$R(\theta, v, \phi) = r_0 \left(\frac{(\cos(\theta))^{k-1}(\cos(v))^{k-1}}{(\cos(\theta)+\cos(v))^{1-k}} \right) exp(bp(\Omega)h(\theta, v, \phi) \qquad (2)$$

Where:

$$h(\theta, v, \phi) = 1 + \left(\frac{1-r_0}{1+G(\theta, v, \phi)} \right) \qquad (3)$$

$$G(\theta, v, \phi) = \left(\left(\frac{\sin(\theta)}{\cos(\theta)} \right)^2 + \left(\frac{\sin(v)}{\cos(v)} \right)^2 + 2\left(\left(\frac{\sin(\theta)}{\cos(\theta)} \right)\left(\frac{\sin(v)}{\cos(v)} \right)\cos(\varphi) \right) \right)^{\frac{1}{2}} \qquad (4)$$

$$p(\Omega) = \cos(\Omega) = \cos(\theta)\cos(v) - \sin(\theta)\sin(v)\cos(\varphi) \qquad (5)$$

Where θ, v, and ϕ are the view angle, illumination angle and relative azimuth.

2.4.2   The Ross-Thick-Li-Sparse (Reciprocal) Model

The RossThick-Li-Sparse-Reciprocal model is a linear combination of three kernel functions and is used as the BRDF representation in the MODIS MCD43 product (Lucht et al., 2000).

The theoretical basis of the RossThick-Li-Sparse-Reciprocal semi-empirical model is that the land surface reflectance is modelled as a sum of three kernels representing basic scattering types (Lucht et al., 2000) depicted in Figure 2.10:

- isotropic scattering (i.e. a constant that is independent of view and illumination angles),
- radiative transfer-type scattering as from horizontally homogeneous leaf canopies (i.e. the Ross-Thick kernel for its assumption of a dense leaf canopy), and
- geometric-optical surface scattering as from scenes containing 3-D objects that cast shadows and are mutually obscured from view at off-nadir angles (i.e. the Li-Sparse kernel for its assumption of a sparse assembly of objects casting shadows on the background which is assumed Lambertian).

Volume scattering BRDF:
leaf/vegetation reflectance

Gap−driven BRDF (Forest):
shadow−driven reflectance
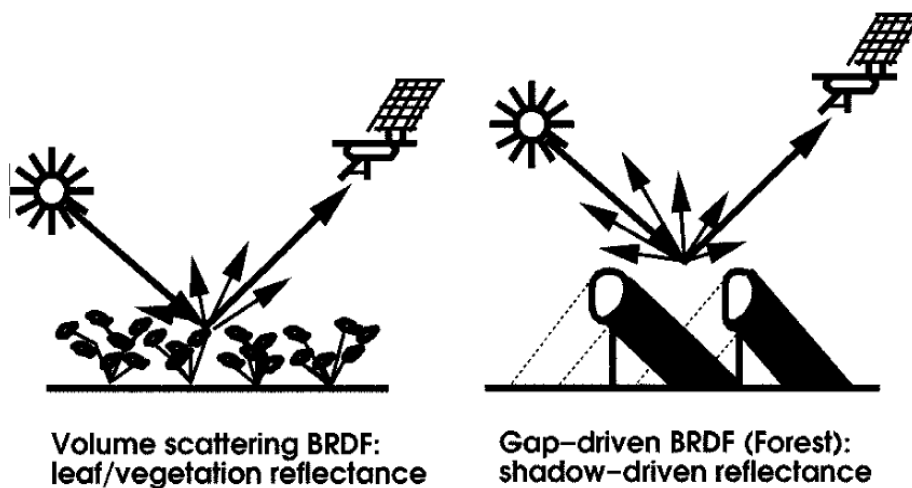
Figure 2.10 Depicts volumetric scattering (left) and geometric scattering (right)

(Lucht et al., 2000)

One may think of the volume scattering term as expressing effects caused by small (inter-leaf) gaps in the canopy and multiple scattering, whereas the geometric-optical term expresses effects caused by larger (inter-crown) gaps (Lucht et al., 2000). The model is shown below (equations 6 – 15), with numerical weights (i.e. f_{iso}, f_{vol} and f_{geo}) applied as a linear multiple of each of the kernel functions:

$$R(\theta, v, \phi, \lambda) = f_{iso}(\lambda) + f_{vol}(\lambda)\, k_{vol}(\theta, v, \phi) + f_{geo}(\lambda)\, k_{geo}(\theta, v, \phi) \qquad (6)$$

Where:

$$f_{iso}(\lambda) = Constant \qquad (7)$$

$$K_{vol} = \frac{\left(\frac{\pi}{2}-\xi\right)\cos(\xi)+\sin(\xi)}{\cos(\theta)+\cos(v)} - \frac{\pi}{4} \qquad (8)$$

$$K_{geo} = \psi - \sec(\theta`) - \sec(v`) + \frac{1}{2}\left(1+\cos(\xi`)\right)\sec(\theta`)\sec(v`) \qquad (9)$$

$$\Psi = \frac{1}{\pi}\left(t-\sin(t)\cos(t)\right)\left(\sec(\theta`)+\sec(v`)\right) \qquad (10)$$

$$\cos(t) = \left(\frac{h}{b}\right)\left(\frac{\sqrt{D^2+(\tan(\theta`)\tan(v`)\sin(\varphi))^2}}{\sec(\theta`)+\sec(v`)}\right) \qquad (11)$$

$$D = \sqrt{\left(\tan(\theta`)\right)^2 + \left(\tan(v`)\right)^2 - 2\tan(\theta`)\tan(v`)\cos(\varphi)} \qquad (12)$$

$$\cos(\xi`) = \cos(\theta`)\cos(v`) + \sin(\theta`)\sin(v`)\cos(\varphi) \qquad (13)$$

$$\theta` = \tan^{-1}\left(\frac{b}{r}\tan(\theta)\right) \qquad (14)$$

$$v` = \tan^{-1}\left(\frac{b}{r}\tan(v)\right) \qquad (15)$$

Where θ, v, ϕ and λ are the view angle, illumination angle, relative azimuth and wavelength. ξ' is the phase angle and is the angle formed between the view and illumination vectors as they intersect on the surface and 'D' is the distance between the illumination source and sensor as considered on a unity radius sphere. Equations (12) and (13) representing the phase angle (ξ') and distance (D) in the Ross-Thick-Li-Sparse-Reciprocal model are the same as equations (4) and (5) respectively in the RPV model.

There are a number of specific properties of the Ross-Thick-Li-Sparse model as shown in equations 6 – 15. The model is reciprocal between view and illumination angles, i.e. a view angle and illumination angle can be interchanged or the direction of light's travel can be reversed to yield the same result. In this form the model is referred to as the Ross-Thick-Li-Sparse-Reciprocal model. Furthermore, the kernels are normalised functions, such that if $\theta = 0$ and $v = 0$ then the kernels equate to 0 and the BRDF equals the isotropic kernel. Plots of the Ross-thick and Li-sparse kernel functions are shown in Figure 2.11.

The model is defined as proportions of a sunlit and shaded scene consisting of randomly distributed spheroids of height-to-centre of crown (h) and crown vertical-to-horizontal radius ratio b/r, where *b* and *r* are relative crown height shape parameters that are pre-selected. For MODIS processing *h/b* = 2 and *b/r* = 1, i.e. spherical crowns are separated from the ground by half their diameter (Lucht et al., 2000).
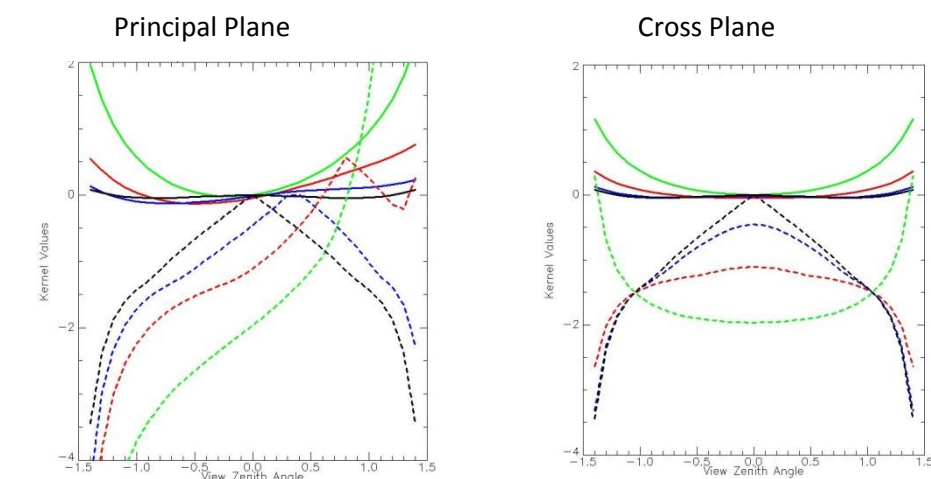
Figure 2.11 - Plots of the Ross-Thick volumetric (solid lines) and Li-Sparse geometric kernels (dashed lines) against view angles in the principal plane, i.e. φ = 0 and cross plane φ = π/2. The solar angle is 0° (black), 20° (blue), 45° (red) and 70° (green).

The Ross-thin and Li-dense kernels are similar in consideration to the Ross-thick and Li-sparse kernels respectively, however they consider the leaf canopy to be thin (rather than thick) and a dense (rather than a sparse) assembly of vegetation canopies.

2.5   Realisation (Inversion) of BRDF Models

BRDF cannot be directly measured as measurements must be based on finite solid angles, whilst BRDF is continuous across the hemisphere. BRDF is 'sampled' (reflectance observed at different illumination and view angles) and may then be modelled in accordance with one of the representations identified in section 2.4. Observations may be made on the ground (in situ) using a spectroradiometer which can be hand held, located on a flux tower or attached to a goniometer. A goniometer, shown in Figure 2.12 is a purpose built frame for observing the ground surface at varying view angles and provides a greater range of observable angles than from a stationary flux tower and a greater level of control and accuracy than hand held devices.

Figure 2.12 (Schaepman, 2006) shows a goniometer used in the field.

In a similar manner, multi-angular views of a surface can be obtained from sensors on an aircraft or EOS. In the case of MISR, observations from fore and aft sensors acquired over a 7 minute interval can be considered quasi-simultaneous (Chopping, 2006). Alternatively, multi-angular observations of the surface can be made through images acquired on successive orbits and this is the approach adopted by MODIS BRDF modelling. In the later case, the assumption is that the surface is temporally invariant over the period in which observations from successive orbits are acquired and observed

reflectance variations from multi-angular observations acquired from successive orbits will be attributed to angular effects.

With a series of reflectance observations of a surface obtained with multiple viewing geometries a best fit process can be applied to BRDF representation, i.e. derivation of the respective BRDF model parameters such that the chosen parameter values within the BRDF minimise the error (squared to removed consideration of the error being positive or negative) between the model and observations. Typically this is performed separately for each pixel and also for each observed EMR wavelength/spectral band.

For the model to be mathematically well defined (i.e. a single solution), the number of reflectance observations required must be equal to or greater than the number of parameters estimated. The greater the number of observations the more redundancy is built into the 'best fit' process. The number of observations used may be practically constrained, e.g. by the 9 fore and aft sensors in the case of MISR. Where in the case of multi-angular observations derived from MODIS, the inclusion of a larger number of observations will be at the expense of the assumption of temporal invariance, i.e. the shorter the window over which observations are acquired the less the surface is likely to have changed. Variations to BRDF models have been proposed that impose conditions of temporal smoothness on the derived BRDF parameters (Quaife and Lewis, 2010, Samain et al., 2007). Modelling with this constraint seeks to extend the temporal window from which multi-angular observations can be obtained and also supports the idea the BRDF parameters should evolve smoothly over time.

There is a relationship between the sensor's field of regard (which enables view angle effects and determines surface coverage), the sensor's spatial resolution and the sensor's revisit frequency. When modelling BRDF from observations obtained from an EOS sensor, a wide field of view, a high spatial resolution and short revisit interval is an ideal. However, achieving one of these objectives is frequently at the expense of the other two objectives. This is why BRDF effects cannot be derived directly from Landsat or other sensors with a 28m or equivalent spatial resolution (Li et al., 2010). Sensors capable of sufficient view angle sampling and short revisit intervals necessary to model BRDF will have a lower spatial resolution. BRDF effects derived from lower resolution sensors will therefore represent surfaces that are heterogeneous in nature and BRDF effects will be the spatial integral of all features present within a pixel. Homogeneous surfaces at the sensors spatial resolution will typically be dried salt lakes or desert areas that are of limited interest other than as a reference surface.

BRDF representations that are linear in form have particular advantages over non-linear models. Linear models can have kernel functions pre-calculated and inversions to determine parameter weights using linear algebra and matrix inversions. This has significant computational savings for global models and avoids long numerical inversion problems (Wanner et al., 1995). Other advantages identified by Wanner et al include easier derivation of albedo from lookup tables rather than numerical integration and allows scaling from one spatial resolution to a coarser one. The RPV model is non linear where as the Ross-Thick-Li-Sparse model is linear in form.

Ideally, the derivation of BRDF parameter model weights from sampling should be representative of the broadest possible range of illumination and viewing angle geometries. Sufficient angular sampling in the derivation of BRDF models from EOS sensors might not always be possible due to flight path or the availability of individual observations made when performing an inversion. Extrapolations of angular geometries beyond those observed may not therefore be valid. Studies have been performed on the RPV and Ross-Thick-Li-Sparse models to test their sensitivity to angular sampling (Lucht and Lewis, 2000). The derived products (i.e. reflectance and albedo) were found to be capable of modelling reflectance at extrapolated view and illumination geometries and less susceptible to noise than the individual BRDF model parameters, i.e. parameters may trade-off magnitude between one another without affecting the overall BRDF shape. In kernel models, the kernels should be orthogonal functions and the absence of kernel-to-kernel correlations is key to reliable BRDF model inversion (Lucht et al., 2000).

Boston University Department of Geography and Centre for Remote Sensing, BRDF and Albedo Research has included Principal Investigators for the MODIS Science Team. Their web site includes a User Guide to the MODIS BRDF modelling (Schaaf, 2012) which is summarised here. Every 8 days, the operational MODIS BRDF/Albedo algorithm makes use of 16 days worth of multi-date data from both Terra and Aqua and a semi-empirical kernel-driven bidirectional reflectance model to determine a global set of parameters describing the BRDF of the land surface (MCD43A1). Combined data from the MODIS instruments on board both Aqua and Terra are used (with only Terra data available before mid-2002). When insufficient high quality reflectance observations are available (currently set to less than seven observations) or a poor representative sampling of high quality reflectance is obtained (as indicated in the quality flags and determined through weights of determination), it is not possible to perform a full inversion. Instead, use is

made of a database of archetypal BRDF parameters to supplement the observational data available and perform a lower quality magnitude inversion. All MODIS Land products supply a per-pixel quality flag indicating whether the algorithm produced results (or not) for that pixel and if so, whether the result is of the highest quality or otherwise (due to some uncertainties in the processing).

When deriving the model parameters, only positive parameter weights are allowed. This is required for physical considerations of the scattering kernels. If the inversion produces a negative parameter, the next best valid value for this parameter is zero, under this imposed condition, the remaining kernel parameters are re-derived (Lucht et al., 2000).

2.6 How BRDF effects are used in remote sensing

Within the remote sensing fields there are three general applications of BRDF effects:

- Standardise images to common view and illumination geometry,
- derivation of surface albedo, and
- the characterisation of the surface features.

2.6.1 Standardising images to a common view and illumination geometry

The view and illumination geometries create a source of variability within remotely sensing reflectance data. Ideally, it is sought to remove this source of variability such that surface features can be compared between images and within individual images. Removal of illumination and view angle variability also allows better mosaics to be created. With an appropriate BRDF model, images can be brought to any required view and illumination geometry, the default being a nadir view. The MODIS BRDF/Albedo Product provides Nadir BRDF-Adjusted Reflectance (NBAR) which is surface reflectance corrected to the standard geometry of nadir view and solar zenith angles at the local solar noon value for the start of the observation period (Schaaf, 2012).

In addition to correcting images to a common view geometry, vegetation indices, leaf area indices (LAI) and measurement of the fraction of photosynthetically active radiation

absorbed by plant canopies (fAPAR) may be improved by consideration of BRDF (Asner et al., 1998).

2.6.2 Surface Albedo

The second application of BRDF effects is for the derivation of surface albedo. Albedo is defined as the ratio of upwelling to downwelling radiative flux at the surface. Downwelling flux may be written as the sum of a direct and a diffuse component (Lucht et al., 2000).

Black sky and white sky albedo mark the extreme cases of complete direct and complete diffuse illumination (Lucht et al., 2000). Black sky albedo is defined as albedo in the absence of a diffuse component and is a function of a solar zenith angle. Pure direct illumination identified as black sky albedo in the MODIS product suite corresponds to Case 3 in Figure 2.6. Black sky albedo can be derived by integrating the BRDF, across the quadrant of view angles (i.e. from 0° to 90°) and then integrating across a full circle of relative azimuths (0° to 360°).

White sky albedo is defined as albedo in the absence of a direct component when the diffuse component is isotropic. Pure diffuse isotropic incident radiation may be best approximated by a thick cloud layer. White sky albedo in the MODIS product suite corresponds to Case 9 in Figure 2.6 (Schaepman-Strub et al., 2006). Integration of the black-sky albedo for all illumination angles in the hemisphere (i.e. from 0° to 180°) provides a measure of white sky albedo. Actual albedo is a value interpolated between black sky and white sky cases and is dependent on the atmosphere's composition and cloud conditions.

Earth-scanning instruments generally acquire data in narrow spectral bands. However, the total energy reflected by the Earth's surface is characterised by the shortwave (0.3 – 5.0um) broadband albedo. Conversion from narrow to broad band albedo is dependent on the atmospheric state and coefficients are determined empirically from computer simulations (Lucht et al., 2000).

Albedo quantifies the radiometric interface between the land surface and the atmosphere. It details total shortwave energy input into the biosphere and is a key influence on the surface energy balance (Lucht et al., 2000). Higher albedo means that

less incident radiation is absorbed and either later re-emitted at longer wavelengths within a spectrum that is a function of blackbody temperature and includes thermal infrared, or available as energy to drive evaporation and transpiration. Better measurement of albedo at continental and global scales is an important factor in climate modelling (Asner et al., 1998).

2.6.3   Characterising of land surfaces

The third application of BRDF is to assist with the characterisation of land surface features. BRDF effects have been applied to the study and characterisation of soils (Pinty et al., 1989, Cheng et al., 2008, Jacquemoud et al., 1992), snow (Zege et al., 2011) and the structure of vegetation (Chopping, 2006). Canopy structure is defined as the vertical and horizontal spatial distribution, orientation and density of foliage and its supporting structures (Chopping, 2006). BRDF theoretical models are derived with consideration of these factors and have the potential to provide additional new information about vegetation structure that is not apparent in spectral data alone, e.g. distinguishing different vegetation species that have the same spectral characteristics by differences in their BRDF effects. The term "spectrodirectional" has been used in regularly in literature to describe the combination of high spectral resolution and multi view angle effects (Schaepman, 2006).

The use of BRDF effects to assist characterise vegetation is the prime focus of this thesis. Past achievements in this area are discussed in the following two sections and include the derivation of metrics from BRDF parameters and how BRDF effects differ at regional and continent scale in association with independently derived land cover classifications.

2.7   Metrics for interpreting vegetation structure using BRDF effects

Just as vegetation indices have been developed by combining reflectance values at different wavelengths into a single numeric value, so too have metrics been derived that combine BRDF parameters that are theoretically derived from vegetation properties and seek to highlight characteristics of the vegetation. Ideal metrics will take the form of a

single numeric value that provides a characterisation of vegetation that includes additional information to spectral data.

Using the Ross-Thick-Li-Sparse-Reciprocal BRDF model which is operationally used in the MODIS BRDF/Albedo algorithm, a metric has been developed combining kernel parameter weights. High vegetation leaf transmittance in the near infrared results in multiple scattering within the canopy and decreases reflectance anisotropy and is best described by the volumetric scattering kernel in the near infrared band. Conversely, the small leaf transmittance in the red band due to chlorophyll absorption causes high anisotropy which is best described by geometric scattering in the red band. Therefore volumetric scattering in the near infrared band and geometric scattering in the red band are the two kernels most sensitive to vegetation (Gao et al., 2003). Based on this, Gao has defined a metric termed the Structural Scattering Index (SSI)(Gao et al., 2003) as:

$$SSI = \ln (f_{nir\,vol} / f_{red\,geo}) \tag{16}$$

Where $f_{nir\,vol}$ is the volumetric weight of the nir band, and

$f_{red\,geo}$ is the geometric weight of the red band.

The SSI has been observed by Gao to have a good linear relationship with the Normalised Difference Vegetation Index (NDVI). NDVI is discussed in section 4.3.1. This allows vegetation with the same NDVI response to be differentiated by its structure based upon its SSI value being above or below the SSI - NDVI trend line, for example vegetation with strong shadowing effects have smaller SSI values. Temporal changes have been observed with SSI and with a Relative Structural Scattering Index (RSSI), being the difference from SSI – NDVI trend line, and is therefore independent of the level of vegetation coverage (Gao et al., 2003).

Two other BRDF derived metrics have been defined as the Anisotropic Factor (ANIF) and the Anisotropic Index (ANIX) (Sandmeier et al., 1998). Sandmeier derived and analysed these metrics from the laboratory study of grasses and watercress.

$$ANIF\,(\lambda, \theta_i, \theta_r, \Phi_i, \Phi_r) \quad = \quad \frac{R\,(\lambda, \theta_i, \theta_r, \Phi_i, \Phi_r)}{R_0\,(\lambda, \theta_i, \Phi_i)} \tag{17}$$

$$\text{ANIX} (\lambda) = \frac{R^{max} (\lambda)}{R^{min} (\lambda)} \tag{18}$$

Where   R is bidirectional reflectance factor

       R_0 is nadir reflectance factor

       λ is wavelength

       θ is zenith angle

       Φ is azimuth angle

       i is the illumination direction

       r is the view direction

       R^{max} is the maximum bidirectional reflectance factor

       R^{min} is the minimum bidirectional reflectance factor

The anisotropy factor (ANIF) describes the proportion of radiation reflected into a specific view direction relative to the nadir reflectance. The anisotropy index (ANIX) gives the amplitude of the bidirectional reflectance variation for a given spectral band for a defined relative azimuth plane. For the principal plane, R^{max} is theoretically measured in the 'hot spot' and R^{min} is near nadir for vegetated surfaces. Sandmeier observed that low reflectance intensities are associated with high anisotropy and higher reflectance intensities are associated with low anisotropy, i.e. for vegetation, red wavelengths have higher directional related reflectance characteristics and near infrared wavelengths have a more isotropic reflectance characteristic. Furthermore, Sandmeier observed variability in reflectance anisotropy between grass lawn and watercress vegetation that was studied and attributed this to canopy structural differences, i.e. greater anisotropy reflectance in the red wavelengths for the more vertically structured grass lawn.

A derivative of the anisotropy index (ANIX) is the Clumping Index (Lacaze and Roujean, 2000). The Clumping Index quantifies the level of foliage grouping within distinct canopy structures relative to a random distribution and thus describes the textural properties of the landscape. The Clumping Index can be modelled from the Normalised Difference Hot spot Dark spot (NDHD = $(p_{HS} - p_{DS})/(p_{HS} + p_{DS})$) (Zhu et al., 2012). The hot spot is where the illumination and view directions coincide, all shadows are hidden by the surface targets that cast them and the result is a maximum backscatter reflectance.

The dark spot contains the maximum shadow observed in the forward scatter direction where reflectance is a minimum (Zhu et al., 2012). Using POLDER data, the Normalised Difference Hot spot Dark spot (NDHD) Index = ((ANIX -1)/(ANIX +1)) (Hill et al., 2008) and has been shown to be linearly related to the Clumping Index (Chen et al., 2005, Chen and Cihlar, 1997). More recently the Clumping Index has been developed from MODIS BRDF data and a global map developed producing a good correlation with field based measurements of Clumping Index and was able to capture structural differences amongst vegetation coverage types (He et al., 2012).

It has been shown in recent studies that BRDF model parameters can be used to increase classification accuracies for vegetation mapping. Combining single-date nadir reflectance with multi-date BRDF model parameters is a feasible approach to increase classification accuracy with lower data dimensionality (Su et al., 2011). Similarly, whilst there is no direct relationship between canopy height and surface reflectance, it has been suggested that BRDF data can be useful in extrapolating limited swath lidar (light detection and ranging) information on canopy vertical structure to larger regional areas (Wang et al., 2010). These studies show that BRDF parameters, whilst not directly and independently used, can be combined with classification techniques and lidar data to provide new potential uses of BRDF measurements from space for improving the accuracy of vegetation studies.

2.8 Past studies in Australia that have utilised BRDF effects to assist with the characterisation of vegetation

There have been numerous studies that have used BRDF effects derived from EOS to assist in the characterisation of vegetation. However, there have been relatively fewer studies that have focused on Australian vegetated landscapes. A summary of the key findings from four recent Australian specific studies are discussed below which have utilised a variety of different sensors, BRDF models and study sites.

Roujean BRDF model parameters from POLDER/ADEOS Level 3 Surface Directional product were compared with 31 vegetation classes derived manually from 1980s Landsat imagery and field observations for the Australian continent (Grant, 2000). The Roujean BRDF model is similar to the Ross-Thick-Li-Sparse model in that it is a linear

kernel model that describes the BRDF effects in terms of isotropic, volumetric and geometric scattering (Roujean et al., 1992). From this study, individual BRDF parameters were identified as noisy and the discrimination of land cover classes on a continental scale by a small number of these parameters would appear difficult. Nevertheless combining twelve – variate POLDER data (3 BRDF parameters by four bands) suggests that multi-angular information gives greater discrimination of land cover classes than using reflectance information alone.

In another study, Roujean BRDF model parameters were again derived from POLDER data for the Australian continent (Lovell and Graetz, 2001). Lovell and Graetz found that spatial variation across the continent influenced BRDF parameter weights more than landform (i.e. topology) or temporal changes during the 8 months of POLDER's operation. They found that the geometric scattering coefficient of the Roujean BRDF model decreased within increased vegetation cover, which may be due to increased uniformity as vegetation cover increases. The volumetric scattering coefficient within the Roujean model did not exhibit as strong a relationship and had a degree of insensitivity to changes in vegetation cover.

Lovell and Graetz defined and calculated a 'spacing to height ratio' as the mean spacing between individual plants and the ratio of this quantity to the average height as derived from a measure of project foliage cover (PFC) from the Australian Federal Government's AUSLIG structural classification system (AUSLIG, 1990). The 'spacing to height ratio' has the advantage of collapsing the description of vegetation structure from two variables (i.e. height and cover) into one variable. They found that the Roujean BRDF model parameters were related to the 'spacing to height ratio' of vegetation, i.e. all the Roujean BRDF parameters in red and near infrared wavelengths increased with larger 'spacing to height ratios'.

In the third study considered, Rahman-Pinty-Verstrate (RPV) BRDF model parameters were derived from MISR data for an area in Southern Queensland (Armston et al., 2006). The results were compared with foliage projective cover (FPC) derived from Landsat data that was supported with extensive field validation for the study area. The derived parameter in the RPV model that describes the degree of forward and back scattering in the red band was incorporated in a regression model to provide a better predictor of FPC from MISR data. The bowl-bell shaped anisotropy parameter from the RPV model contained information independent of FPC.

In the fourth study considered, tropical savannas in the Northern Territory were used as a study site and Rahman-Pinty-Verstrate (RPV) BRDF model parameters were derived from MISR data and Ross-Thick-Li-Sparse BRDF model parameters taken from the MODIS MCD43 product (Hill et al., 2008). Their results show complimentary information about savannas' vegetation structure within the high-level BRDF products from both MISR and MODIS sensors. Distinct differences between individual spatially defined savanna communities were found and considerable evidence of seasonal trends related to the aspect ratio effects of canopy cover and tree heights. However, a definitive relationship between tree density, arrangements, canopy shape and tree heights could not be obtained with broad descriptive structure classes. Hill summarises by stating that shadow casting and arrangement of open space and tree clumps need to be quantitatively characterised and generalised to the scale of MISR and MODIS pixels. The structure of surfaces should be described in terms of the arrangements, density and light-interception properties of the vegetation and angular and shadowing influences of the terrain and canopy architecture (Hill et al., 2008).

The four Australian studies discussed above are similar in that they are focused on large land area extents for which respective BRDF parameters showed distinct statistical relationships with independently defined land cover metrics. However all results were impacted by noise and the results were not interpretable at a pixel scale.

2.9   Gaps, issues and opportunities identified in past studies

There are a number of issues repeatedly identified in BRDF research and the studies cited above; they are: noise, understanding BRDF effects at different spatial scales (i.e. derived from in-situ, airborne or satellite) and understanding BRDF effects in heterogeneous surfaces where multiple feature are present. These issues are very much interrelated.

2.9.1   Noise

Noise is always a problem in any field of satellite measurement (Gao et al., 2003). To address noise, BRDF models have been developed that place the constraint of temporal

smoothing on derived BRDF parameters (Quaife and Lewis, 2010) and some studies have removed potentially 'contaminated' pixels (Armston et al., 2006). Also, to minimise noise associated with individual BRDF parameters that may be correlated with one another, the use of linear combinations of parameters may be preferable to the consideration of individual parameters (Lucht and Lewis, 2000). Noise associated with BRDF parameters makes characterisation of vegetation at a pixel level problematic. If the sources of noise can be identified, minimised or removed when considering BRDF effects from EOS sensors, the remaining signal may enable a clearer characterisation of land surface properties.

2.9.2   Scale and homogeneity

Past satellite studies have tended to focus on large land area extents ranging from regional to continental scales. Such scales allow the statistical treatment of noise within the data and the generalisation of land cover types.

Measurement of BRDF effects have been derived from laboratory scale studies (Sandmeier et al., 1998, Huete, 1987), measurements from flux towers (Liu et al., 2009), observations from aircraft (Roman et al., 2011) and from satellites (Grant, 2000, Lovell and Graetz, 2001, Armston et al., 2006). A difficulty is reconciling BRDF effects at different spatial scales, i.e. BRDF associated with leaf structure, plant structure, ecosystems, regional, continental and global scales.

The use of moderate to coarse spatial resolution satellite sensors in BRDF studies means that pixels will tend to represent heterogeneous surfaces and that the resulting BRDF effects are the spatial integral of all features present in each pixel. Liu (Liu et al., 2009) states that the site heterogeneity and spatial scale mismatch between MODIS and ground observations are the major factors contributing to discrepancy between MODIS albedo and field measurements. Most BRDF models are derived with consideration to plant canopy structures and shadow casting between plants, however BRDF derived from EOS sensor observations are at a much larger scale. Retrieval models used in remote sensing are usually developed at a local scale, implying that models are merely suitable when the medium where the process takes place is homogeneous. If these models are directly applied at different scales, they may lead to different retrieval models for different scales. Processes which appear homogeneous at a local scale may

become heterogeneous at a large scale and parameters and factors which are important at one scale may become less important at another (Wu and Li, 2009).

2.10 Summary

Bi-directional Reflectance Distribution Functions (BRDF) seek to characterise changes in a surface's reflectance associated with variations in view and illumination angles, i.e. reflected EMR is not scattered uniformly in all directions from the Earth's surface (Schaaf, 2012); (Diner et al., 1999). BRDF cannot be directly measured (Schaepman-Strub et al., 2006). Surface reflectance can be sampled at different illumination and view geometries and modelled with mathematical functions. Numerical parameters within BRDF models are derived by 'best fitting' the model to the observed reflectance at different view an illumination directions (Lucht et al., 2000). BRDF effects have been used in past studies to assist in the characterisation of vegetation as they can provide additional information not apparent in spectral data alone (Schaepman, 2006). Past studies have identified surface homogeneity, scale and noise as issues at a pixel level when seeking to use BRDF effects to assist with the characterisation of vegetation. The use of EOS sensor derived datasets where angular effects are realised, combined with study areas that enable noise, scale and homogeneity aspects to be well considered may offer an opportunity to further understanding of how BRDF effects can be used to assist with the characterisation of vegetation and answer the research questions proposed within this thesis.

3   Datasets

This chapter identifies the principal dataset used within this thesis, the rationale for its use and the availability of the dataset via the Australian Commonwealth Science Industry and Research Organisation (CSIRO). The choice of the dataset and study areas (introduced in the next chapter) seek to address issues of noise, scale and homogeneity, and thus isolate BRDF effects associated with the characterisation of vegetation.

3.1   Rationale for using the MODIS BRDF (MCD43) dataset

The principal dataset used within this thesis is NASA's Moderate Resolution Imaging Spectroradiometer (MODIS) BRDF product, i.e. the MCD43 product which incorporates several sub-products. The rationale for using this dataset is that MCD43 represents an "off the shelf" BRDF representation. The MCD43 product is fully operational and incorporates pre-processing elements that may not be available in other datasets and would otherwise need to be additionally incorporated into this research, e.g. MCD43 is atmospherically corrected and geo-located. This means that these operational processing aspects associated with derivation of BRDF parameters can be omitted, thus enabling a focus to be on the interpretation of BRDF effects to assist with the characterisation of vegetation.

The MCD43 product has been validated (Schaaf et al., 2002, Liu et al., 2009, Liang et al., 2002) and is derived from MODIS which is one of the most comprehensively calibrated sub-systems ever flown on a remote sensing satellite (Jensen, 2007). The MCD43 product is derived using the Ross-Thick-Li-Sparse-Reciprocal BRDF model (Lucht et al., 2000) which has ubiquitous application due to it being the best overall kernel combination for fitting to a range of surfaces BRDF measurements (Armston et al., 2006). Furthermore, the MCD43 product is planned to be used as the basis for atmospheric and BRDF corrections of Landsat images for Australia (Li et al., 2010) which will further extend the penetration of the MCD43 product.

The MCD43 product has a 10+ year history, worldwide coverage, daily revisit frequencies and is widely used. This means that any additional information content that

can be extracted from this dataset, however small, will potentially yield a benefit and further the understanding of how BRDF effects can be used to assist with the characterisation of vegetation.

MODIS products for terrestrial applications are created and maintained by the Land Processes Distribution Active Archive Centre (LPDAAC, http://lpdaac.usgs.gov) using processing algorithms developed by product science teams. These products include surface reflectance, land surface temperature, vegetation indices, thermal anomalies (fire hot spots), leaf area indices and a variety of albedo and BRDF related products. The LPDAAC creates these products for the MODIS instruments at a variety of spatial resolutions and at daily, 8-day and 16-day intervals. These are distributed in sinusoidal projection in HDF_EOS format files (tiles) each covering approximately 10 x 10 degrees of the Earth's surface.

To facilitate utilisation of the MODIS data sets within CSIRO and the Australian environment research community, the CSIRO have obtained all the available tiles for selected products covering the Australian continent (including Tasmania) mosaiced and remapped into the same Geographic (rectilinear latitude/longitude) projection using the MODIS Re-projection Tool (MRT) software distributed by the LPDAAC. The actual data and meta data have not been changed (Paget and King, 2008). The CSIRO's re-projection of the MCD43 product to a map grid of the Australian continent provides immediate, ready access to a very broad range of possible study areas and temporal periods.

The specific datasets accessed from the CSIRO (https://rs.nci.org.au/lpdaac/) are:

- MCD43A1 (BRDF parameter weights (x 3) for each of the seven bands at 500m resolution),
- MCD43A2 quality flag files from which three separate datasets were accessed:
    - 500m Albedo quality (overall BRDF inversion quality indicator), where:
        - "0" – processed, good quality (full BRDF inversion)
        - "1" – processed, see other QA (magnitude BRDF inversions).
    - Ancillary quality files (bit word files) identifying the solar zenith angle at local solar noon, platforms used in making observations for the BRDF inversion (i.e. Terra, Aqua or both) and the surface type (land or water).
    - Band Quality files (bit word files), identifying BRDF inversion quality for each of the seven bands separately, where:

- "0" – best quality, full inversions (WoDs, RMSE majority good),
- "1" – good quality, full inversion,
- "2" – Magnitude inversion (number of observations >=7),
- "3" – Magnitude inversion (number of observations >=3&<7),
- "4" – fill value

- MCD43A4 (Nadir BRDF-Adjusted Reflectance (NBAR) for each of the seven bands).

Data files from the CSIRO are in compressed format and were decompressed using 7-Zip software. All data access was collection 5. All data represents 8-day interval epochs. Epochs accessed were from March 2000 to March 2010, being a total of 463 epochs. The extraction of pixels from HDF databases, analysis and presentation of results (e.g. scatter plots and map formats) has been undertaken using Interactive Data Language (IDL) software from ITT Visual Information Solutions.

4 Do MODIS BRDF effects vary between soil and vegetation?

4.1 Selection criteria for study areas

In the literature review chapter, noise and homogeneity of study areas were identified as issues when using BRDF to assist with the characterisation of vegetation. In past studies these issues tend to have been addressed by studying large land area extents ranging from regional to continental scales. By using large land areas, these issues may be averaged or generalised in the interpretation of the derived BRDF parameters. Another approach has been the study of homogeneous vegetated areas. However, using the MODIS BRDF product, which has a 500-m pixel size, locating suitable homogeneous areas may be difficult. Sparsely vegetated homogeneous surfaces tend to be semi-arid or desert and dense vegetation areas tend to be virgin native forests. Even using these types of study areas, issues of homogeneity at the sensor's spatial resolution may still be problematic. Furthermore, a detailed in situ survey and knowledge of the study area is necessary and this must be aligned to the temporal periods at which MODIS BRDF was derived. In situ surveys become increasing difficult for large land areas and may require repeated site surveys if the areas are temporally variant.

An alternative approach to addressing issues of noise and homogeneity is to use single species cropped fields that are sufficiently large such that the pixels studied fall completely within the surface area of the cropped field. With MODIS's 10+ year history, temporal variations in the BRDF parameters can be compared with the known cropping status of the field. This approach seeks to answer the first three research questions; do BRDF effects vary between bare soil and vegetation, which BRDF parameters correlate strongest with the cropping cycle and with vegetation indices? To support this approach, several criteria must be met for the study sites, i.e. the field must represent the minimum management unit, be a single crop species, fields must have dimensions greater than 1 km x 1 km and property management records must be available in lieu of in-situ survey.

The cropped field must represent the minimum management unit, i.e. the entire area of the field must always be cultivated, sowed and harvested at the same time. These

activities must not be temporally staggered over the field or applied only to a portion of the field's area. This also implies that the field must have a single crop variety planted for each cropping cycle. The planting of different crops in different cropping cycles is not an issue in this context as the field will still be homogeneous at each epoch.

The MODIS BRDF product has a 500-m spatial resolution, however suitable study areas necessitate fields being significantly larger than 500-m x 500-m. The geo-location (latitude and longitude) for the centre of a pixel is recorded as metadata within the dataset. The ground position that the pixel occupies vary nominally +/- 250-m in any direction from its geo-location reference. Studies have found that the geo-location of pixels to be much more accurate than +/- 250-m, i.e. in the range of +/- 50-m (Masuoka et al., 1998). Using fields with dimensions of at least 1 km x 1 km means that even at the theoretical upper limit of geo-location inaccuracy, the extracted pixel will still always fall completely within the area of the field and thus any consideration of geo-location errors can be effectively ignored within this approach and a homogeneous surface may be consider to exist at each epoch. Consideration is only given here to geo-location accuracies. Enlargement of pixels' ground IFOV will be discussed later and was found to be a very significant issue.

Property management records of the field must be available in order that there is independent data for comparison of the MODIS MCD43 BRDF parameters. The minimal requirement is identifying the crop type, date of planting and date of harvest. Any additional information regarding cultivation, pest/weed control or fertilisation application is useful additional data.

Furthermore, cropped fields should ideally be topographically flat and have irrigated farming practised. Flat topology eliminates any issues with slope or aspect that may impact the derivation of BRDF parameters. Given that Australia is largely a flat continent and large extent cropped fields tend to be on flat topology for practical reasons of farm management, topography will generally not be an issue for fields meeting the above criteria. Using irrigated crops for study sites will tend to minimise impacts on vegetation cover that might otherwise be associated with weather events, e.g. cyclones, rain or droughts. Furthermore temporal comparisons between cropping years are likely to be consistent.

Vegetated surfaces meeting the criteria identified in this section can be considered homogeneous at each epoch but temporally heterogeneous, however with just two

features present, i.e. soil and crop in varying mixes. In addition, the transition between the bare soil and mature closed canopy should be smooth. Such study sites minimise issues of noise and spatial homogeneity. Cropped fields with the above characteristics provide study areas that enable the clearest possible distinction between the BRDF effects of bare soil and vegetation.

4.2   Study areas for a temporal transect of single species cropped fields

This chapter considers a temporal transect of a pixel from a single species cropped field in order to assist in the understanding of how BRDF effects can be used to assist with the characterisation of vegetation. Specifically, this chapter seeks to answer the first three research questions; do BRDF effects vary between bare soil and vegetation, which BRDF parameters correlate strongest with the cropping cycle and with vegetation indices? Considering the criteria for study areas indentified in section 4.1, section 4.2 introduces two study areas that meet these criteria. The locations of the two study areas, the nature and characteristics of crops grown and history obtained from property management are also discussed in section 4.2. Section 4.3 provides a summary of the MODIS BRDF data extracted for these fields, i.e. time series plots of vegetation indices, BRDF parameter weights and correlations between BRDF parameters. Finally, section 4.4 introduces a model to assist interpret the BRDF effects in order to answer research question 4, and the results from the application of this modelling will be discussed in section 4.4.

No fields were found that were sufficiently large that multiple neighbouring pixels could be used as study areas, e.g. to have 2 or more neighbouring pixels falling fully within the area of the field. For such to occur, fields meeting the criteria in section 4.1 would need to have areas of several square kilometres, i.e. these would be exceedingly large fields and unlikely to exist. Cropped fields that are 1 km^2 in area and represent the minimum management unit are very large by farm management standards and are not common. However, two sites have been identified that meet the criteria identified in section 4.1; they being cotton grown in South West Queensland and sugar cane grown in Northern Queensland, Australia. The use of different crop types not only allows consideration of the BRDF effects between soil and crop but also between crop varieties. The location,

an overview of the crop and information obtained from property management will be discussed in section 4.2 for the two study areas.

4.2.1 Cotton and wheat grown at Cubbie Station, SW Queensland

Cubbie Station comprises approximately 93,000 hectares and is located near St George in South West Queensland. The total enterprise is large employing more than 50 staff directly and a further 120 contract staff. The prime business is irrigated cropping of cotton, wheat, sorghum, sunflowers, barley, chickpea and corn. Further details can be found at their web site http://www.cubbie.com.au. The location of Cubbie Station is shown in Figure 4.1 being Lat 27° 41'S and Long 148° 03'E.
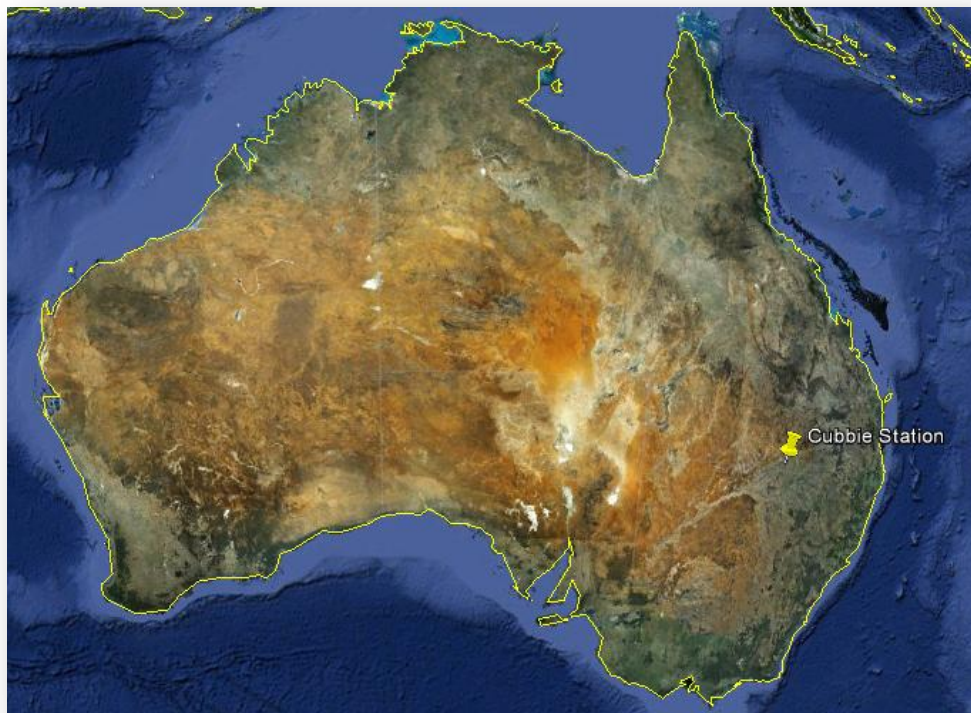
Figure 4.1 – Location of Cubbie Station (Source : Google Earth)

Three fields at Cubbie Station have been identified that have a continuous and well defined cropping history over the past 10 years. These fields are designated by property management as fields 2, 3, 7. Partial information about two additional fields designated

10 and 13 has also been obtained. The location of these fields on Cubbie Station is shown in Figure 4.2.

Figure 4.2 – Location of study areas/fields at Cubbie Station. The red square represents the size of a MODIS 500-m pixel. (Source : Google Earth)

Table 4.3 shows a summary of the cropping history for fields 2, 3 and 7 at Cubbie Station. In addition to crop planting and harvest dates, Cubbie Station also provided dates for cultivation, fertilisation, herbicidal spraying and stubble removal activities performed on these fields.

Table 4.3 – Cropping History Summary

Year/Field	2 (160 ha)	3 (146 ha)	7 (147 ha)
2000	Cotton planted 27/9/2000, harvested 10-20/3 2001	Cotton planted 26/9/2000, harvested 10-20/3/2001	Cotton planted 29/9/2000, harvested 10-20/3/2001
2001	Cotton planted 10/10/2001, harvested 25/3 – 5/4 2002	Cotton planted 5/10/2001, harvested 25/3 – 5/4/2002	Cotton planted 16/10/2001, harvested 25/3 – 5/4/2002
2002	Fallow	Fallow	Fallow
2003	Fallow	Fallow	Fallow
2004	Cotton planted	Cotton planted	Cotton planted

Year/Field	2 (160 ha)	3 (146 ha)	7 (147 ha)
	6/10/2004, harvested 20-28/3 2005	27/9/2004, harvested 20-28/3/2005	28/9/2004, harvested 20-28/3/2005
2005	Cotton planted 5/10/2005, harvested 28/3/2006	Cotton planted 1/10/2005, harvested 3/4/2006	Cotton planted 3/10/2005, harvested 31/3/2006
2006	Fallow	Fallow	Fallow
2007	Fallow	Fallow	Fallow
2008	Wheat planted 24/6/2008, harvested 1-9/12/2008	Wheat planted 24/6/2008, harvested 27/11/2008	Wheat planted 26/6/2008, harvested 1/12/2008
2009	Cotton planted 1/10/2009, harvested 21/4/2010	Cotton planted 1/10/2009, harvested 23/4/2010	Cotton planted 5/10/2009, harvested 27/4/2010
2010	Cotton Planned	Cotton Planned	Cotton Planned

Figure 4.4 - In a clockwise direction from the top left, shows the densification of cotton

from planting to a mature crop

(source : http://cottonaustralia.com.au/)

Cotton Australia (http://cottonaustralia.com.au/) is the peak body representing the cotton growing industry and provides general information about the cultivation of cotton which is summarised here. Cotton is planted in rows on raised beds that allow for drainage. Whilst the width between rows may vary (narrower rows allowing greater crop density), Cubbie Station adopts a 1-m standard. Cotton is planted from seed in the spring and takes between 4 and 14 days for seedlings to appear. Cotton plants mature over the summer months and grow to between 1 – 1.5-m in height. In late summer and autumn, the crop is sprayed with defoliant prior to harvesting. Following harvest the stubble is removed by being ploughed back into the soil. The soil is cultivated and sprayed for weeds during fallow years and spraying may be continued in the early months after the crop has been planted until the crop density prohibits machinery access between the rows. Figure 4.4 shows the characteristic densification of a cotton crop from when seedlings first appear through the bare soil, through to a mature crop where soil is no longer visible.

4.2.2   Sugar cane grown by Davco Farming in Northern Queensland

Davco Farming is an irrigated sugar cane farming business located 24 km west of Ayr in North Queensland and has been growing sugar cane since 1987. The location of the property is shown in Figure 4.5, being Lat 19° 41'S and Long 147° 14'E. Davco Farming provides background information about their operations on their web site (http://davcofarming.com/). The property includes a number of fields greater than 1 km^2 in area that are managed as a single management unit. Cropping history was provided for field 1 as shown in Table 4.7 with advice that the fields 2 and 3 had similar practises (i.e. managed as a single unit) although harvest dates were not known. These specific fields on the property are identified in Figure 4.6. It can be seen in Figure 4.6 that many of the neighbouring fields are 'patch work' in appearance which indicates that they represent several smaller management units, although their sole crop remains sugar cane.
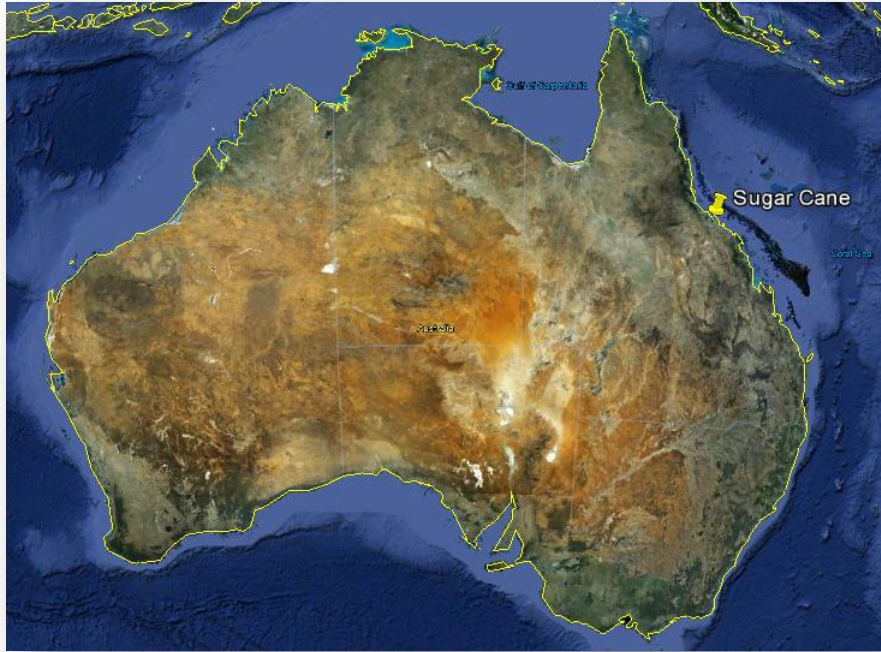
Figure 4.5 – Location of the sugar cane study area at Davco Farming.

(Source : Google Earth)
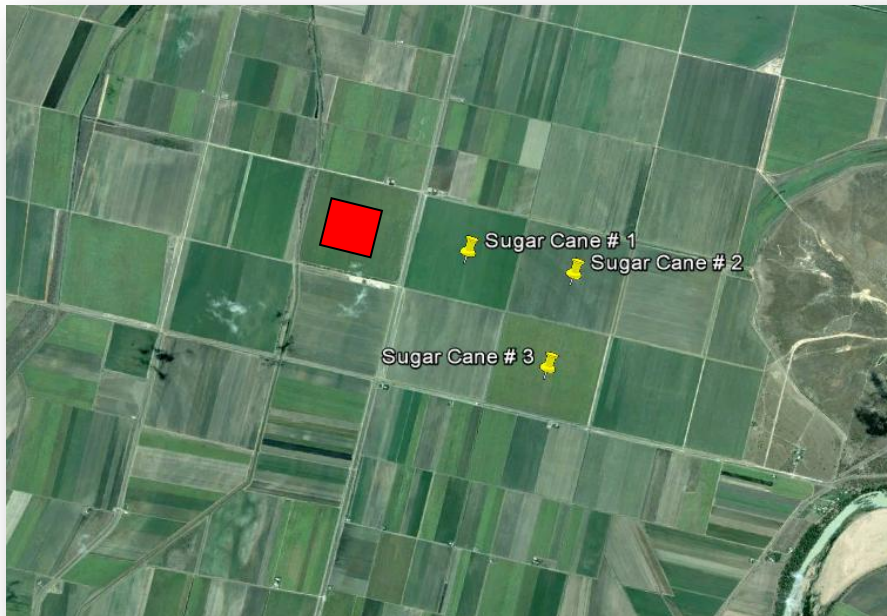
Figure 4.6 – Davco Farming sugar cane fields designated 1, 2 and 3 used as study areas. The

red square represents a MODIS 500-m pixel. (Source : Google Earth)

Table 4.7 – Summary of cane cropping history for Davco Farming field 1

Year	Field 1 (110.17 h.a)
2000	-
2001	-
2002	-
2003	-
2004	Planted March/April 2004
2005	Harvested June 2005
2006	Harvested June 2006
2007	(partial harvest)
2008	(partial harvest)
2009	Harvested 5-12/8/2009
2010	Ploughed out October 2010

The Cane Growers Association (http://www.canegrowers.com.au/) is the peak body in Australia representing sugar cane growers and provides general information about sugar cane cultivation via their web site which is summarised here. Sugar cane is grown in Australia in the coast plains from Northern Queensland to Northern New South Wales. Sugar cane is grown by replanting fully grown cane stalks that are cut into lengths about 40 cm in length called "setts". After a few weeks new shoots grow from buds on the joints of the setts. Up to 12 stalks grow from each sett, forming what is known as a stool of sugar cane. The crop typically takes 9 -16 months to grown in Queensland and up to 24 months in southern regions which are cooler. A mature crop grows to between 2 and 4-m in height. The crop is harvested from the base of the plant along the rows and cane leaf litter is discarded on the field to assist minimise soil erosion, moisture loss and suppresses weeds. Typically, a cropping cycle comprises one planting and several regrowth (ratoon) crops, i.e. the cane is allowed to naturally regrow after harvesting. Yields from successive ratoons tend to diminish until the field is ploughed out and replanted again from newly planted setts. Figure 4.8 illustrates two stages of crop cycle, i.e. shortly after planting where the crop rows are evident though to harvest at maturity.
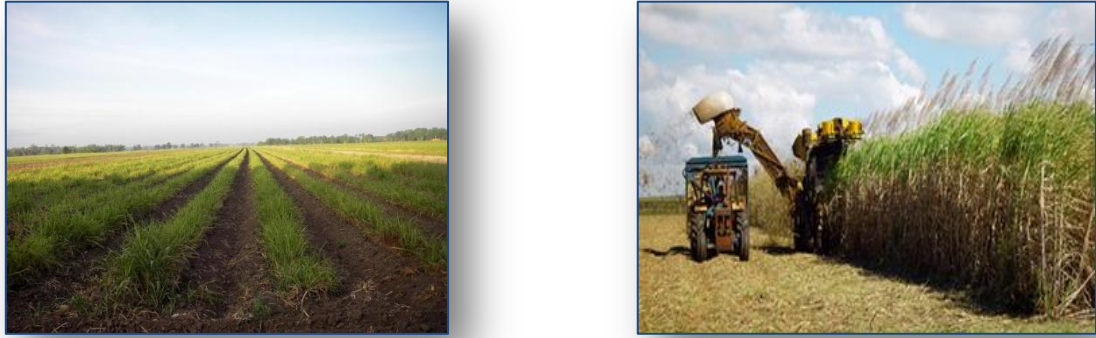
Figure 4.8 – Two stages of cane crop growth (Source :

http://www.bing.com/images/search?q=pictures+of+sugar+cane+growing&FORM=IGRE

&qpvt=pictures+of+sugar+cane+growing#)

4.2.3   Confirmation of study areas homogeneity

To provide further validation of the homogeneity of these study areas, a requirement discussed in section 4.1, data has been obtained from the Australian National Carbon Accounting System (NCAS) for a sample period. The Australian NCAS was developed by the Department of Climate Change (formerly the Australian Greenhouse Office). The NCAS is a multi-temporal dataset derived from Landsat Multispectral Scanner (MSS), Thematic Mapper (TM) and Enhanced Thematic Mapper Plus (ETM+) data and re-sampled to a spatial resolution of 25 metres (Furby et al., 2009); (Farmer et al., 2011). The higher spatial resolution of the NCAS data and validations done in support of this dataset make it a benchmark standard for comparison purposes, i.e. the NCAS dataset may be considered a best available dataset. The NCAS dataset is distributed through Geoscience Australia and more details of the product can be found on their web site (www.ga.gov.au).

Normalised Difference Vegetation Index (NDVI) has been derived from the NCAS dataset for the two study area which are shown in Figure 4.9. (NDVI will be discussed in section 4.3.1.) Absolute values for NDVI derived from NCAS dataset are not specifically relevant or intended for comparison to MODIS data. However, the higher resolution NCAS dataset is able to show that NDVI is generally evenly distributed within respective fields, which supports the spatial homogeneity requirement identified in section 4.1. It can be

observed that field 3 at Cubbie Station appears at little more variable than fields 2 and 7 but less variable than many of the surrounding fields.
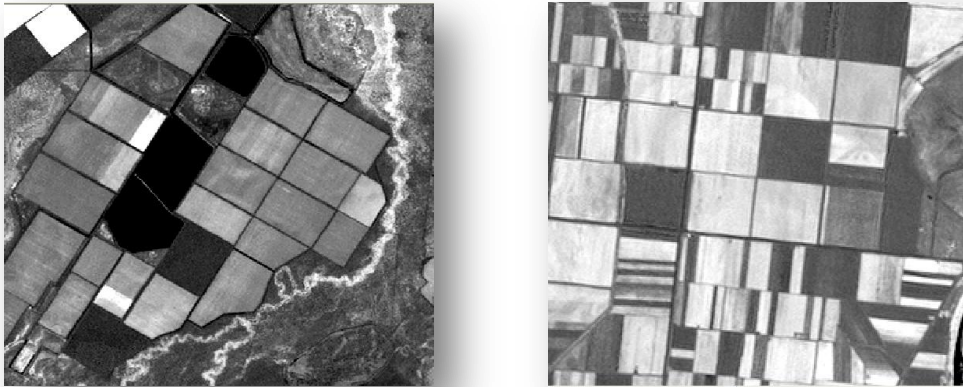
Figure 4.9 – NDVI (derived from NCAS dataset) shown as a grey scale for Cubbie Station (Left) and Davco Farming (right). Cubbie Station mosaic complied between 27/2 – 19/4/2005 (l5atm_2005_AGO_sh55_ne_geo.ers). Davco Farming mosaic complied between 17/7 – 11/8/2004 (l5atm_2004_AGO_se55_se_geo.ers).

Each of the fields described above can be represented by a single (MODIS 500-m) pixel based upon Latitude and Longitude coordinates at the centre of the field. For the respective fields, pixels were extracted for the 10 years between March 2000 and March 2010 representing 463 (8 day interval) epochs.

4.3   Vegetation indices, BRDF parameter and their correlations

Section 4.3 is partitioned into two subsections. Section 4.3.1 contains time series plots for two vegetation indices and time series plots for individual BRDF parameter weights representing a field from each of the two study areas. Section 4.3.2 examines the correlations between BRDF parameter weights and the correlations between the BRDF parameter weights and vegetation indices. Section 4.3 concludes with a summary analysis of both time series and correlation plots.

A small number of epochs contained no data/filler values. Where this occurred, it tended to be for all data for that epoch. Values were interpolated between the previous and next epoch.

4.3.1 Time series plots of vegetation indices and BRDF parameter weights

Molecules in a typical green plant have evolved to absorb wavelengths of EMR in the visible region of the spectrum efficiently. This supports the plants food-making processes via photosynthesis. Chlorophyll *a* and *b* are most important in absorbing blue wavelengths of EMR (approximately 0.45um) and red wavelengths of EMR (approximately 0.65um), with relatively lower absorption and higher reflectance for green wavelengths of EMR (approximately 0.55um), which causes healthy vegetation to appear green. In a typically healthy green leaf, the near infrared reflectance increases dramatically in the region from 0.7 to 1.2um. Plants have adapted to either reflect or transmit (and be reflected by lower leaves) these near infrared wavelengths of EMR and thus avoid their absorption which may lead to the plant becoming too warm. The inverse relationship between reflectance in visible light (particularly at red wavelengths of EMR) and near infrared wavelengths of EMR are related to plant biomass and stress and are the basis of many vegetation indices (Tucker, 1979); (Bannari et al., 1995); (Jensen, 2007); (Sabins, 1997).

Vegetation indices are dimensionless, radiometric measures that indicate the relative abundance and activity of green vegetation, including leaf-area-index (LAI), percentage green cover, chlorophyll content, green biomass, and absorbed photosynthetically active radiation (APAR). Two vegetation indices that are considered sufficiently significant to have derived products in the MODIS product suite (i.e. MOD13Q1) are the Normalised Difference Vegetation Index (NDVI) and Enhanced Vegetation Index (EVI) (Justice et al., 1998). Figures 4.10 and 4.11 show NDVI and EVI, derived here directly from MODIS's Nadir BRDF Adjusted Reflectance (NBAR) (MCD43A4) product and defined as:

$$\text{NDVI} = \frac{R_2 - R_1}{R_1 + R_2} \qquad\qquad (19)$$

$$\text{EVI} = 2.5\left(\frac{R_2 - R_1}{R_2 + C_1 R_1 - C_2 R_3 + L}\right) \qquad\qquad (20)$$

Where R_1 is NBAR MODIS band 1 (red),

   R_2 is NBAR MODIS band 2 (near infrared),

   R_3 is NBAR MODIS band 3 (blue), and

   C_1, C_2 and L are empirically determined values of 6.0, 7.5 and 1.0 respectively

The saturation of NDVI at high leaf areas and its sensitivity to soil is a disadvantage associated with NDVI. EVI was developed by the MODIS Land Discipline Group for use with MODIS data and is a modification of NDVI with a soil adjustment factor. EVI has also improved sensitivity in high biomass landscapes (Jensen, 2007, Justice et al., 1998).
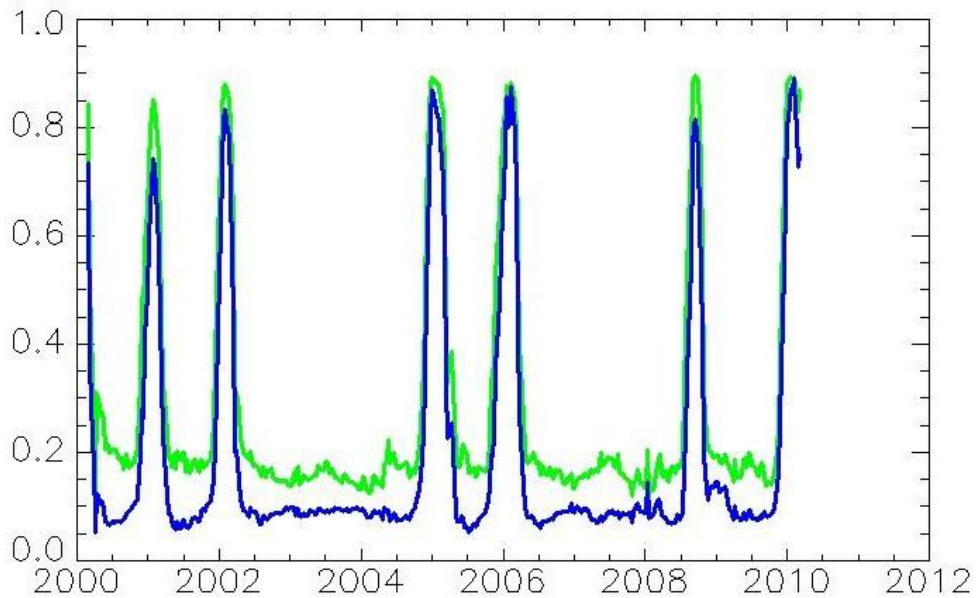

Figure 4.10 – NBAR NDVI (green) and NBAR EVI (blue) on the y-axis for field 7 at Cubbie Station against time on the x-axis.
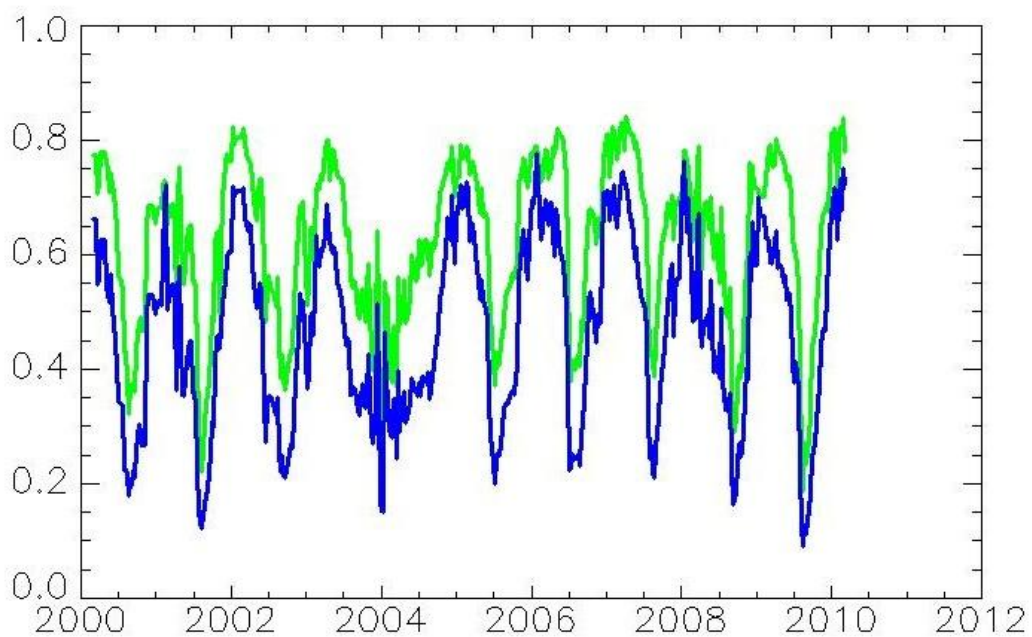

Figure 4.11 – NBAR NDVI (green) and NBAR EVI (blue) on the y-axis for Davco field 1 against time on the x-axis

Some comments can be made from the NDVI and EVI time series plots:

The vegetation indices correlate very well to the cropping cycles for respective fields as advised by property management. This provides a common sense check between MODIS data and property management records. Furthermore, it suggests that vegetation indices can be used validly as a metric describing the cropping cycle and are able to distinguishing between soil and crop for the study areas.

The cotton/wheat grown at Cubbie Station has a clearer profile of the cropping cycle than sugar cane grown at Davco Farming. This is reasonably be attributed to nature of the crop management, i.e. stubble is ploughed out to bare soil after the harvesting where sugar cane is naturally allowed to regrow after harvesting.

The "peaks" and "troughs" in the vegetation indices associated with the crop cycles are relatively consistent in magnitude between years which should support consistency in intra-year comparisons of BRDF parameters.

The wheat crop grown at Cubbie Station in 2008 has a similar NDVI and EVI profile to the cotton crop grown in other years and is indistinguishable other than via the slightly shorter temporal presence of the crop.

The replanting of the sugar cane crop in 2004 is distinguishable from the regrowth crops in other years. In 2008 the sugar cane crop appears as though it has been partially harvested or subjected to a staggered harvest.

For the other fields at Cubbie Station identified above and Davco Farming fields 2 and 3, very similar time series plots were apparent, i.e. the cropping cycle was clearly evident and matched farm management records where available.

The MODIS MCD43 product includes quality flags to indicate if there were quality issues in the BRDF inversion process, e.g. cloud cover reducing the number of observations included in the inversion. Adverse quality issues can be handled in one of three ways. Firstly, adverse quality issues can be ignored, and the archetypical default values provided by the MCD43 product used in such instances. Secondly, values can be interpolated between the last epoch that had no adverse quality issues and the next epoch with no adverse quality issues. This being similar to the process applied when there was missing data at an epoch. This approach may be suitable for when there are sequentially only a small number of epochs with quality issues, but may be less appropriate for extended periods. Thirdly, only consider ranges of continuous temporal

epochs which all have no adverse quality inversion issues. However, this approach will reduce the number of observations (from the maximum of 463) used in deriving summary statistics, e.g. correlations.

For the times series plots and the computed correlations below, adverse BRDF quality inversions were ignored and the archetypical values provided by the MODIS product used. Restricting time series plots and correlations to only consider temporal ranges where no adverse quality inversion issues were present did not appear to have a significant effect on plots or correlation results.

Figures 4.12 and 4.13 show time series plots of the individual BRDF parameter weights for cotton/wheat grown at Cubbie Station field 7 and for sugar cane at Davco Farming field 1, i.e. for each field, there are 21 separate plots being 7 bands x 3 parameter weights.

Isotropic Weight	Volumetric Weight	Geometric Weight
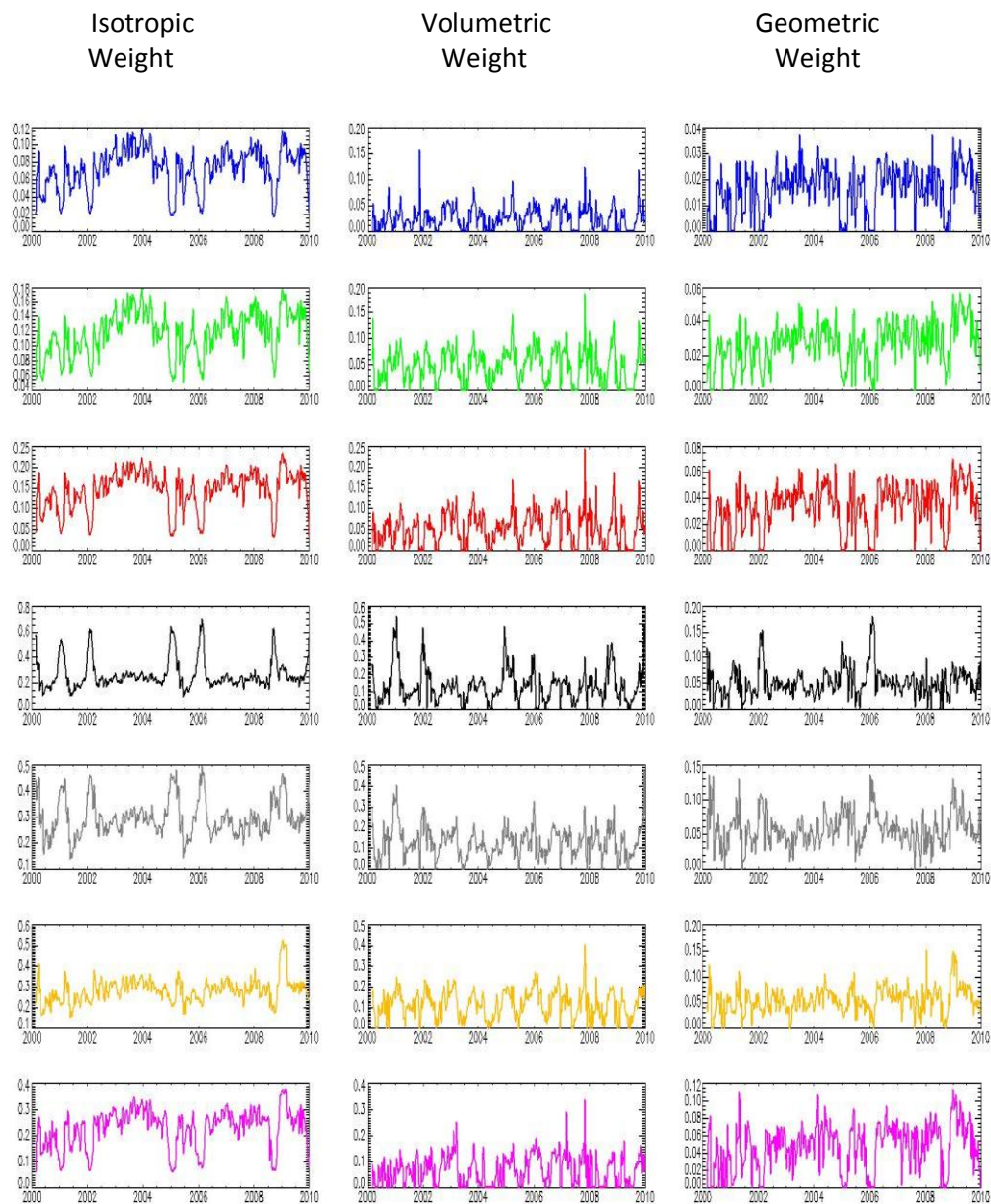
Figure 4.12 – Temporal profile of individual BRDF parameter weights (y-axis) for Cubbie Station field 7 plotted against time (x-axis). Left column being the isotropic parameter, centre column being volumetric (Ross-thick) parameter weight and the right column being the geometric (Li-Sparse) parameter weight. Blue being blue (band 3), green being green (band 4), red being red (band 1), black being NIR (band 2), grey being IR 1.24um (band 5), gold being IR 1.63um (band 6) and magenta being IR 2.13um (band 7). NB – the parameter weights on the y-axis are at different scales for each plot. This has been done to assist visualisation of the temporal variations associated with the parameter.

Isotropic
Weight

Volumetric
Weight

Geometric
Weight
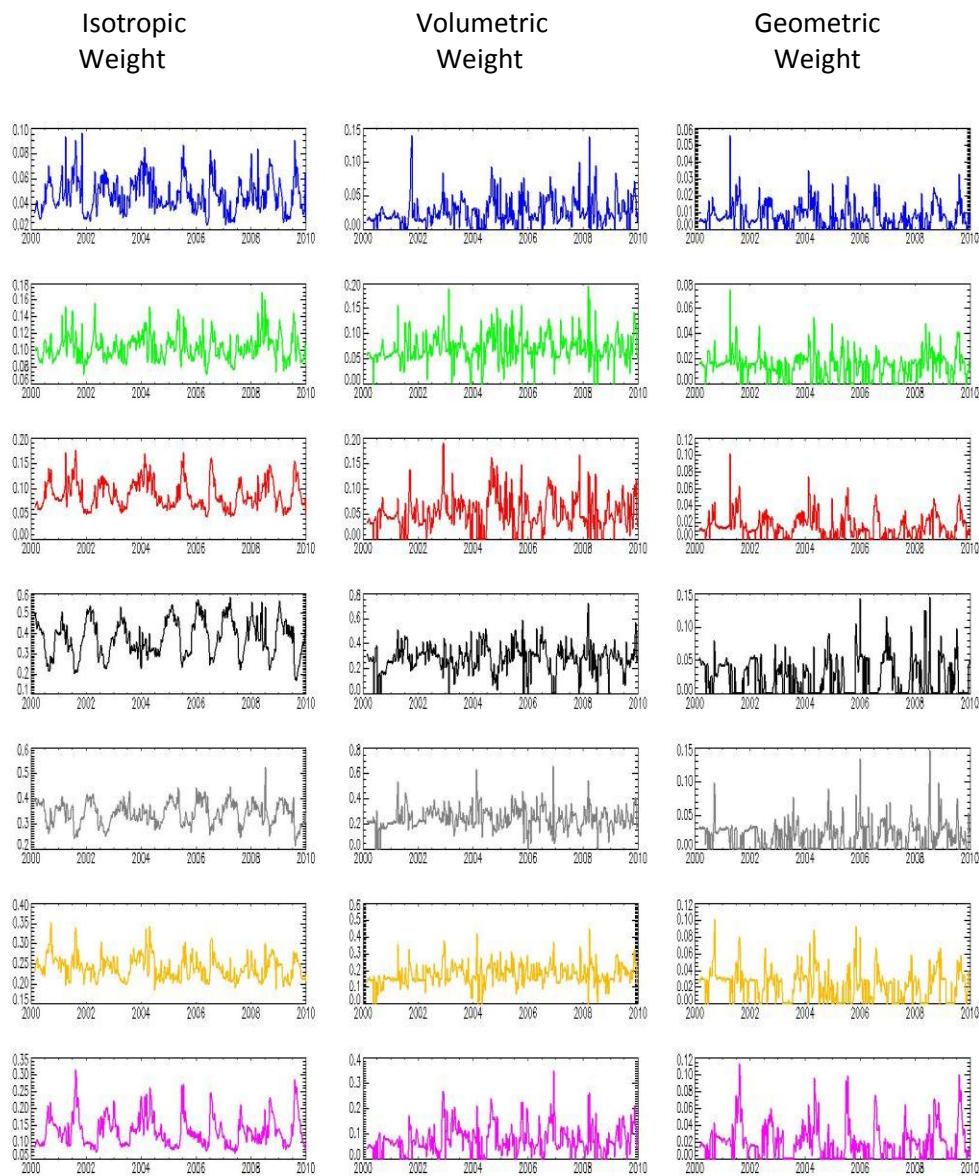
4.13 - Temporal profile of individual BRDF parameter weights (y-axis) for sugar cane at Davco Farming field 1 plotted against time (x-axis). The definition of the plots is the same as Figure 4.12.

The isotropic parameter weights (particularly for the near infrared band) display the strongest relationship with the cropping cycle. This is expected for the parameter with the strongest association to the spectral characteristics of vegetation. Isotropic parameters in neighbouring bands tend to display similar relationships. The volumetric and geometric weights appear noisy. For example, variability within these parameters is

apparent for periods of fallow soil on Cubbie Station field 7 although there is not the equivalent variability in NBAR NDVI or NBAR EVI during these same periods.

4.3.2 Correlations

As quantitative means of analysing the BRDF parameter weights, the correlation coefficient between each of the 21 BRDF parameter weights has been computed. Correlations are displayed as intensity matrices in Figures 4.14 and 4.15; being for Cubbie Station field 7 and Davco Farming field 1 respectively. Positive correlations are shown in the upper right triangle and negative correlations shown in the lower left triangle. Stronger correlations (positive or negative) are shown as brighter red through to zero correlations which are shown as black. Correlations between the variable and itself, (i.e. having correlations of 1), appear along the diagonal from top left to lower right.
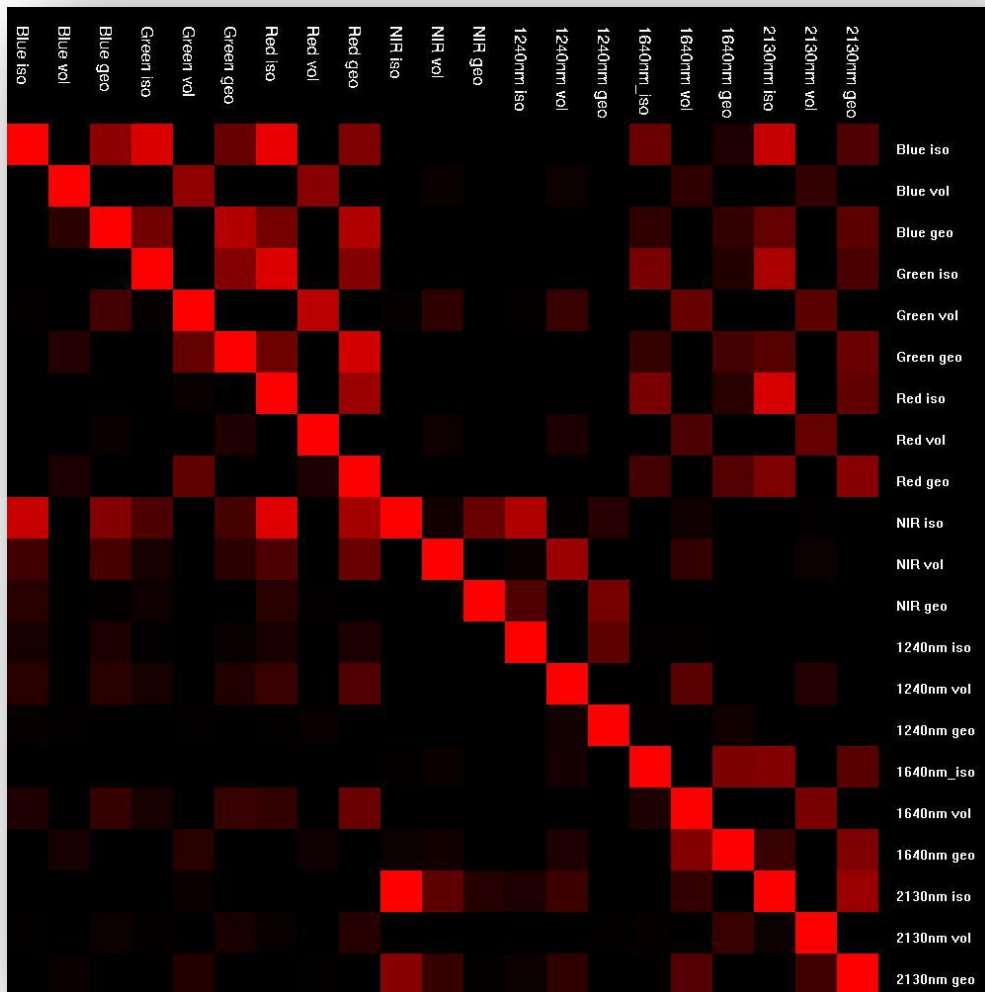
Figure 4.14 – Correlation between each of the 21 BRDF parameters, derived over 463 epochs for Cubbie Station field 7. Different intensity scales between positive and negative correlations are used to better assist visualisation.
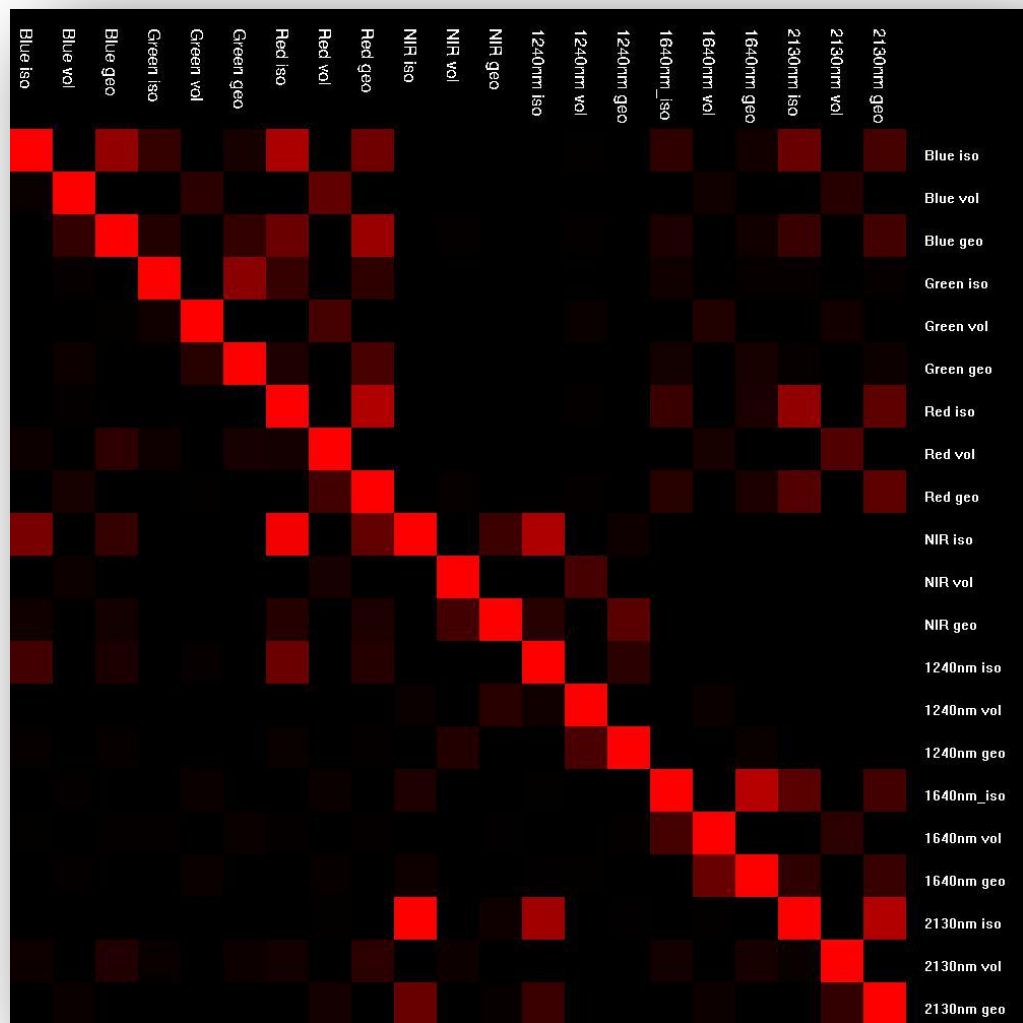
Figure 4.15 – Correlation between each of the 21 BRDF parameters, derived over 463 epochs for Davco Farming field 1. Definition of the plot is the same as Figure 4.14.

In addition to correlations between each of the 21 BRDF parameter weights, correlations between each of the BRDF parameter weights and NBAR NDVI have also be computed and are shown in Figure 4.16 for cotton/wheat grown at Cubbie Station field 7 and sugar cane grown at Davco Farming field 1. Strong correlations between BRDF parameters and NBAR NDVI can be considered a good indicator that the BRDF parameter is related to biomass, but conversely it can also be taken that the BRDF parameter represents minimal additional information than contained in spectral data.
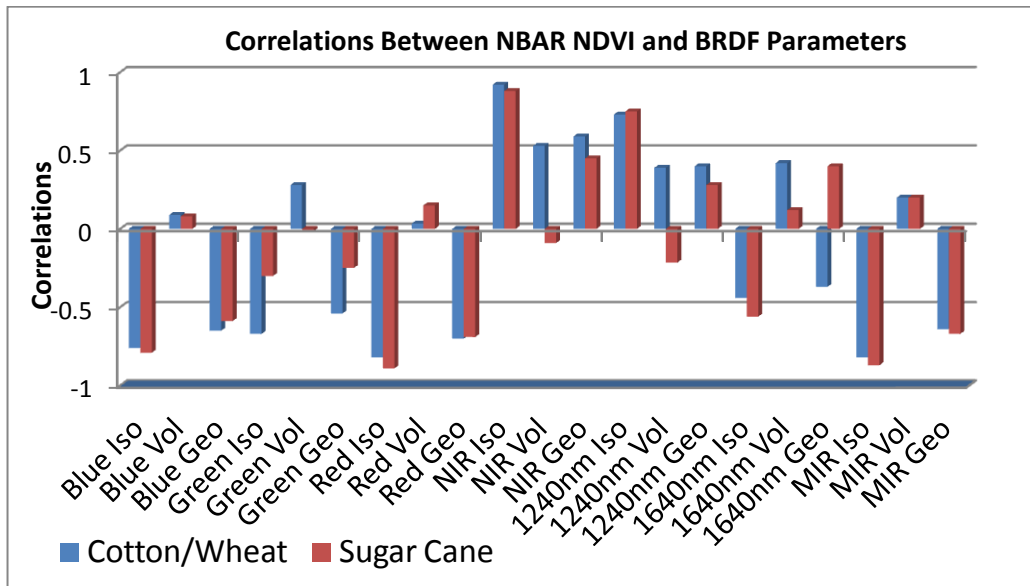
Figure 4.16 – Correlations between NBAR NDVI and the 21 individual BRDF parameter weights.

The isotropic parameter weights for both study areas exhibit the strongest correlation between each other (refer Figures 4.14 and 4.15) and the strongest correlation between the BRDF parameter weights and NBAR NDVI (refer Figure 4.16).

The correlations shown in Figure 4.16 between the isotropic parameter weights and NBAR NDVI are similar in magnitude and sign for both cotton/wheat and sugar cane crops. However, the correlations for all green band parameter weights exhibit significantly smaller values for sugar cane than for the cotton/wheat crop.

Across all bands, the geometric parameter weights generally demonstrate stronger correlations than the volumetric parameter weights.

In figure 4.16, cotton/wheat exhibits an inverse correlation with NBAR NDVI compared to sugar cane for the NIR volumetric parameter weight, for the 1240nm volumetric parameter and for the 1640nm geometric parameter.

To remove effects associated with isotropic parameter weights, the volumetric and geometric parameters have been divided by respective isotropic weights before computing the correlations with NBAR NDVI. The results of this are shown in Figure 4.17, noting that the correlations for the isotropic parameters will be the same as displayed in Figure 4.16.
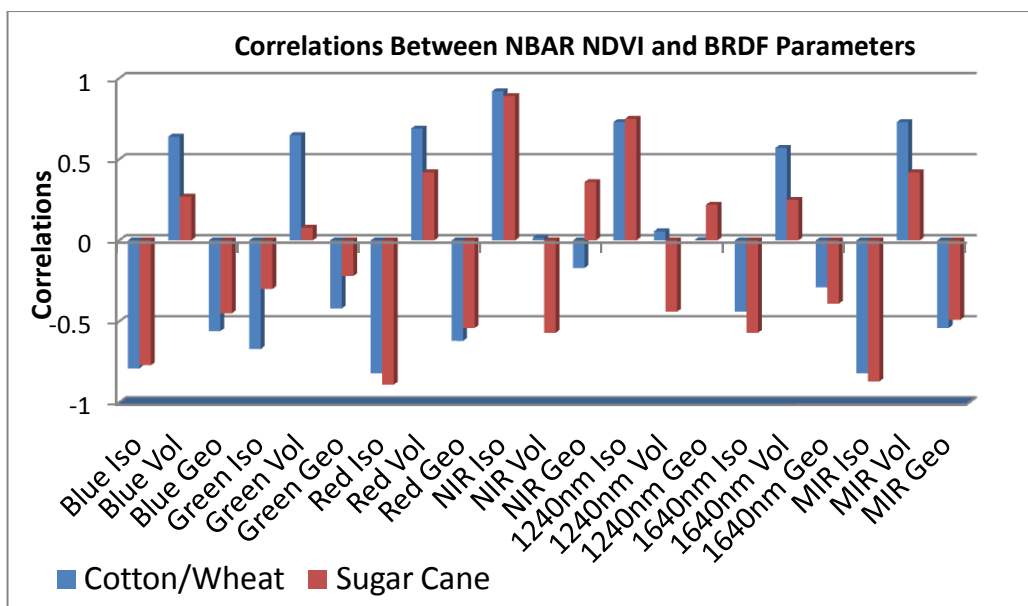
Figure 4.17 – Correlations between NBAR NDVI and the 21 individual BRDF parameter weights, where the volumetric and geometric weights have been divided by their respective isotropic parameter weight.

For both study areas, the correlations shown in Figures 4.16 and 4.17 for the volumetric and the geometric parameter weights in each band are the inverse of one another, i.e. if the volumetric parameter weight has a positive correlation with NBAR NDVI, then the geometric parameter in the same band exhibits a negative correlation with NBAR NDVI and vice versa.

Excluding the above mentioned relationships that appear associated with reflectance characteristics, it is difficult to interpret a simple, direct relationship between individual BRDF parameter weights with the crop cycle. Therefore, it does not appear possible to answer research question 1 – 3 using the approach described in this chapter.

4.4 Can BRDF effects be used to describe the height of vegetation?

Whilst still considering single species cropped fields as study sites, an alternative approach to interpreting BRDF effects may be to combine BRDF parameter weights, e.g. this being the basis of the Structural Scattering Index (SSI) which combines near infrared

volumetric and red geometric parameters (Gao et al., 2003). It is observed in Figures 4.16 and 4.17 that the infrared volumetric parameter appears to provide some distinction between cotton/wheat and sugar cane crops. An extension of this approach is to consider how vegetation indices vary with BRDF effects. This has been considered in previous studies (Huete, 1987, Tian et al., 2010). A benefit of considering vegetation indices is that they introduce an absolute measure into modelling. Where BRDF effects associated with an individual reflectance bands can only be considered as relative measures, vegetation indices may be directly interpreted with a physical characteristic, e.g. percentage of vegetation cover within a pixel. Consideration of BRDF effects on vegetation indices also has the benefit removing correlations between individual BRDF parameters and reduces the number of parameters being considered. Figure 4.18 shows NDVI and EVI profiles for Cubbie Station field 7 over eight consecutive months from planting in 2004 to harvesting of the cotton crop in 2005. NDVI and EVI profiles have been generated using MODIS BRDF model parameters of band 1 (red), band 2(nir) and band 3 (blue) for respective epochs multiplied by the kernel functions for view angles ranging from 0° to 60°, whilst setting solar and relative azimuth angles equal to 0°.

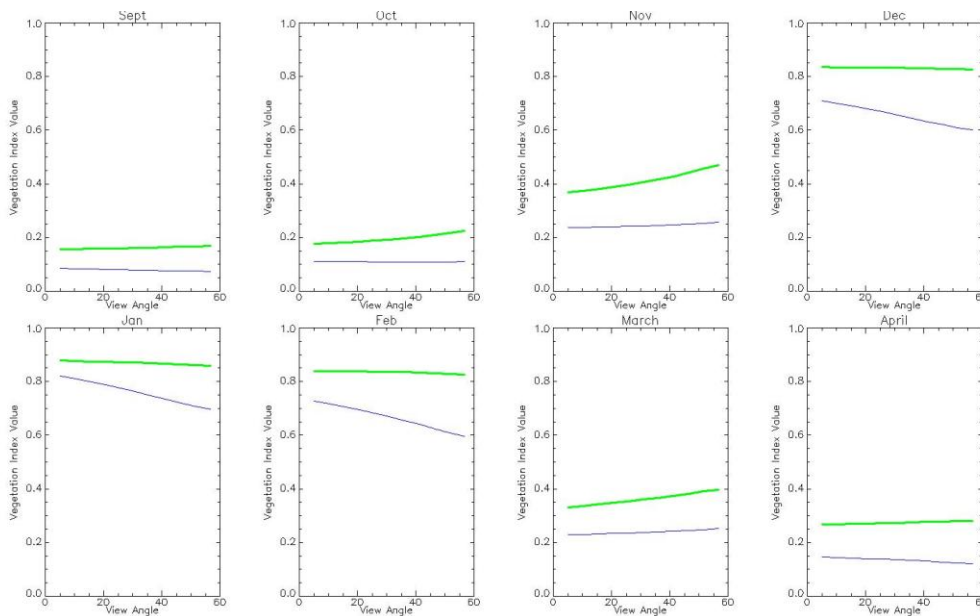Figure 4.18 – Profiles of NDVI (green) and EVI (blue) on the y-axis against view angle on the x-axis for Cubbie Station field 7 from mid-September 2004 to mid-April 2005. Illumination angle and relative azimuth have been set equal to 0°.

A general observation made from Figure 4.18 (also observed for other crop cycles on this field, for other fields at Cubbie Station and for sugar cane fields at Davco Farming) is that NDVI and EVI tend to exhibit an increasing profile with view angle for low crop densities and a decreasing profile with view angle for high crop densities. Rising profiles of NDVI with view angle for sparsely vegetated surfaces has previously been identified (Bannari et al., 1995) as have falling profiles with denser vegetation cover (Tian et al., 2010, Huete, 1987).

4.4.1 Introduction of a simple geometric optical model to re-express MODIS BRDF effects in terms of an alternative set of parameters

As a means of analysing BRDF effects associated with vegetation indices, the MODIS BRDF product (MCD43) can be used to forward model vegetation indices at various viewing and illumination geometries. These derived values for vegetation indices can be considered to be 'observations' which can in turn be modelled, i.e. a model for analysing the MODIS BRDF model. The re-modelling of derived values for vegetation indices can be considered a re-expression or re-casting of the MODIS BRDF as an alternate parameter set, i.e. principally the vegetation index being modelled. Furthermore, variability in viewing and illumination geometries can be controlled to simplify re-modelling, e.g. consideration of changes in the view zenith angle only. Given the reciprocity of the Ross-Thick-Li-Sparse model the same result will also achievable by interchanging the view angle with the illumination angle.

This re-modelling approach may be considered independent of the vegetation index being used, e.g. NDVI or EVI. However, plots as per 4.18 for vegetation indices against view angle, indicate that NDVI provided more consistent profiles, i.e. consistently having a rising profile when NDVI was low and a falling profile when NDVI was high. Given the wide spread use of NDVI, its relative simplicity and consideration that other indices (e.g. EVI) are enhancements of NDVI's fundamentals (i.e. reflectance differences between near infrared and red bands exhibited by vegetation), the focus hereafter is towards use of NDVI only in development of a model for quantifying changes in vegetation indices associated with view angle.

With the above considerations, a model is introduced that seeks to re-express MODIS BRDF in terms of an alternative set of parameters: $NDVI_{max}$ (being crop components),

NDVI $_{min}$ (being bare soil components), vegetation density and a height-to-width ratio of vegetation components. This approach seeks to answer the fourth research question; can BRDF effects be used to measure the height of vegetation?

4.4.2   Model formulation

A surface pixel on the cropped fields being studied can be considered to be a mix of soil components and crop canopy components. If a pixel is defined as having a dimensionless area of 1 (that is 1 x 1), a random distribution of vegetation prisms may be considered on the surface having dimensions d x d x (H x d) where; 'd' is a dimensionless value between 0 and 1 representing the length and width of the vegetation prism in the horizontal plane and 'H' is a dimensionless height-to-width ratio of the vegetation. Geometrically a height-to-width-ratio of 1 represents cubes of vegetation, values greater than 1 being taller elongated vegetation such as pine trees and values less than 1 being low and flat vegetation. This enables vegetation cover within the pixel to be defined as a fraction of the pixel's dimensions. The use of prism shaped objects to represent vegetation has the benefit of computational simplicity and the shape of protrusions should not be important with prisms having been used in past BRDF models (Roujean et al., 1992). Larger viewing angles will bring the vertical surface of the vegetation into view and obscure an area of soil.

Based on the geometry of these surfaces, an expression for changes in NDVI as a function of viewing angle can be described as the sum of the horizontal and vertical surface components. Visually the model is depicted by Figure 4.19 and mathematically the model is described by equations 21 – 23.
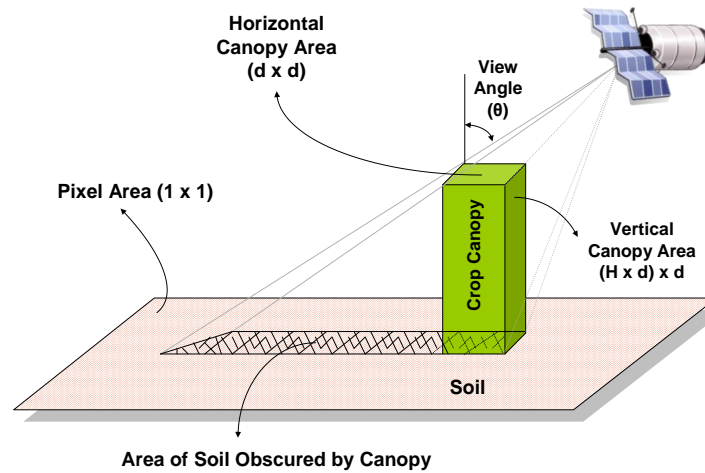
Figure 4.19 - A single 'prism' of vegetation is depicted on a flat surface of soil with an area of soil obscured via the vegetation prism based on the viewing geometry from the sensor.

$$\text{NDVI}_{\text{Total}}(\theta) = \text{NDVI}_{\text{horizontal}}(\theta) + \text{NDVI}_{\text{vertical}}(\theta) \qquad (21)$$

$$\text{NDVI}_{\text{horizontal}}(\theta) = D\,\text{NDVI}_{\text{max}}(\theta) + (1\text{-}D)\,\text{NDVI}_{\text{min}}(\theta) \qquad (22)$$

$$\text{NDVI}_{\text{vertical}}(\theta) = H\,D\,\tan(\theta)\left[\text{NDVI}_{\text{max}}(\theta) - \text{NDVI}_{\text{min}}(\theta)\right] \qquad (23)$$

where: H is the height-to-width ratio of vegetation prisms

(which may be constrained to an arbitrary range),

D = $\sum d^2$ and represents the density of vegetation cover with a

range $0 \leq D \leq 1$, with value 0 being for all soil and no

vegetation and 1 being for complete vegetation coverage

and no soil, and

` θ is the viewing angle.

Values for the two model parameters (H and D) can be determined by numerical methods that provide a best fit (lowest root mean squared error (RMSE)) between the model and NDVI derived from the MODIS BRDF parameters across a range of viewing angles 0° to 57°; this being at the upper limit of MODIS's angular sampling (Wanner et al., 1997). In this approach, values for NDVI derived from the MODIS BRDF

representation across a range of viewing angles effectively become 'observations'. The model represents a semi-empirical approach replacing the wavelength-specific isotropic, volumetric and geometric parameters within the MODIS BRDF model with the alternate parameter set of : NDVI $_{max}$ NDVI $_{min}$ vegetation density (D) and a height-to-width ratio (H) which offer more direct interpretation of vegetation structure. The model may also be thought of as a mixing model, where the end members are soil and crop and the determination of the component quantities are based upon both spectral and angular effects measured in NDVI.

Equation (22) is the linear combination of soil and canopy NDVI response on the horizontal plane for the case when only the horizontal vegetation surfaces are present (H = 0). Equation (23) is the additional contribution that the vertical plane of the canopy makes to the observed NDVI response as a function of the viewing angle including the additional soil obscuration relative to the H = 0 case. The total NDVI response (i.e. Equation (21)), is therefore the sum of Equations (22) and (23).

It is implicit that when bare soil only is present NDVI (θ) = NDVI $_{min}$ (θ). For this to occur the crop density must be zero (i.e. D = 0). Similarly, when no soil layer is present, meaning a closed canopy exists (i.e. D = 1) then NDVI (θ) = NDVI $_{max}$ (θ) and will do so if and only if H = 0. If viewed at zenith (i.e. θ = 0) or the vegetation has no vertical profile (i.e. H = 0), then Equation (23) becomes zero.

Increases in NDVI (θ) as a consequence of higher viewing angles will be greatest when:

- the NDVI difference between canopy and soil is greatest, and/or
- the height-to-width ratio of the vegetation is large (that is larger values of H), and/or
- the density of vegetation is higher (that is larger values of D).

4.4.3 Model assumptions

The model assumes that the vegetation prisms do not overlap from the satellite viewpoint and neglects shadows. The model assumes that the NDVI response from the horizontal and vertical surfaces of the vegetation prisms are the same and that all variations in NDVI, as a function of view angle changes, are associated with geometric considerations only, i.e. vegetation obscuration of the soil layer. The model also assumes that the NDVI response from the vegetation (and the lower soil layer) is

constant across the crop growth cycle and all changes in NDVI observed are due to the density and height of vegetation over the soil layer. It is implicit that the model does not include any consideration of an understory layer (i.e. the effects of a third layer which is additional to the soil and crop layers) on the NDVI response.

The model is independent of the number of vegetation prisms present within a pixel. For a given density (D) and height-to-width ratio (H), a single large prism of vegetation (as depicted in Figure 4.19) or a large number of small prisms (as would realistically be expected) will make visible the same surface areas of soil and crop at the same viewing angle. The volume that the vegetation occupies as a fraction of the pixel's dimensions in 3-D space will be a function of the number of individual vegetation prisms present in a pixel, density (D) and the height-to-width ratio (H), however consideration of the number of individual vegetation prisms can be ignored, as the resulting vegetation volume is not considered within this model. The formation of this model is also valid for vegetation grown in rows (i.e. horizontally elongated prisms) provided all views are considered to have been made perpendicular to the orientation of the rows.

Application of this model is based on changes in viewing angle only. Values for the solar zenith angle and relative azimuth must be determined and fixed when generating 'observations' using MODIS's BRDF representation which the model seeks to interpret. In application of this model a 0° solar zenith angle and a 0° relative azimuth have been used. Using 0° for the solar zenith angle will make consideration of the relative azimuth selected irrelevant. A 0° solar zenith angle and 0° viewing angle will represent the 'hot spot', which is the angularly narrow reflectance enhancement around the antisolar direction. The range of viewing angles from 0° to 57° used for deriving the model parameters represents consistent viewing away from the hot spot without the need to consider viewing angles that will cross the hot spot. This enables the model to remain relatively simple in its formation. The MODIS BRDF representation is reciprocal between solar and viewing angle, therefore whilst a 0° solar zenith angle may not have been observed by MODIS in deriving the BRDF representation, a 0° viewing angle may have been observed and will yield the same BRDF result. Past studies have shown that linear BRDF models can be stably extrapolated to zero zenith angles (Lucht, 2000). Furthermore, as the study sites are 19° and 28° south Latitude respectively, with an annual cropping cycle during the summer months, large solar zenith angles are avoided and shadowing effects minimised. A solar zenith angle of 0° eliminates shadow effects in the model.

4.4.4   Determination of model end-members

In applying this model, a representative characteristic profile for NDVI $_{min}$ (θ) being bare soil and NDVI $_{max}$ (θ) being crop canopy must first be determined. This acknowledges that soil and crop canopy end-members also have angular profiles that vary with viewing angle. The NDVI response of end member states (i.e. NDVI $_{crop/max}$ (θ) and NDVI $_{soil/min}$ (θ)) are obtained from observations of bare soil prior to planting and the mature crop canopy prior to harvest respectively. The characteristic profiles for soil and vegetation canopy should be uniquely defined for each field and may vary according to the soil type, the amount of vegetation mass, stubble, leaf littler and weeds present in the soil layer and vary for the mature canopy for different crops varieties. A simple expression that provides a good fit for soils, crop canopies for all the study sites was found in the form of:

NDVI $_{min}$ (θ) = a $_{min}$ + b $_{min}$ tan (θ)   (24)

NDVI $_{max}$ (θ) = a $_{max}$ + b $_{max}$ tan (θ)   (25)

Values for 'a' and 'b' can be derived that provide a best fit (minimum RMSE) for representative samples of soil and crop derived from the MCD43 product across a range of viewing angles. The end-member angular signatures expressed by Equations (24) and Equations (25) can be substituted into Equations (21-23). Expressions in other forms (e.g. a polynomial in θ) may equally provide good characteristic profiles for soil and crop canopy. There is no specific interpretation implied from the parameters or in the structure of Equations (24) and (25), other than the constant 'a' represents the isotropic NDVI response from the soil and crop respectively. The format of equations 24 and 25 allows the model algorithm for determination of best fit parameters to be applied iteratively, i.e. firstly to derived end-member profiles for soil and crop canopy and secondly with substituted end-member profiles in equations 21 – 23 applied to epochs where there exist soil and crop in varying mixes.

Several observations have been made at epochs that are representative of bare soil and crop and the derived end-member results averaged. Fields on Cubbie Station appeared

less variable that sugar cane fields, which is reasonably explained by the clearer cropping cycle associated with cotton and wheat compared to sugar cane. The resulting end member profiles are shown in Table 4.20.

Table 4.20 – End Member Profiles

Field	NDVI - End Member Profiles
Cubbie Field 2	$0.1 + 0.06 \tan(\theta)$ – soil $0.9 - 0.039 \tan(\theta)$ - crop
Cubbie Field 7	$0.1 + 0.046 \tan(\theta)$ – soil $0.9 - 0.039 \tan(\theta)$ - crop
Davco field 1	$0.21 + 0.135 \tan(\theta)$ – soil $0.85 + 0.0 \tan(\theta)$ - crop
Davco field 3	$0.21 + 0.15 \tan(\theta)$ – soil $0.86 + 0.0 \tan(\theta)$ - crop

Cubbie Station fields 2 and 7 have cotton grown in each cropping cycle expect for 2008 when wheat was planted in both fields. In deriving the crop canopy end-member no discernible difference could be found between cotton and wheat.
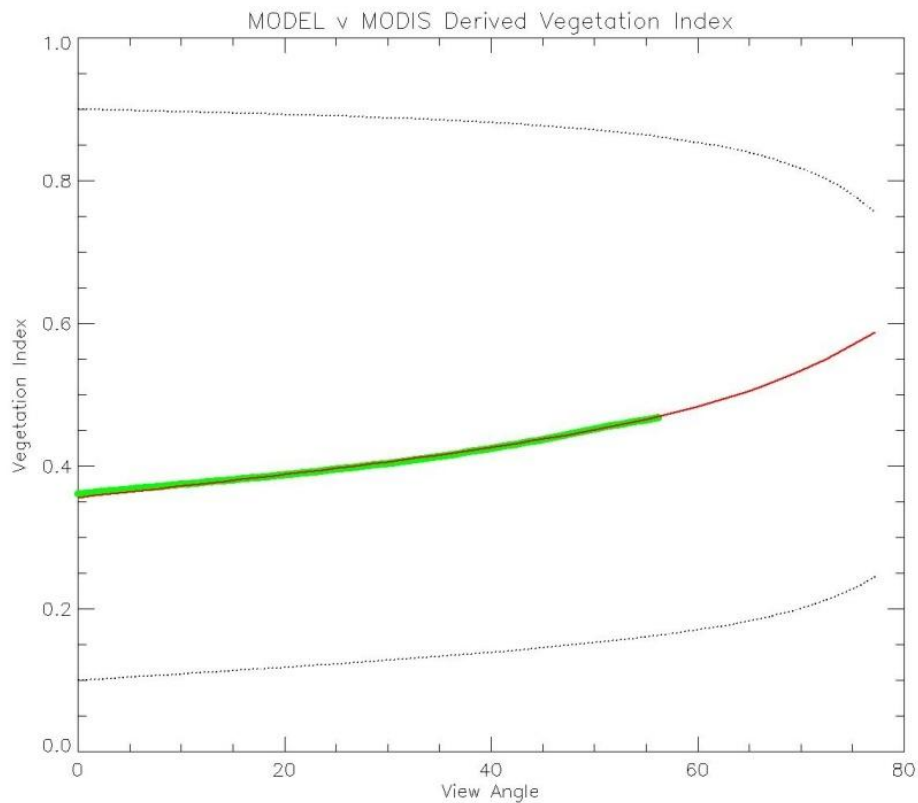
Figure 4.21 - Graphical representation of the model.

Figure 4.21 shows a graphical consideration of the model at a single epoch. The green line is the NDVI profile derived from the MODIS BRDF parameters for cotton grown at Cubbie Station field 7 approximately seven week after planting. The red line is the derived model (i.e. best fit to the green line). For a given density of vegetation, larger positive values for the height-to-width ratio will be associated with stepper rising profile of NDVI with view angle. Similarly, for a given density of vegetation, larger negative values for the height-to-width ratio will be associated with a sharper falling profile of NDVI with view angle. Independent of the density of vegetation, zero height-to-width ratios will generate a flat NDVI profile, i.e. NDIV is invariant to view angle. The lower dashed black line is the characteristic end member NDVI profile for bare soil and the upper dashed black line is the characteristic end member NDVI profile for mature cotton. The viewing angle has been extended to 80° to enable better visualisation of the respective curves shapes.

4.4.5   Results

The model has been applied to Cubbie Station fields 2 and 7 and Davco Farming fields 1 and 3. Whilst detailed cropping records for Davco Farming field 3 were not available, Davco property managers indicated a similar cropping practise to that of field 1 which is supported by time series plots of vegetation indices for this field. Cubbie Station fields 2 and 7 have cotton grown each cropping cycle except for 2008 when wheat was grown. No discernible difference could be found between the cotton and wheat crops in the results discussed below.

The results are considered in three ways, firstly how well the model fits MODIS BRDF modelling, time series plots of the two derived parameters and finally scatter plots of the two derived parameters against NBAR NDVI.

Goodness of fit

The two parameters derived from this model can be considered a re-expression of the MODIS BRDF model as an alternate parameter set that offer a more direct interpretation. For the derived values to have validity, the model must provide a good fit to NDVI derived from MODIS BRDF modelling across the same range of view angles. To test this, two quantities are considered, i.e. the root mean squared error (RMSE) and the correlation between NDVI derived from the model (when the best fit parameters are substituted back) and NDVI derived from MODIS BRDF modelling across the same range of view angles. The results for the four fields are shown in Figure 4.22. To enable visualisation at the same scale as the correlations, the RMSE have been multiplied by a factor of 100.
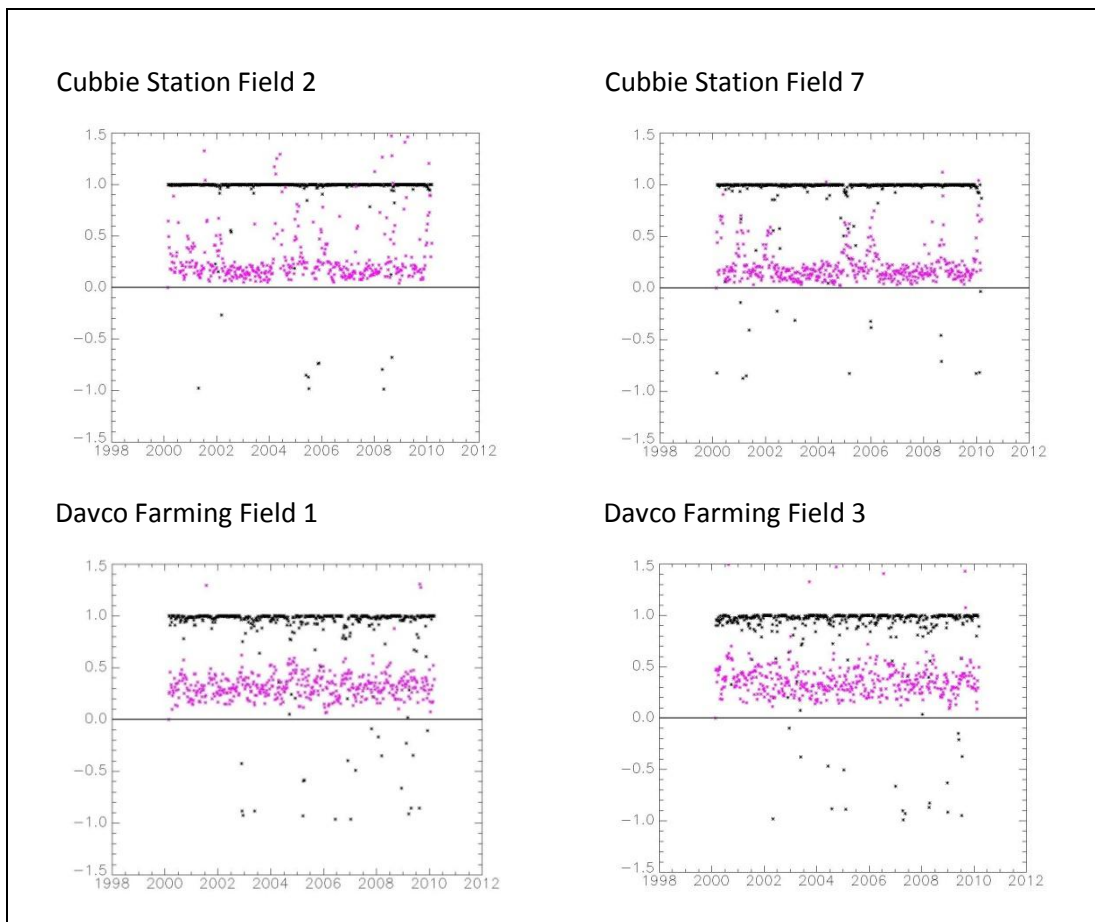
Figure 4.22 – Time series plots of correlations (black) and RMSE x 100 (magenta) on the
y-axis against time on the x-axis

Correlations and RMSE for all four fields indicate that the model provides a good and
consistent fit to MODIS BRDF modelling. Cubbie Station fields provide better results
than sugar cane fields at Davco Farming, i.e. correlations closer to 1 and having lower
RMSE. A discussed above, the fields at Cubbie Station exhibit a clearer and distinct
pattern associated with the cropping cycle than do the sugar cane fields at Davco
Farming. Furthermore, for the two Cubbie Station fields the RMSE appears related to
the cropping cycle, i.e. larger RMSE when the crop is present, but still these values
appear generally less than 0.005 NDVI.

Time series plots of derived parameters

The study areas were selected because they are most likely to provide clear distinction between bare soil and crop canopy, and temporal changes in BRDF effects could be related to the crop cycle. With the same consideration, the two parameters derived from the model (i.e. density and height-to-width ratio) have been plotted against time. These are shown in Figure 4.23.
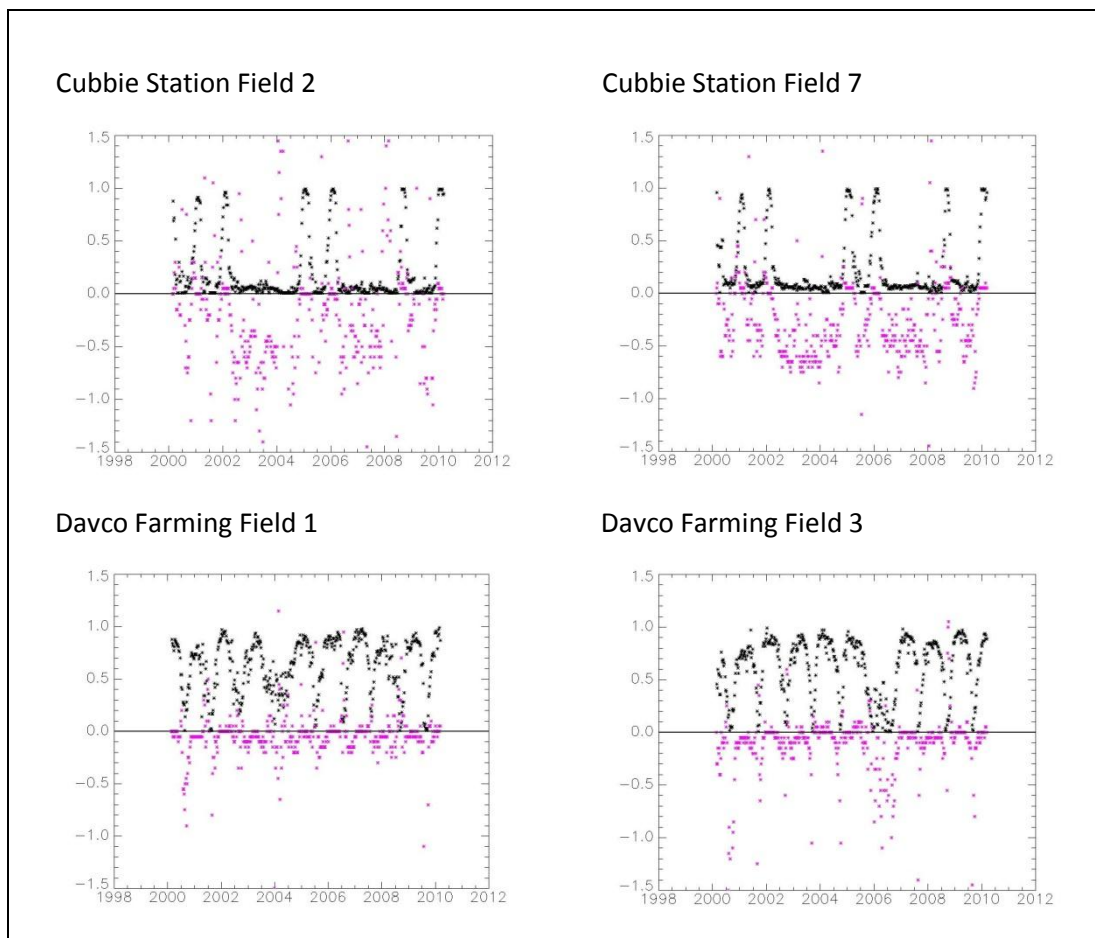
Figure 4.23 – Time series plots of derived height-to-width ratio (magenta) and density (black)

The derived density appears to well match the cropping cycle, i.e. alternating between 0 (i.e. bare soil) and 1 (i.e. mature crop canopy). The height-to-width ratio (which was

allowed to range between -5 and +5) shows significant more variability, including a predominance of negative values.

Scatter plots of derived parameters against NBAR NDVI

A third means of analysing the result is to plot the two derived parameters against NBAR NDVI which may be considered to represent biomass. Scatter plots for the two derived parameters against NBAR NDVI are shown in Figure 4.24 and 4.25.
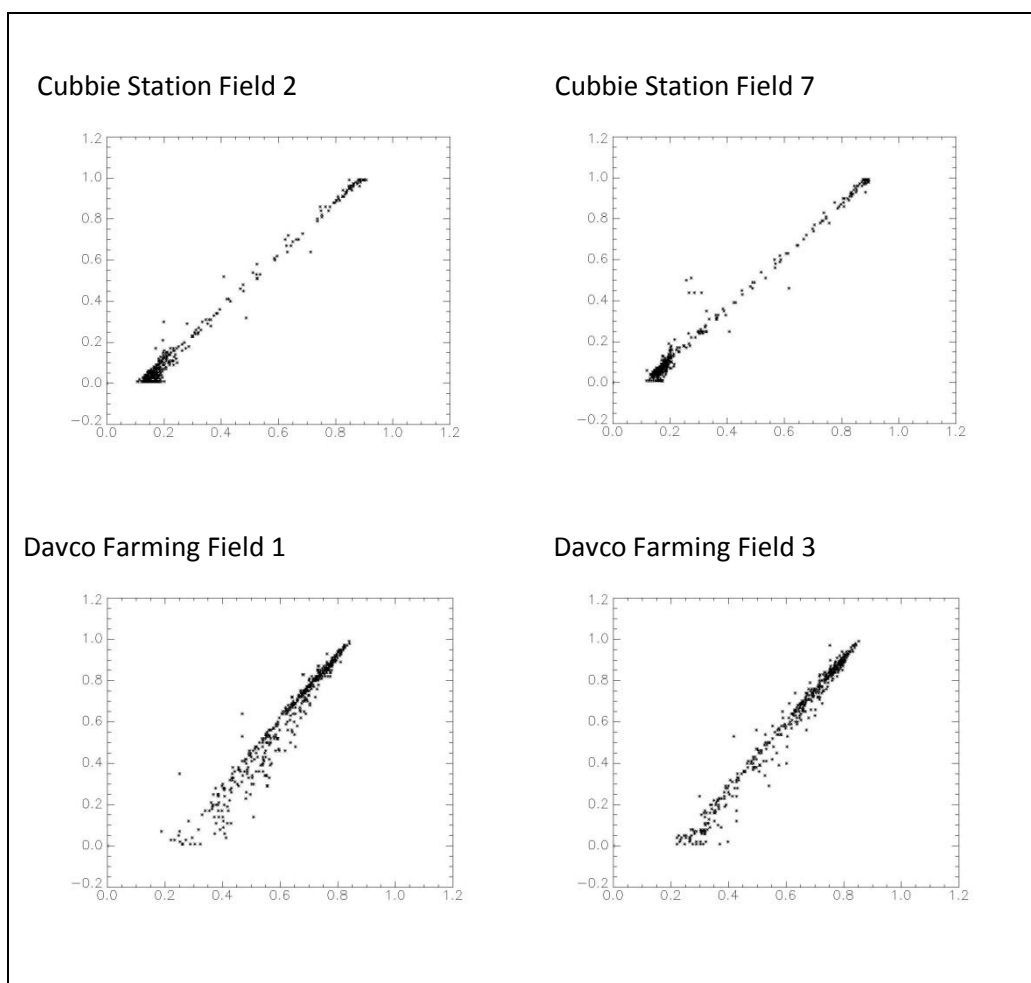
Figure 4.24 – Derived density (y-axis) against NBAR NDVI (x-axis)

The derived density parameter provides a very good linear relationship with NBAR NDVI (correlations > 0.97), effectively mapping NBAR NDVI onto density values in the range of

0 to 1. This strong relationship between derived density and NBAR NDVI is as expected.
Cubbie Station fields demonstrate a stronger relationship between the derived density
and NBAR NDVI than the Davco Farming fields, this being consistent with the time series
plots and the explanation given above.

Cubbie Station Field 2

Cubbie Station Field 7

Davco Farming Field 1

Davco Farming Field 3
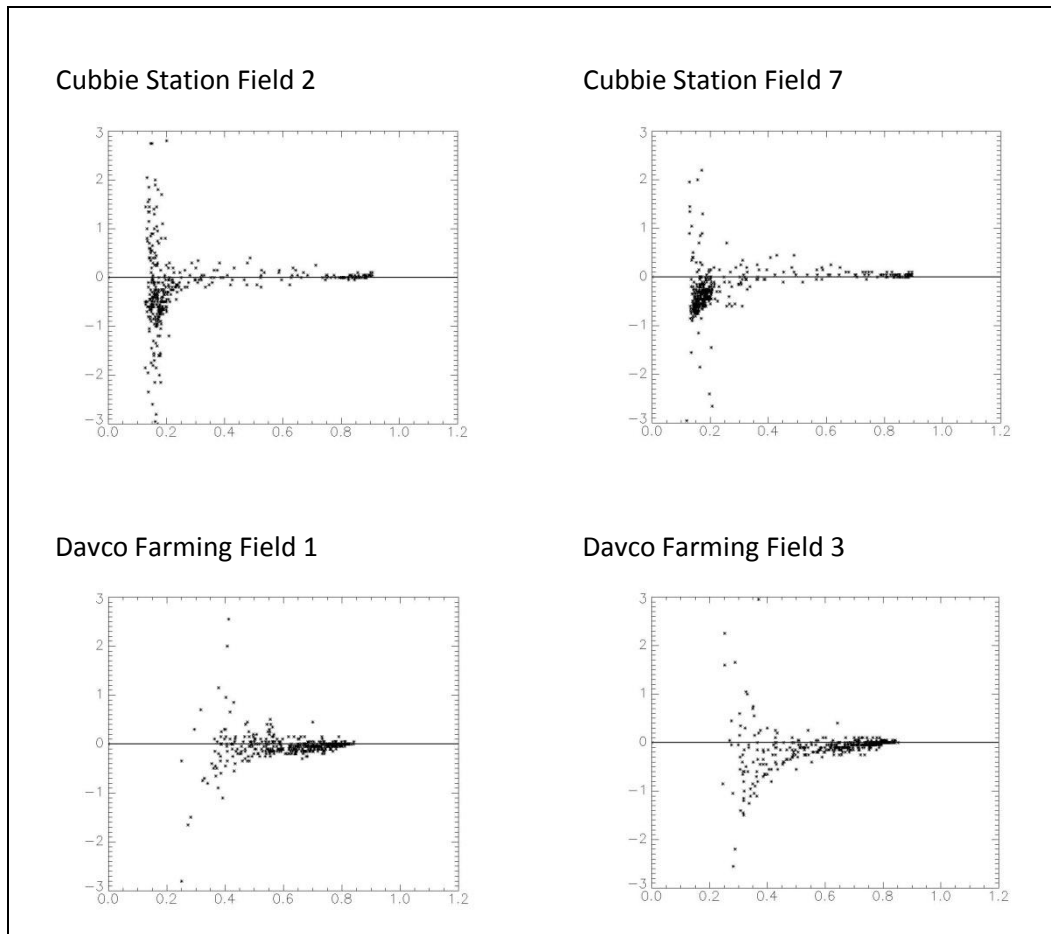
Figure 4.25 – Derived height-to-width ratio (y-axis) against NBAR NDVI (x-axis)

Perhaps the more significant derived variable is the height-to-width ratio, as this
parameter is more closely related to vertical structure of vegetation that is theoretically
the basis of BRDF modelling and related to research question 4. Figure 4.25 shows large
variances in the height-to-width ratio for low NBAR NDVI values and smaller variances
for high NBAR NDVI values. For higher NBAR NDVI values the height-to-width ratio
approaches zero, however for low vegetation densities a mean height-to-width ratio is
difficult to determine.

An explanation of the result for low NBAR NDVI values (i.e. densities approaching 0) is that the profile of NDVI as a function of view angle is required to approach the shape of the bare soil end member. This requires (by equation 22) that the vegetation density be constrained to values near 0. Therefore the derived height-to-width ratio must account for all the variability between the model and the bare soil end-member. It can also be stated that if no vegetation is present, determination of its height is meaningless.

At higher NBAR NDVI values (i.e. densities approaching 1), the profile of NDVI as a function of the view angle is required to approach the shape of the closed canopy end-member. This is only possible if equation 23 approaches 0. For equation 23 to approach zero and the density to approach 1, the derived height-to-width ratio must approach 0. It can also be stated that if there is a closed canopy, there can be no interpretation of height above an unseen layer of soil. Furthermore, as the model does not take into account mutual obscuration of vegetation components, vegetation densities greater than say 50% (D=0.5) will begin to appear as closed canopies at the upper range of MODIS viewing angles which may begin to influence the derived height-to-width values.

The derived height-to-width ratio provides consistent results with conditions theoretically expected by the model, but does not appear to provide interpretable results as the vegetation density approaches the upper or lower limits, i.e. approaching the end member states. Notwithstanding, the derived height-to-width ratio may still provide interpretable results when vegetation densities are between 10-50% coverage, i.e. where soil and crop elements are both present and mutual obscuration of vegetation components unlikely. Figure 4.26 shows the combined results for the four fields together in the one plot. For NBAR NDVI in the range of 0.3 to 0.5, the height-to-width ratio for sugar cane at Davco Farming appears greater in magnitude (positive and negative) than that of cotton/wheat crops at Cubbie Station. Whilst not strong, this difference in the height-to-width ratio may allow distinction between crop types with the same NBAR NDVI response.
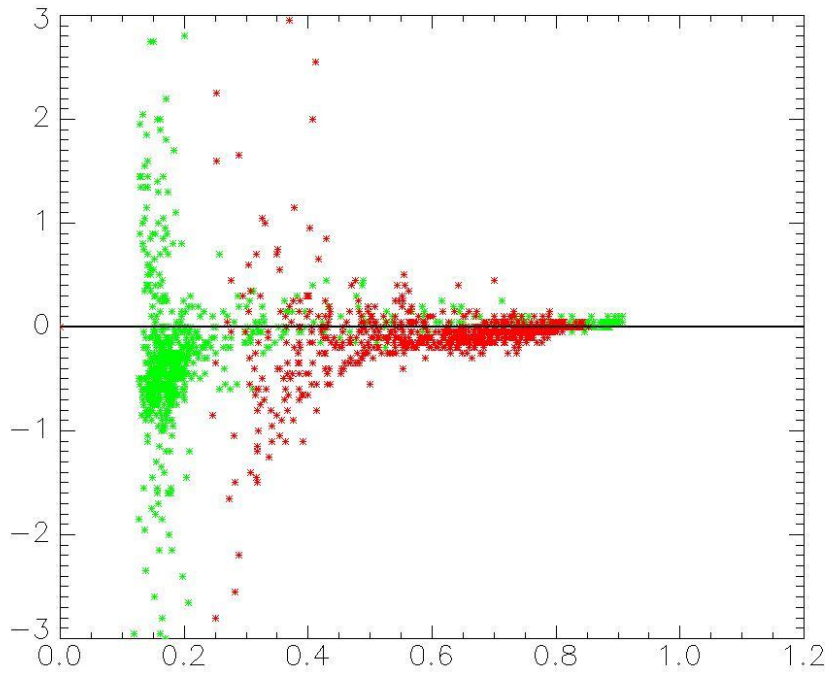
Figure 4.26 – Derived height-to-width ratio (y-axis) against NBAR NDVI (x-axis), Cubbie Station Fields 2 & 7 (green) and Davco Farming Fields 1 & 3 (red).

Issues associated with the results

The model (with derived best fit density and height-to-width ratios substituted) provides a good fit and therefore can be considered a valid re-expression of MODIS BRDF modelling. However, the derived parameters, especially the height-to-width ratio appear noisy and are difficult to interpret as intended by the model, i.e. as a measure of the height of the vegetation. There are three specific aspects from the application of this model that appear inconsistent or are particularly difficult to explain; the derived height-to-width ratio includes negative values, tends to be of a smaller magnitude than might be expected from physical geometric considerations, and finally the results appear insensitive to crop row orientations. Each of these aspects will be discussed separately below.

The model is based solely on geometric physical considerations where vegetation components are vertical protrusions on a flat soil layer. Therefore only positive derived height-to-width ratios are permissible if applying physical geometric considerations. Zero being the lowest permissible value for the derived height-to-width and interpreted as a three dimensionally flat surface. Values less than zero have no clear physical

interpretation. For very high or very low vegetation densities, the NDVI profile must approach that of the respective end member profiles, and negative values for the height-to-with ratio may be reasonably be excused in these extreme cases (refer previous discussion). However for vegetation densities in between these extremes, the large number of negative values across the range of NBAR NDVI values tends to suggest either excessive noise or additional explanation is needed.

Secondly, the derived height-to-width ratios appear smaller in magnitude than might be expected from a parameter describing physical structure of vegetation as intended by the model. For cotton, which is planted in rows one metre apart and with individual plants growing to just over a metre in height, a height-to-width ratio of 1 might be expected, i.e. plants being as high as they are wide. Derived values for the height-to-width ratio are significantly and consistently less than 1 and appear inconsistent with the physical description of vegetation as defined by the model. An assumption of the model is that for equal surface areas the NDVI response from the vertical and horizontal surfaces of vegetation prisms will be the same. The smaller than expected magnitude of the derived height-to-width ratio may be explained if the NDVI response from the vertical surface was less than for the horizontal surface for an equivalent area. However this consideration necessitates introducing additional assumptions or parameters to the model. With similar considerations, it might also be expected that for vegetation of a given density and height that NDVI would 'plateau' at a particular view angle, i.e. there will be no further increase in NDVI at larger view angles. The geometric explanation of this is that at a given density and height, vegetation no longer obscures the under layer of soil but will begin to obscure other vegetation components and appear as a closed canopy at that and any greater view angles. This is not what is observed. For example, in Figure 4.18 the plot for November shows NDVI of 0.4 at the nadir view which might correspond to approximately a 30% crop cover. The profile of this curve with view angle should be much steeper than what is observed, such that at a 60° view zenith angle the NDVI response should be approaching the NDVI response of a closed canopy. Considering the geometric nature of the model presented here, the view angle at which NDVI should 'plateau' can be determined as a function of the density and height-to-width ratio, which is depicted in Figure 4.27 and expressed by the equation 26.

In section 4.4.3 it was discussed that the model is independent of the number of vegetation prisms present within a pixel, i.e. modelling is equivalent for one large prism of vegetation or a large number of small vegetation prisms as only the surface areas are

being considered, not the volume the prisms create in a 3-D space. This similarly applies when determining the view angle at which NDVI can be expected to plateau, and it is more easily depicted with consideration of two neighbouring pixels, each containing a single prism or row of vegetation as shown in Figure 4.27. The red line in Figure 4.27 represents the minimum view angle at which mutual obscuration of vegetation will become apparent. For a given density and height of vegetation, NDVI should not increase further for larger view angles.

$$\theta° = \tan^{-1}\left(\frac{1-d}{Hd}\right) \tag{26}$$

Where: H is the height-to-width ratio of vegetation prisms,

d is the derived density, and

θ° is the zenith view angle at which mutual obscuration of the vegetation components will begin to occur, i.e. the surface will appear as a closed canopy.
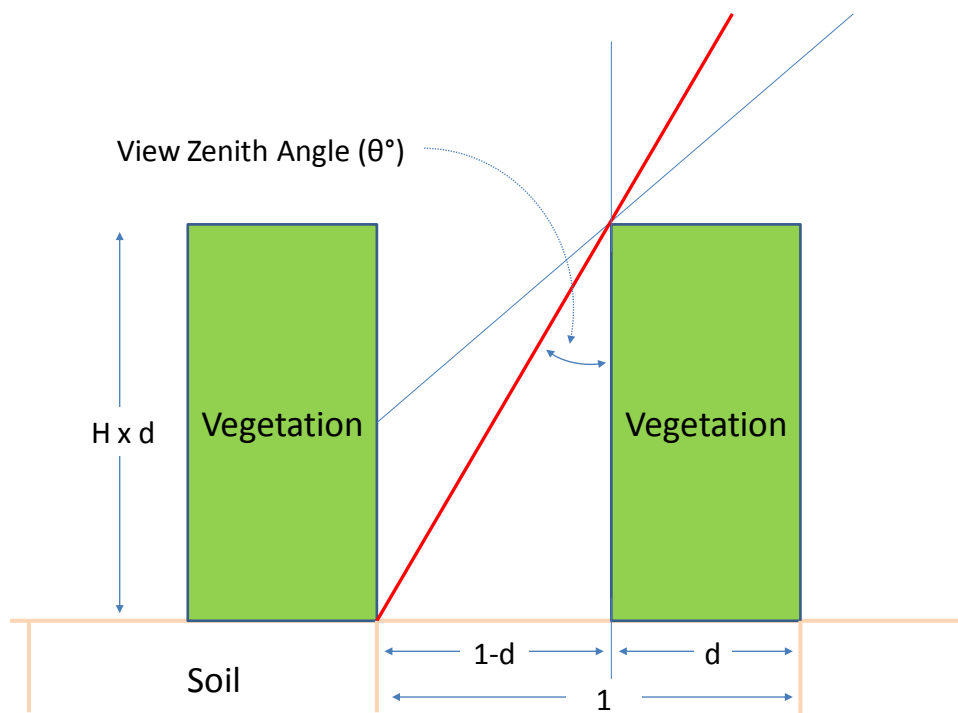
Figure 4.27 – Two neighbouring pixels, each with a single prism of vegetation depicting the derivation of equation 26.

Figure 4.28 shows that derived height-to-width ratio plotted against the derived vegetation density. The height-to-width ratio appears consistently smaller in magnitude

than might be expected if NDVI is to 'plateau' as expected where the physical geometry of the surface is the sole consideration.
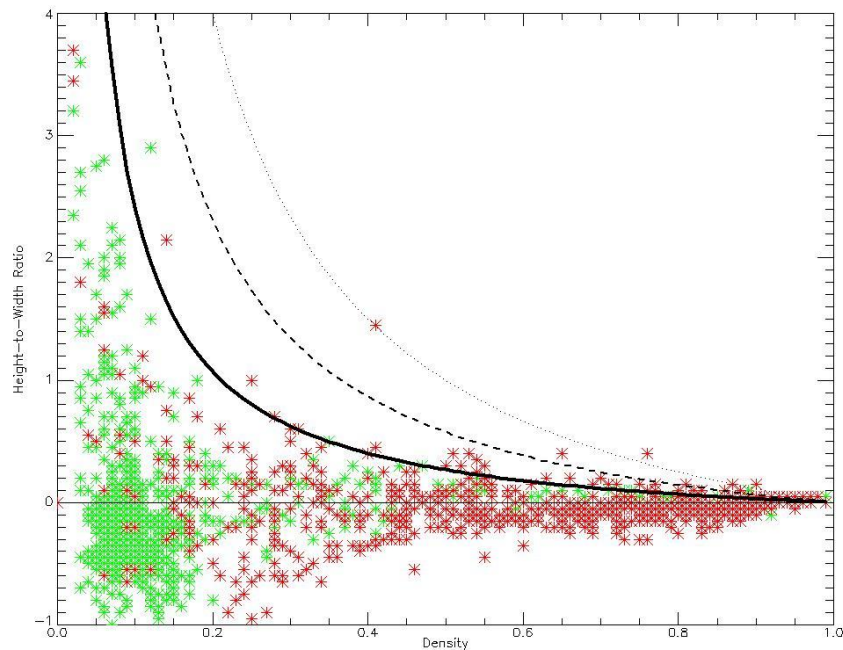
Figure 4.28 - Derived height-to-width ratio (y-axis) against density (x-axis) for cotton (green) and sugar cane (red). Curves are for 'plateau' view angles of 45° (dotted), 60° (dashed) and 75° (solid).

The final result from the model that is difficult to explain is that results appear insensitive to the row orientation of the crops. The MODIS BRDF parameters are derived on the assumption that the arrangement of surface scattering and shading elements is random with no preferred azimuth (Lucht et al., 2000). The model described here as a re-expression of MODIS BRDF is also derived on the assumption of randomly distributed objects or all views are made perpendicular to the direction of the crop rows. The cropped fields being studied are not random: they grow in rows as do nearly all planted crops. BRDF effects may therefore be expected to vary as a consequence of the absolute viewing azimuth used in deriving the MODIS BRDF representation: that is variations in the distribution of raw observations that are viewed along the rows compared to across the rows. It may be expected that if the crop row direction coincides with the view direction, there will be mutual obscuration of vegetation components rather than obscuration of the soil layer and therefore the NDVI response may appear invariant to view angle. The inclusion of a large number of views along the

rows within the MODIS BRDF inversion may therefore influence derived MODIS BRDF parameters and the results of the model described within the thesis for interpreting the MODIS BRDF product.

To determine if crop row orientations impact the derived height-to-width ratio, which is a re-expression of the MODIS BRDF model, two cotton fields at Cubbie Station with a SW – NE row orientation (i.e. fields 2 and 7) and two fields with a NW – SE row orientation (i.e. fields 10 and 13) have been included, giving crop row orientations of 90° to one another. End-member profiles for Cubbie Station fields 10 and 13 being as per table 4.29 and fields 2 and 7 being as per table 4.20.

Table 4.29 – End member profiles

Field	NDVI - End Member Profiles
Cubbie Field 10	$0.1 + 0.035 \tan(\theta)$ – soil $0.9 - 0.036 \tan(\theta)$ - crop
Cubbie Field 13	$0.1 + 0.05 \tan(\theta)$ – soil $0.9 - 0.038 \tan(\theta)$ - crop

If, for the inversion of the MODIS BRDF parameter weights a disproportionate number of views have been included that are along the rows for fields with one orientation, then a disproportionate number of views will have been made across the rows for fields with the opposite row orientation at the same epoch. If the crop's row orientation is contributing to variations in the BRDF effects, a bias in the height-to-width ratio for field pairs with the same orientation should be matched with the opposite bias for nearby field pairs with an orthogonal row orientation.
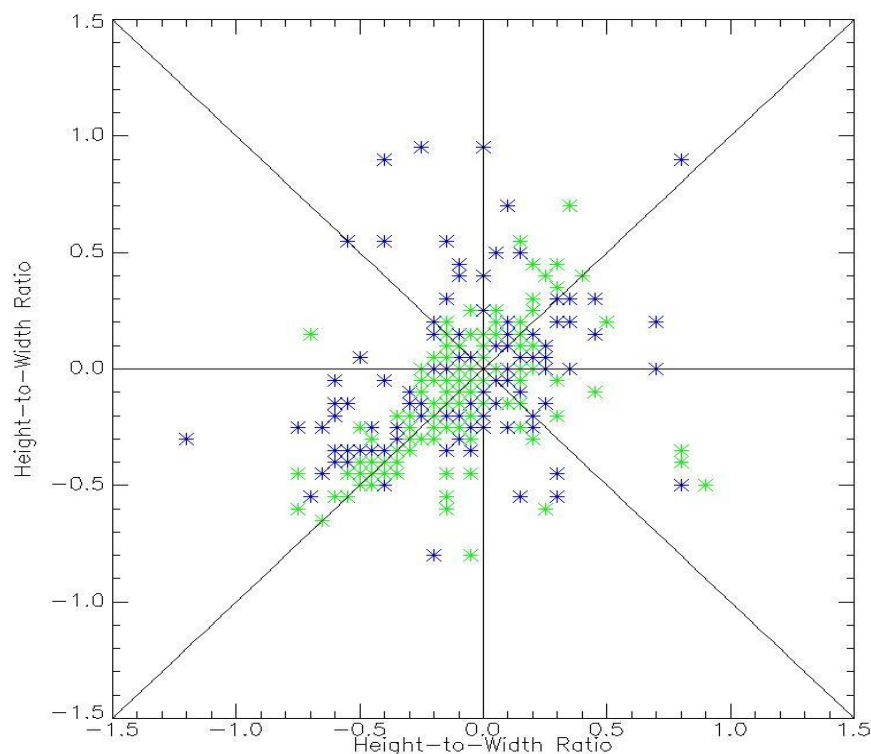
Figure 4.30 - Scatter plot of height-to-width ratios for cotton fields for the same epochs. The scatter plot includes all (6) permutations of two fields from the four available. Pairs of fields with the same crop row orientation are shown in green and fields with opposite orientations are shown in blue.

Only crop densities in the range of 10 - 50% are included within this scatter plot, because bare soil or a closed canopy are not considered to exhibit a row structure and/or would be impacted by mutual canopy obscuration.

Whilst not a strong relationship, Figure 4.30 shows a positive relationship clustering along the +45° or 1:1 relationship line irrespective of the orientation of the fields, indicating that row orientation effects are not a factor in variations in the height-to-width ratio. If effects associated with crop row orientations were an influence on MODIS BRDF modelling and the subsequently modelling described in this thesis, then positive height-to-width ratios for one orientation should be matched by negative height-to-width ratios for fields with the opposite row orientation, i.e. -45° relationship line. Furthermore, it follows from Figure 4.30 that row orientation effects are not related to negative height-to-width ratios, i.e. negative values for the derived height-to-width ratio do not appear the result of a disproportionate number of views that have been made along the direction of the crops' rows in determining MODS BRDF parameter weights.

4.5 Summary of results for a temporal transect of single species cropped fields

Consideration of a temporal transect on the fields with the criteria identified in section 4.1 should provide the best possible opportunity to examine how BRDF effects vary between bare soil and vegetation. In this approach, issues associated with noise and homogeneity are well considered and minimised. Temporal changes in BRDF parameters can be identified by their association with a field's known cropping cycle. However, a clear simple relationship between the MODIS BRDF parameter weights and the cropping cycle was not evident.

A simple semi-empirical geometric optical model was introduced to re-express BRDF effects in terms of the NDVI response from soil, the NDVI response from the vegetation canopy, the density and a height-to-width ratio of vegetation components. The model, (with best fit parameters substituted) provided a very good fit to MODIS BRDF modelling and is therefore considered a valid re-expression of MODIS BRDF modelling. The derived height-to-width ratio appears to provide some distinction between surfaces with a similar NDVI response. However, the results are generally weak and raise new issues that are difficult to explain. The results suggest a deficiency in the model or that noise will always be a significant issue and the ability to interpret the physical structure of vegetation at a pixel level is effectively unachievable with this approach and dataset. An answer to the research questions was not achieved.

5 Broadening the applicability of the model

5.1 Introduction

A limitation of the model introduced in chapter 4 was that it described vegetation in terms of two end members that need to be determined. A priori use of homogeneous, single species cropped fields as a study area enabled determination of end members, (i.e. soil and crop) by making observations at the appropriate epochs in the cropping cycle. End member profiles were derived by averaging several observations at the relevant epochs, however the results may be sensitive to the end member profiles used in modelling. Furthermore, for the model described in chapter 4 to be applied more widely, end members would need to be obtained in a different manner and generally more than just two end members would be required to describe a complex heterogeneous surface, e.g. the influence from an understory layer may need to be considered. Modelling may be achieved by identifying end members from different homogeneous locations and then applying, as per the model described in chapter 4, to a third/alternate location. However, this approach is likely to introduce more variability and complexity into the modelling.

An alternative approach is to assign the end members of soil and vegetation to NDVI responses of 0 and 1 respectively with no angular variability, i.e. equation 24 = 0 and equation 25 = 1. These being theoretical extreme values for the respective components and if no angular variability is considered, a minimum of assumption can be considered imposed. When these end members are substituted into Equations 21 – 23 the model becomes:

NDVI (θ°) = NDVI(0°) (1+H tan (θ°))   (27)

Where: θ is the view zenith angle,

      H is the height-to-width ratio of vegetation prisms, and

      NDVI (0°) is derived from the normalised difference between

      the near infrared and red band isotropic parameter weights.

Equation 27 broadens the applicability of the model described in the previous chapter and is much simpler in form. It has a very similar structure as Roujean's geometric scattering equation (Roujean et al., 1992). The model necessitates the derivation of only one parameter (i.e. 'H'), which can be derived in the same manner as previously described in chapter 4, i.e. the value for H that achieves the lowest RMSE to NDVI derived from MODIS BRDF across the same range of view angles. NDVI (0°) implicitly represents the density of the vegetation cover. Given the high correlation between the derived density and NDVI discussed in chapter 4, the use of NDVI as a direct representation of density appears reasonable. With this broader approach any limitations the model may have in physically describing vegetation may be ignored as ***the derived height-to-width ratio can be considered an abstract, single numeric value that quantifies the relationship between NDVI and view angle.***

Given the form of equation 27, a height-to-width ratio (H) equal to zero implies a 3-D flat surface and the NDVI response will therefore be invariant to changes in view angle, i.e. isotropic. Also, when viewed at nadir (i.e. $\theta = 0$), NDVI (0°) will equal the normalised difference of the near infrared and red isotropic parameters.

To test this modified model, it was applied to the same temporal transect of single species crop fields considered in the previous chapter. This allowed comparison with previous results and testing of the sensitivity of the model to the selection of end member profiles.

In addition to applying the model to fields of cotton/wheat at Cubbie Station and sugar cane at Davco Farming, an additional surface has also been included as the determination of end member profiles are no longer required. A surface that is homogeneous and generally temporally invariant is well suited as an additional study surface when no particular knowledge or validation of the surface has been undertaken. Two random pixels from the Simpson Desert on the South Australian/Northern Territory border have been selected as an additional surface. Both pixels display low NDVI response over the 463 epochs (10 years) which is consistent with a temporally invariant, low vegetated density desert environment. The NDVI response for the two selected pixels in the Simpson Desert is very similar to that of bare soil on Cubbie Station fields, i.e. an NDVI response of 0.2. The derived height-to-width ratios for this additional surface and Cubbie Station can be compared, in order to test if the height-to-width ratio provides any distinction between two surfaces that exhibit similar NDVI responses.
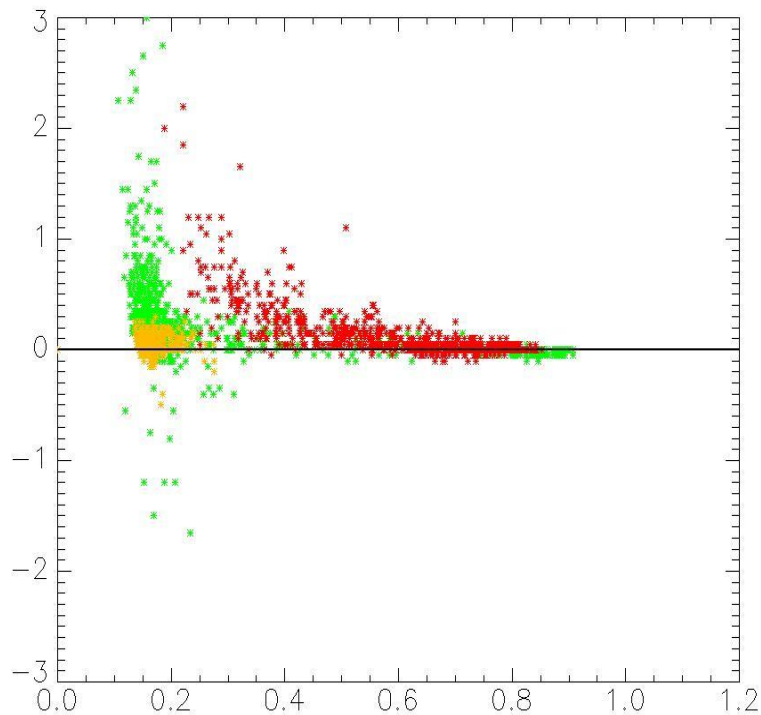
Figure 5.1 – Derived height-to-width ratio (y-axis) against NBAR NDVI (x-axis), '0' and '1' end members having been used in modelling. Cubbie Station fields 2 and 7 (green), Davco Farming fields 1 and 3 (red) and two random pixels from the Simpson Desert (gold).

The results shown in Figure 5.1 differ significantly from those shown in Figure 4.26. There is a greater propensity for positive derived height-to-width values, although a significant number remain negative. In the range of NBAR NDVI values from 0.3 to 0.5, (as discussed above, being the most appropriate range from which the height-to-width ratio may be interpreted) there appears a much clearer distinction between cotton/wheat at Cubbie Station and sugar cane at Davco Farming. A similar distinction can also be made between the periods of bare soil at Cubbie Station and pixels taken from the Simpson Desert, i.e. whilst both have the same NBAR NDVI response, the pixels at Cubbie Station exhibit larger height-to-width ratios. An explanation for this is unclear, however it suggests that residual vegetation (e.g. crop litter or weeds) which is more likely to be present on Cubbie Station fields than in the Simpson Desert could be the cause of differences in the derived height-to-width ratio, i.e. the height-to-width ratio may be detecting low levels of vegetation that are insufficient to appear in spectral data and therefore not evident in the NDVI response.

The re-expression of MODIS BRDF modelling described by equation 27 provides a very good fit (with best fit values for 'H' substituted back into equation 27) to MODIS's BRDF modelling, i.e. correlations close to 1 and low RMSE. Therefore equation 27 represents a valid re-expression of MODIS BRDF where the height-to-with ratio is considered a single numeric value describing the relationship between NDVI and view angle. Whilst the issues identified in section 4.4 remain unexplained and an interpretation of the results unclear, the height-to-width ratio (derived with 0 and 1 end members) may be able to provide a means of distinguishing different surfaces with the same NBAR NDVI response. In this manner the height-to-width ratio, derived from MODIS BRDF modelling which expresses the relationship between NDVI and view angle as a single numeric value may provide an answer to research questions 3 and 4 which are explored further in the next section.

5.2 Spatial Transect (Melbourne to Darwin, Australia)

The use of transects is a standard method to examine spatial patterns within vegetation studies (Hutley et al., 2011). Leveraging the continental scale of the MODIS BRDF data set available via the CSIRO and considering the above results, a next step was to apply the modified model to a spatial transect. A transect from Melbourne to Darwin includes a wide variety of Australian bioregions and is shown in Figure 5.2. The derived height-to-width ratio can be compared with spatially distinct surfaces covers along the transect line, e.g. forest near Melbourne, crop farming, the mallee in northern Victoria, arid desert and tropical savanna in Northern Australia. The northern third of this transect includes the region covered by the Northern Australian Tropical Transect (NATT) which has been the subject of numerous studies and provides a relatively constant gradient with respect to rainfall and vegetation with the inland distance (Hutley et al., 2011). The transect line can also be taken at different times of year and temporal variations in the results compared.

Figure 5.2 – Spatial transect location between Melbourne (Lat 37° 49' S, Long 144° 58' E)
and Darwin(Lat 12° 27' S, Long 128° 51' E) (Source Google Earth)

The transect line between Melbourne and Darwin is a distance of approximately
3,100km. 6,180 MODIS 500-m resolution pixels representing the transect line have been
extracted from the MCD43 dataset and the model, described by equation (27), has been
applied enabling derivation of a height-to-width ratio (H) for each pixel. Pixels have
been extracted representing four epochs; the first week of July 2005 and 2006 (i.e.
winter), and the last week of January 2005 and 2006 (i.e. summer).

5.3 Results

The results are considered in the same manner as the temporal transect of a single pixel.
Firstly, how well the model fits with NDVI derived from MODIS BRDF modelling.
Secondly, plotting the derived height-to-width ratio along the transect line and finally by
plotting the height-to-width ratio against NBAR NDVI.

5.3.1   Goodness of fit

As discussed in chapter 4, the model must provide a good fit to MODIS BRDF derived NDVI for the height-to-width ratio to have validity. Additionally, it is appropriate to further consider the MODIS BRDF quality flags and the impact that the quality of the MODIS BRDF inversion has on the results.

In Figure 5.3 the correlations and RMSE indicate that the model (equation 27) provides a good and consistent fit to MODIS BRDF modelling for the four selected epochs, i.e. correlations close to 1 and low RMSE. The RMSE appears higher nearer Melbourne and Darwin and lower across the arid regions of central Australia. The RMSE may be related to NBAR NDVI, i.e. higher NBAR NDVI is associated with higher RMSE, although the RMSE is always less than 0.005 (NDVI). This is consistent with the RMSE associated with the temporal transect.

In Figure 5.3, the near infrared band (band 2) quality flag for pixels that are not 'best quality inversions' are shown as green points along the x-axis. The MODIS BRDF inversion quality is lower in the southern and central Australia during winter when cloud cover is likely to be present and lower in the northern regions during summer when cloud cover associated with the wet season is likely to be present. Furthermore, when the MODIS BRDF quality flag indicate best quality inversions, the fit between the model and MODIS BRDF is strongest, i.e. higher correlations and lower RMSE. This further supports the model as a valid re-expression of MODIS BRDF modelling.
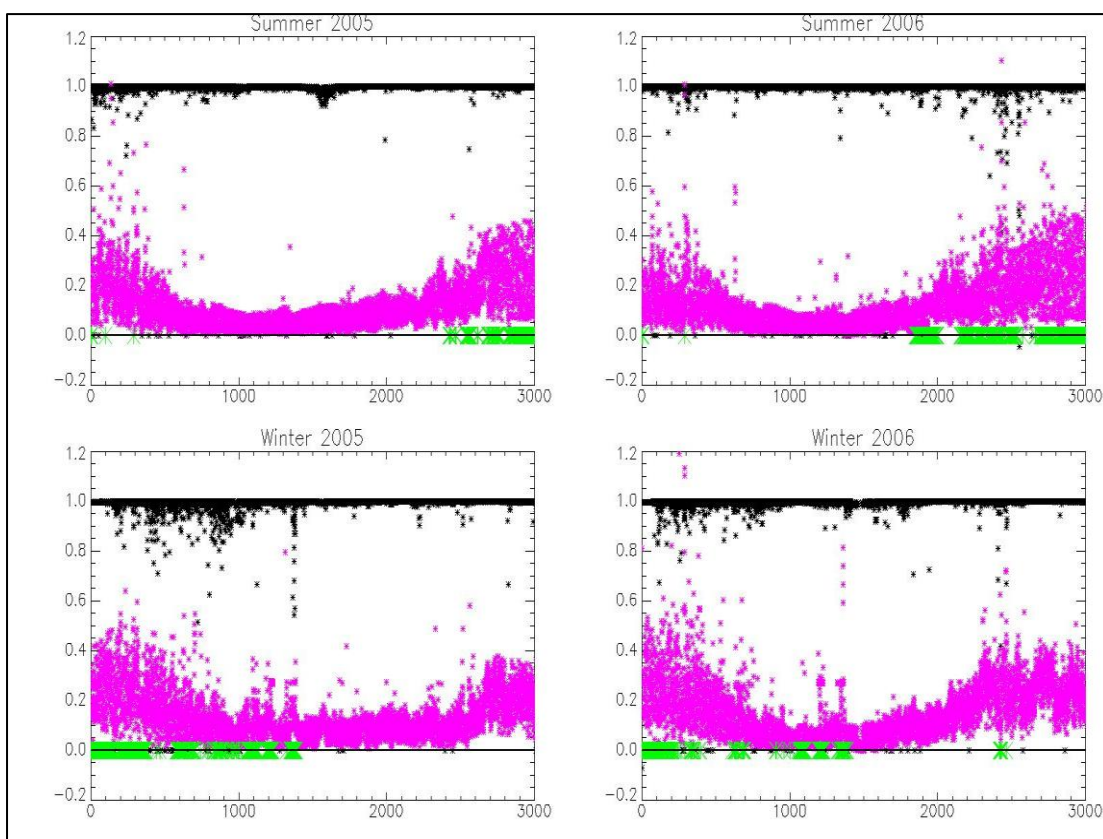
Figure 5.3 - Correlations (black), RMSE x100 (magenta) on the y-axis. The x-axis represents distance in kilometres from Melbourne. MODIS NIR Band QA Flags for pixels which are not 'best quality' inversions are shown as green points along the x-axis. Winter epochs being taken from the first week of July and summer epochs being taken from the last week of January in respective years.

5.3.2 Derived height-to-width ratio and NBAR NDVI along the transect

In Figures 5.4, 5.5 and 5.6 the derived height-to-width ratios have been removed from the plots if the MODIS BRDF band quality flag is other than "best quality inversion", or the RMSE for derivation of the height-to-width ratio is greater than 0.005, or the correlation between the model and NDVI derived from MODIS BRDF is less than 0.9. This seeks to remove from consideration a small number of pixels where the model and derived height-to-width ratio did not provide a good fit with MODIS BRDF modelling.

Figure 5.4 – NBAR NDVI (green) and derived height-to-width ratio (red) (y-axis) against distance in kilometres along transect from Melbourne (x-axis).

In order to better visualise the results, the plot from summer 2005 (top left in Figure 5.4) has been partitioned and enlarged for three separate sections of the transect and is displayed in Figure 5.5, i.e. Melbourne to 1,000km, 1 – 2,000km and 2,000km to Darwin. The summer 2005 epoch was selected for enlargement as the band QA data, shown in Figure 5.3, indicates better quality BRDF inversions than the other three investigated epochs. Only the area close to Darwin indicate BRDF inversion quality issues, with this most likely being a reduction in the number of observations due to cloud cover in the summer wet season and appears as "missing data" in the plot.

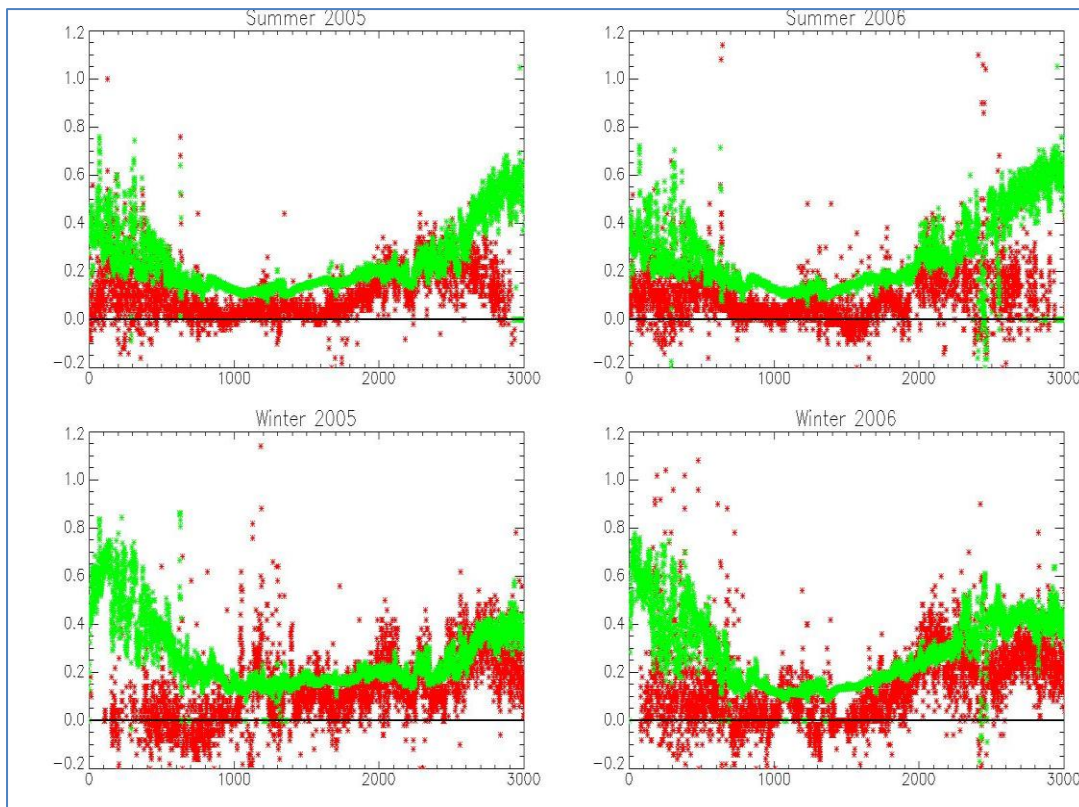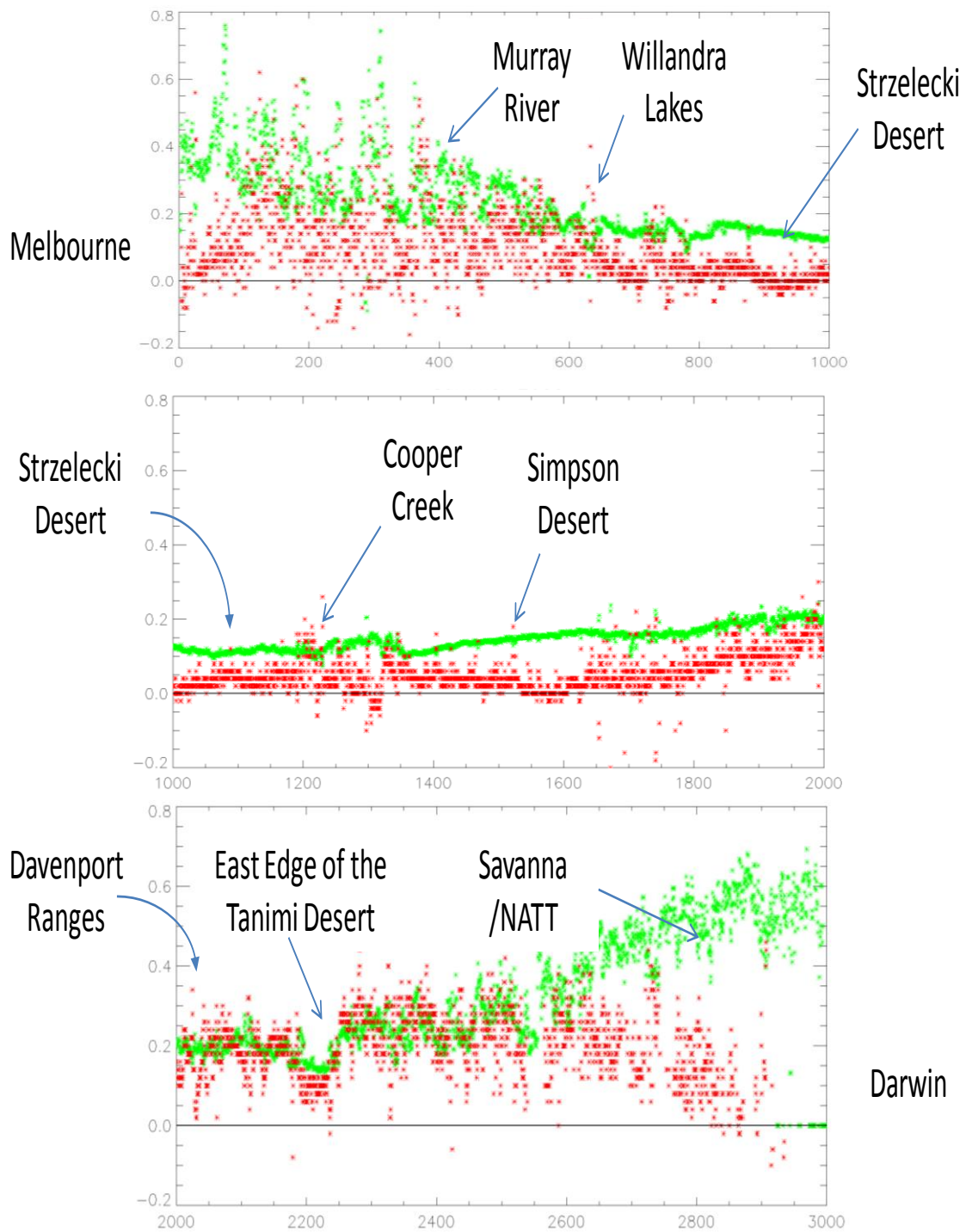Figure 5.5 - NBAR NDVI (green) and derived height-to-width ratio (red) (y-axis) against distance in kilometres along transect from Melbourne (x-axis), for the summer 2005 epoch, partitioned and enlarged into three separate plots.

Nadir BRDF Adjusted Reflectance (NBAR) NDVI derived from the MODIS MCD43 product has been determined for pixels along the transect line. Within Figures 5.4 and 5.5 NBAR NDVI exhibits the expected profile, i.e. falling NBAR NDVI moving North West from Melbourne, low NBAR NDVI across the arid centre of Australia and rising again in tropical areas approaching Darwin. NBAR NDVI was higher in winter than summer in the southern regions near Melbourne. The opposite pattern is observed in the northern regions approaching Darwin, i.e. higher NBAR NDVI during the summer wet season and lower NBAR NDVI during the winter dry season.

In Figure 5.4 there appear a series of prominent spikes in the height-to-width ratio that correspond spatially to specific surface features along the transect line. For winter epochs, at approximately 600km, 1,100km, 1,200km and 1,280km along the transect from Melbourne there are four positive spikes in the height-to-width ratio. These appear without significant corresponding changes in NBAR NDVI. Spatially, these align to the Willandra lakes in Mungo National Park, Tooncatchyin, Cooper and Warburton Creeks which feed into Lake Eyre. A similar effect, but less well defined occurs around the Davenport range in the Northern Territory (approx 2,000km from Melbourne). These spikes in the height-to-width ratio are more prominent in winter. During summer epochs, the increases in the height-to-width ratio at these locations are significantly less pronounced, but it is still possible to detect them as a general rise in the height-to-width ratio. The spatial extent and degree of definition of these spikes in the height-to-width ratio varies between years, e.g. more extensive in winter 2005 than in winter 2006.

In contrast to the four areas of prominence in the height-to-width ratio, the height-to-width ratio is consistently low during summer in areas 800 – 1,000km and 1,400 – 1,700km along the transect line from Melbourne. These areas correspond spatially to an area South West of the Strzelecki Desert and the Simpson Desert through which the transect passes. These areas are particularly arid and generally have very low, uniform vegetation cover as evidenced by the NBAR NDVI response. Additionally, the variability of the height-to-width ratio at these locations is comparatively low compared to the variability in the height-to-width ratio shown at other locations along the transect line and this is most evident in the centre plot of Figure 5.5, i.e. lower variability in the NBAR NDVI response corresponds to low variability in the derived height-to-width ratio.

It is difficult to fully understand or explain the underlying cause of height-to-width ratio variations at these locations without specific surface cover knowledge at these particular epochs (e.g. rainfall and flood events). However where the height-to-width ratio spikes,

the corresponding location is a water related feature. Where the height-to-width ratio is consistently low in comparison to NBAR NDVI, the corresponding surface feature is related to a general absence of water features, e.g. Simpson Desert. This suggests that these particular variations in the height-to-width ratio may be associated with the presence of vegetation, although with an insufficient density to influence a significant change in NBAR NDVI. The height-to-width ratio may be sufficiently sensitive and able to amplify the presence of low density vegetation from the background soil, i.e. vegetation that is only apparent when viewed at an angle. Consistent with this, when there is effectively no vegetation cover present (i.e. sand dunes in the Simpson Deserts), NDVI is invariant to viewing angle and the derived height-to-width ratio will be close to zero and may indicate that the NBAR NDVI response is from bare soil alone.

A final observation evident in Figures 5.4 and 5.5 is that is that the height-to-width ratio is generally larger in value for areas in northern Australia than southern Australia and this appears independent of the NBAR NDVI response. This appears consistent for both summer and winter epochs. Whilst an association with latitude or the solar angle appear likely factors, a definitive cause is unclear.

The derived height-to-width ratio has also been plotted against NBAR NDVI which is shown in Figures 5.6. Considering Figures 5.6 the following general observations can be made; for lower NBAR NDVI values (e.g. < 0.4) there is a positive relationship between NBAR NDVI and the height-to-width ratio, for higher NBAR NDVI values (e.g. > 0.4) a negative relationship exists. The height-to-width ratio progressively tends towards zero at higher NBAR NDVI values.

The general relationship between the derived height-to-width ratio and NBAR NDVI is not strong, e.g. a positive relationship with NBAR NDVI up to 0.4 and then a negative relationship beyond 0.4. This peak in the derived height-to-width ratio corresponding to NBAR NDVI of 0.4 is consistent with the results from the temporal transect, if larger height-to-width ratios associated with bare soil at Cubbie Station are considered an exception. Considering figures 5.4, 5.5 and 5.6, the derived height-to-width ratio appears more variable in winter than summer epochs.
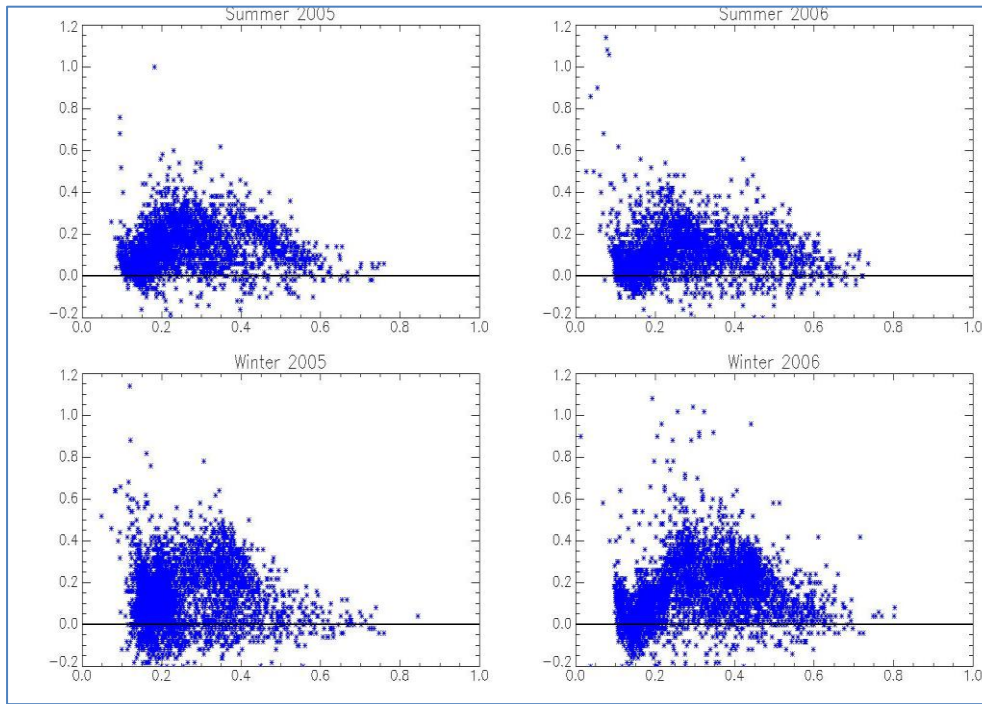
Figure 5.6 – Derived height-to-width ratio (y-axis) against NBAR NDVI (x-axis)

5.4 Summary of results from the spatial transect

A model for re-expressing the MODIS BRDF representation in terms of an alternative parameter set was described in chapter 4. In order to broaden the applicability of the model, the two model end members of soil and vegetation were assigned values of 0 and 1 respectively and substituted into the model developed in chapter 4. The modified model (described by equation 27) was applied to a spatial transect between Melbourne and Darwin and also to the previously considered temporal transect associated with single species cropped fields.

The modified model provides a good fit with NDVI derived from MODIS BRDF and therefore is considered a valid re-expression of MODIS BRDF with an alternative set of parameters. **The modified model enables derivation of a single parameter which describes the relationship between NDVI and view angle, i.e. the height-to-width ratio (H).** In this context, negative values, which were problematic in a geometric sense (refer chapter 4) may be valid with this broader interpretation.

Whilst derived values for the height-to-width ratio are noisy, the derived values are not spatially random. Derived results are partially consistent between the temporal transect

and spatial transect. The height-to-width ratio appears able to distinguish vegetation cover that is otherwise not distinguishable by its NDVI response, e.g. larger height-to-width ratios may be distinguishing bare soil associated with cropped fields from arid desert soils, identify low density vegetation surround waterways and distinguish different crop varieties that have the same NDVI response. In answer to research question 4; the height-to-width ratio (derived from MODIS BRDF modelling) appears to provide some additional information to spectral data, although an understanding of the underlying surface characteristic responsible for these variations in the height-to-width ratio is unclear.

6 Exploring the spatial relationship of BRDF effects

6.1 Introduction

The model described in previous chapters has been applied to a temporal transect of a single pixel (i.e. a point) and a spatial transect (i.e. a line). A logical extension might be to apply the model to a surface area. Applying the model to a surface area will enable the resulting derived height-to-width ratio to be displayed in a map format. This in turn allows the spatial relationship between features with differing height-to-width ratios to be considered.

In analysing the spatial transect between Melbourne and Darwin, surface features were identified by their distance along the transect line as measured using Google Earth. Due to map projection differences between CSIRO's continental grid and Google Earth, the exact location of corresponding features was an approximation. Whilst this was good enough for the general location of large scale features corresponding to variations in the derived height-to-width ratio, it is limited in understanding the exact position of features and their surrounds at a pixel scale. The application of the model to a surface area with well defined geo-location of pixels can address this limitation experienced in the previous chapters. Application of the model to a surface area enables scale issues at the pixel level in BRDF modelling to be considered. Issues of scale in BRDF modelling were identified in the literature review as an issue but not considered in the two previous chapters.

In chapter 5 the derived height-to-width ratio (being a single numeric value describing the relationship between NDVI and view angle derived from a re-expression of MODIS BRDF modelling) appeared to offer some additional information to spectral data, however an understanding of the underlying surface characteristics responsible for these variations in the height-to-width ratio is unclear. This chapter seeks to explore the spatial relationship of the height-to-width ratio in order to explain observed variations and in doing so answer research questions 3 and 4.

6.2 Location of study area

The selection of a study surface area is somewhat arbitrary, although several conditions are desirable. An area with generally low vegetation cover is preferable as mutual obscuration of vegetation is not considered by the model and unlikely to be an issue in areas of low vegetation density. The model does not consider the influence of an understory layer which may also be seasonally variable. The use of a semi-arid study area reduces possible effects of an understory layer, which is not considered by this modelling approach, but may be a more significant in woodland areas. Topographically flat areas are also preferable as issues associated with aspect and slope in the derivation of MODIS BRDF can be ignored. Areas that are temporally invariant support better MODIS BRDF inversions (as indicated by quality flags) and allow comparison of results from different epochs, e.g. consecutive epochs or inter year epochs from the same time of year/season. Many semi-arid areas in central Australia meet these criteria. The area through which the spatial transect passed displaying prominences around water courses is a good site given the already observed variability in the height-to-width ratio that appeared associated with water features.

The temporal transect represented 463 epochs, the spatial transect 6,180 pixels. The surface study areas should be sufficiently large to make large scale features clearly visible but, too large an area will introduce data processing issues.

A surface study area in the north east of South Australia has been selected, being latitude 28° 00' to 29° 00' South and longitude 138° 00' to 139° 30' East, i.e. 1 ½ ° longitude by 1° latitude representing approximately 18,000 km^2. Figure 6.1 shows this area on a locator map. Figure 6.2 is an enlargement showing surrounding features and the approximate location of the transect line discussed in chapter 5. Figure 6.3 is MODIS NBAR NDVI of the surface study area representing 319 x 213 MODIS 500-m pixels.
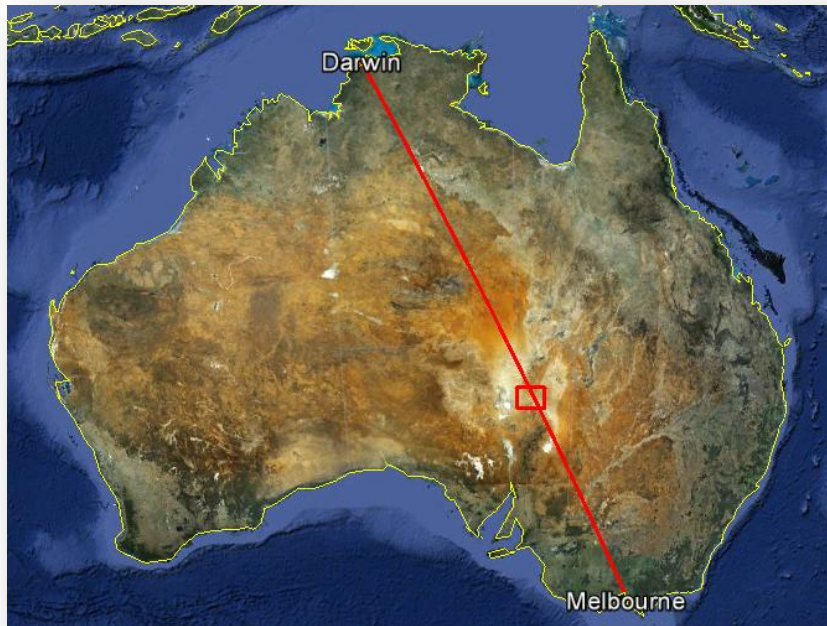
Figure 6.1 – The Australian continent showing the location of the study surface area

(Source : Google Earth)
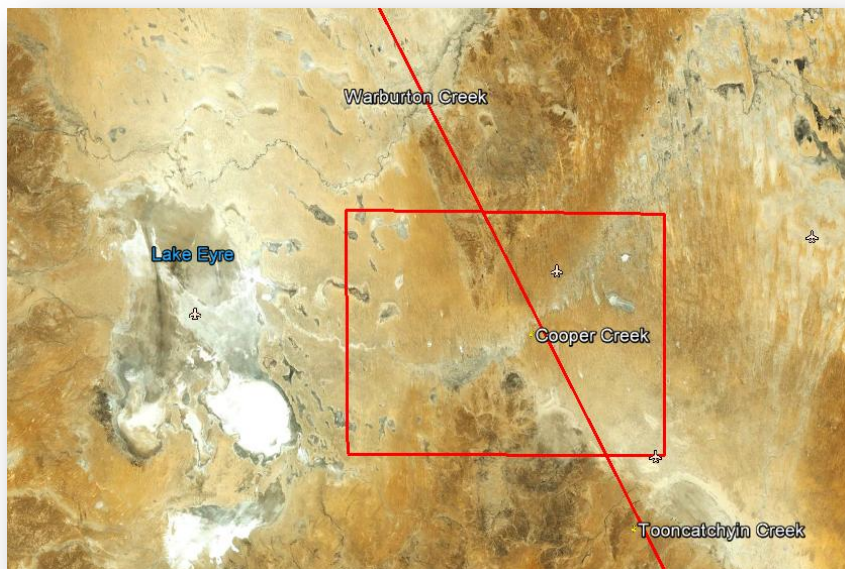
Figure 6.2 – Enlargement of the surface study area and surrounds

(Source : Google Earth)
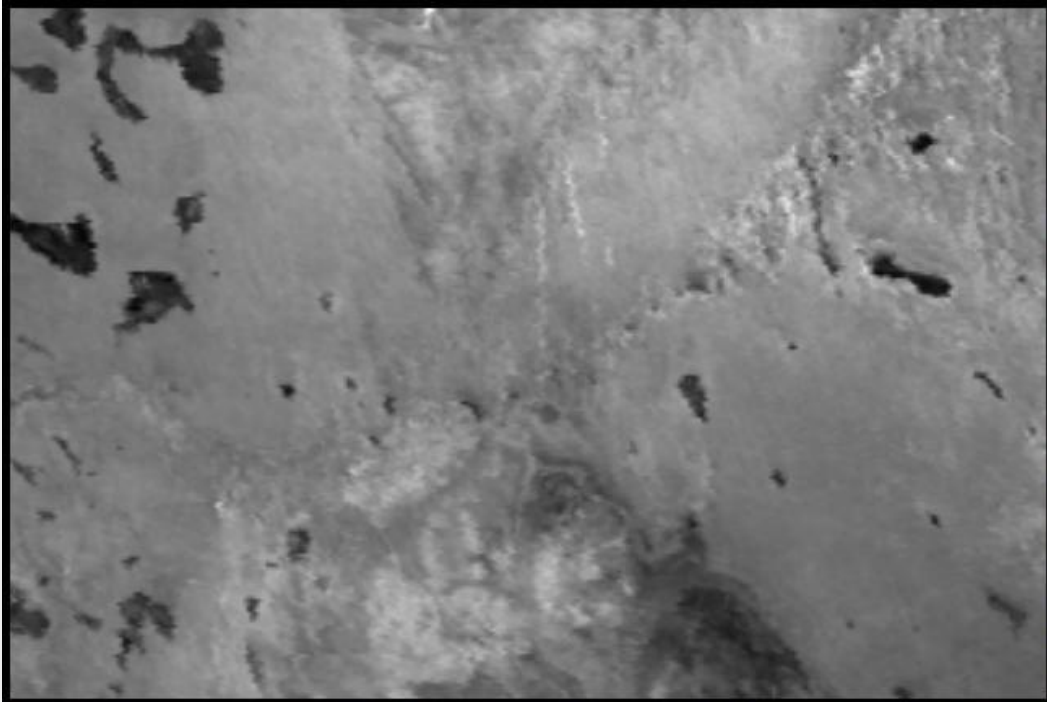
Figure 6.3 – Grey scaled image of MODIS NBAR NDVI for the surface study area for the 18th February 2005 epoch.

The surface study area is sparsely vegetated, i.e. NBAR NDVI maximum is 0.22. The major feature is Cooper Creek running from the top right to centre left of the image in Figure 6.3. The dark areas being dried salt lakes.

MODIS BRDF band quality flags have been extracted for the area and generally indicate poor quality inversions during winter epochs. The poorer quality inversions are consistent with the spatial transect through this area during the winter epochs. Summer epochs generally show no adverse BRDF quality issues across the entire study area, i.e. 'best quality inversions'. As discussed in chapters 4 and 5, for the derived height-to-width ratio to have validity, MODIS BRDF (which the model described here seeks to interpret/re-expression) should be derived without inversion quality issues.

6.3 Results

The height-to-width ratio (H) of pixels in the surface study area has been derived in the same manner as the temporal and spatial transects, i.e. derived values for H (as per equation 27) that achieve the lowest RMSE to NDVI derived from MODIS BRDF across the same range of view angles. In this manner, the derived height-to-width ratio expresses the relationship between NDVI and view angle as a single numeric value.

The results can again be considered in the same manner as the temporal and spatial transects, i.e. how well the model fits with NDVI derived from MODIS BRDF modelling and the examination of the values for the derived height-to-width ratio across the surface study area. For the temporal and spatial transect, values for the derived height-to-width ratio could only be shown as a plot. For a surface area the derived height-to-width ratio can be depicted as a colour intensity map and the results spatially contextualised with surrounding surface features.

6.3.1 Goodness of fit

With the derived best fit height-to-width ratio (H) substituted back into equation 27, the model generally provides a good fit to NDVI derived across the same range of view angles based on the MODIS BRDF representation, i.e. correlation close to 1 and low RMSE. Figure 6.4 shows correlations and RMSE in map format of the study area for the 18/2/2005 epoch, i.e. summer. To assist visualisation within Figure 6.4, correlations are displayed with a floor value of 0.99, i.e. correlations <0.99 are shown as black and as a grey scale for values in the range 0.99 to 1. RMSE are displayed with a ceiling value of 0.00025, i.e. RMSE > 0.00025 are displayed white and as a blue scale for values in the range 0 – 0.00025. There is some evidence of non random spatial distribution of the correlations and RMSE across the study area, although this is not ideal, the numerical variations are very small.
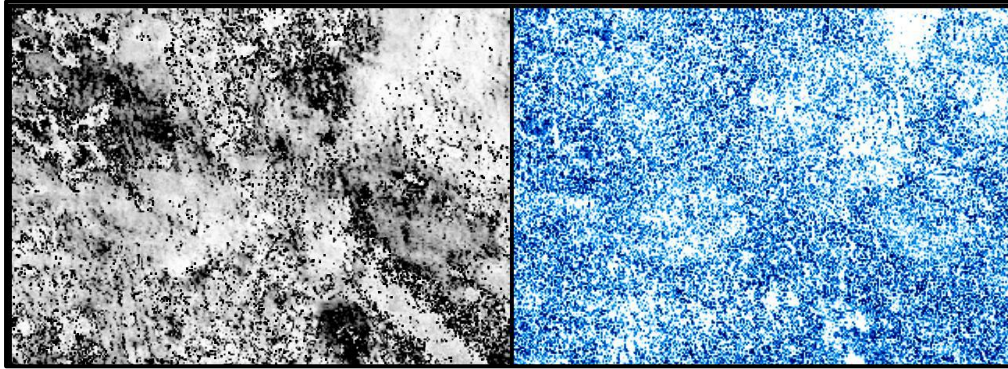
Figure 6.4 – Left - Correlations between the model (i.e. equation 27 with substituted 'best fit' height-to-width ratios) and NDVI derived from MODIS BRDF parameters for the study area across the same range of view zenith angles, where white indicates better correlations and darker grey areas lower correlations. Right - RMSE in derivation of the height-to-width ratio, where white indicates larger RMSE and darker blue areas indicates lower RMSE.
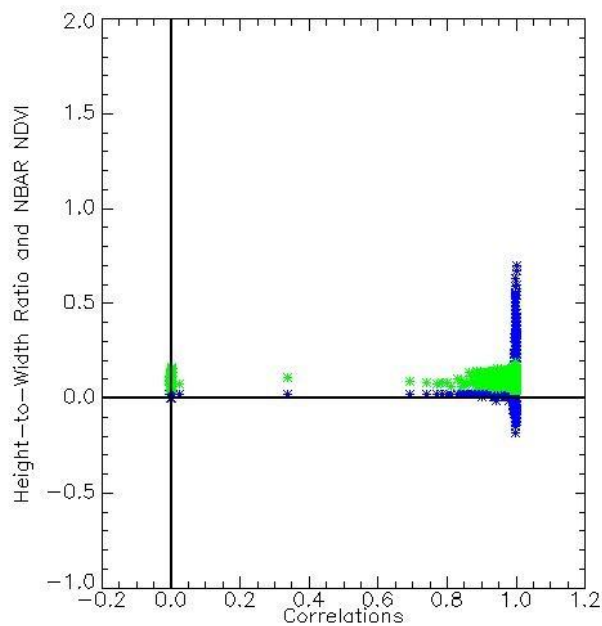
Figure 6.5 – Derived height-to-width ratio (blue) and NBAR NDVI (green) on the y-axis plotted against correlations on the x-axis

Correlations between the model (with best fit values for the derived height-to-width ratio substituted) and NDVI derived from MODIS BRDF modelling across the same range of view angles is shown as a scatter plot in Figure 6.5. In addition to showing correlations being generally close to 1, Figure 6.5 shows that that for weaker

correlations the derived height-to-width ratio tends to be 0. Correlations also appear independent of the NBAR NDVI response, i.e. the model fits equal well across all NBAR NDVI response levels although NBAR NDVI is generally very low across the entire study area. In summary, the model (i.e. equation 27) and the height-to-width ratio derived from it can be considered a valid re-expression of MODIS BRDF modelling.

6.3.2   Height-to-width ratio map

The height-to-width ratio has been derived across the surface study area for the 18th February 2005 epoch. The derived height-to-width ratios ranged from -0.18 to 0.7. To support better visualisation of the results, outlying values have been replaced with ceiling values of 0.3 and floor values of -0.1 respectively, and the image in Figure 6.6 has had brightness values scaled within this range. White/lighter coloured areas indicate higher values and darker areas indicate lower/negative height-to-width ratio values.

An advantage of applying the model to a surface area is that it allows the results to be displayed in a map format that enables spatial patterns associated with the derived height-to-width ratio to be considered. The results are not spatially random and appear related to surface features. Higher values are generally evident in areas surrounding Cooper Creek. The derived height-to-width ratio also exhibit larger values on the rim of dried salt lakes. These are most likely to be the features that appeared as 'spikes' along the spatial transect in chapter 5. Figure 6.7 shows an enlargement for the top left corner of the surface study area. In the enlargement, the positive height-to-width ratios appear accompanied by negative values in areas immediately outside the rim of the dried salt lakes. This effect appears more prominent on the East/West boundaries than the North/South boundaries of the dried salt lakes. The large positive and negative values for the derived height-to-width ratio appear spatially related to a common surface feature, i.e. the rim of dried salt lakes This is significant because MODIS BRDF and the height-to-width ratio are derived independently for each pixel, yet the effects for pixels inside and outside of the dried salt lake appear (inversely) related.
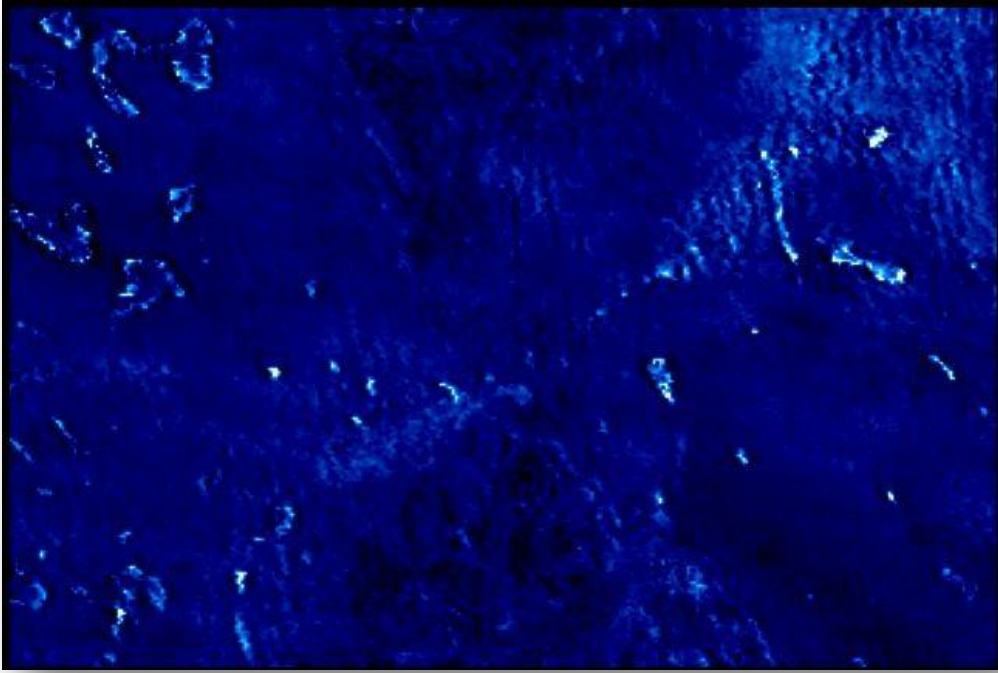
Figure 6.6 – Derived height-to-width ratio for the surface study area for the epoch 18th Feb 2005.
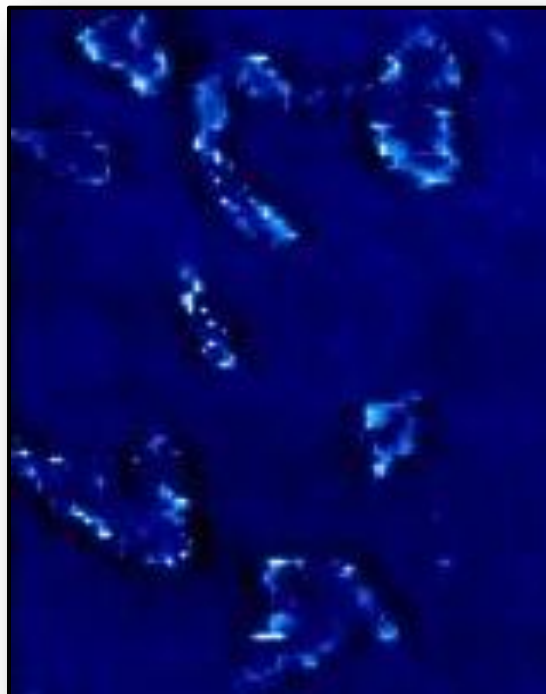

Figure 6.7 – Derived height-to-width ratio, an enlargement of the top left corner of study area

The model, from which the height-to-width ratio is derived, is theoretically based on vertical prism shaped protrusions of vegetation above a layer of bare soil, i.e. the vertical profile of these vegetation protrusions being responsible for the variation in NDVI associated with view angle. Considered geometrically, larger height-to-width ratios represent tall thin vegetation. Providing a geometric interpretation of negative height-to-width values is unclear, as discussed in chapters 4 and 5. A possible geometric explanation for the negative values in very arid areas is that vegetation is below the soil layer, e.g. in crevasses between rocks. In this case, the soil layer will obscure the vegetation at higher view angles and produce a negative height-to-width ratio. The vegetation may also be microscopic in nature rather than at a scale associated with cultivated crops. Whilst the corresponding positive and negative height-to-width ratios may theoretically be explained in this manner for some dried salt lakes, it is perhaps less easy to extend this explanation across the whole study area of 18,000 km^2 where this effect appears broadly evident. Given the historical nature of data, the size of the study area and the characteristic being described, in-situ studies may be problematic in confirming or otherwise these interpretations of the resulting height-to-width ratio.

The Australian National Carbon Accounting System (NCAS) was used in chapter 4 to verify the homogeneity of single species cropped fields and data from the NCAS has also been obtained for this surface area. The NCAS dataset is at a 25m spatial resolution. The study area in central Australia is covered by the SH54 North West tile from the NCAS dataset. The NCAS dataset 2005 tile was created with images acquired during the period between 24/1/2005 and 22/3/20005 and corresponds to the epochs from which MODIS data is being examined. The relatively short time period over which images were acquired should minimise temporal variations in the resulting mosaic and better enable comparison with MODIS data for an epoch within this date range. NDVI has been derived from NCAS dataset for the dried salt lake at the centre of Figure 6.7 and is shown in Figure 6.8 (left image). NDVI derived from NCAS dataset suggests that there is no appreciable difference in the NDVI response between the surface of dried salt lakes and the inside rim, nor are there any appreciable difference in the NDVI response between areas immediately outside of the dried salt lakes and from areas further removed.
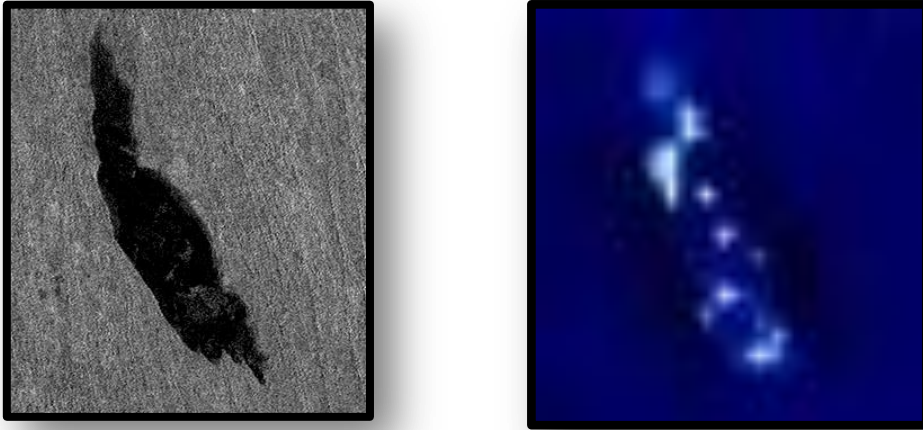
Figure 6.8 – (Left) NDVI derived from the Australian NCAS dataset at a nominal 25 m spatial resolution showing the region around the salt lake in the centre of Figure 6.7. The derived height-to-width ratio (right) is shown for the salt lake at the centre of Figure 6.7, being at MODIS's 500-m resolution.

Whilst the variations in the derived height-to-width ratio surrounding the dried salt lakes appear singularly the most prominent effect in Figure 6.6, larger derived height-to-width ratios are also evident in a broad area from the top right to the centre left of Figure 6.6. This area corresponds to Cooper Creek. A vegetation structural interpretation for these variations in the height-to-width ratio across the study area is unclear with regard to answering research questions 3 and 4.

6.4   An alternative interpretation of the results

An alternative explanation is that the height-to-width ratio is not describing the directional scattering of reflected light based on vegetation's vertical structure within the pixel, but is highlighting an artefact in MODIS BRDF modelling. MODIS BRDF modelling utilises successive observations of a pixel for the determination of RossThick-LiSparse parameter weights. For sensors with a wide field of view such as MODIS, the size of the ground IFOV grows significantly towards the edge of the swath (Lucht et al., 2000). Also the location on the ground represented by a pixel may nominally vary up to +/- 250-m as a consequence of satellite flight path and altitude variations.

In determining the MODIS BRDF model parameter weights for pixels on the inside rim of a dried salt lake; if observations used in the determination of the MODIS BRDF model happen to include within its ground IFOV some area having a higher NDVI response from outside of the dried salt lake, the MODIS BRDF model will attribute the higher NDVI response to angular effects. This will tend to result in larger angular variations for pixels on the inside rim of the dried salt lake. The model described by equation 27 in chapter 5 and applied to this surface area will interpret larger angular effects as larger height-to-width ratio which will appear as brighter areas in Figures 6.6 and 6.7. The inverse will occur for pixels just outside the area of the dried salt lake, and the model will interpret these angular effects as negative height-to-width ratios which will appear as darker areas in Figures 6.6 and 6.7. This effect may also explain the results from the temporal and spatial transects that were difficult to interpret and appeared subject to noise. For example, noise may not random but systemic due to variations in the location and size of a pixel's ground IFOV used in MODIS's BRDF inversion.

To explore the possibility that the geo-location accuracy and/or the size of a pixel's ground IFOV is the cause of the observed variations in the height-to-width ratio, the following sections (i.e. 6.4.1 – 6.4.4) consider known issues associated with pixel geo-location, enlargement of pixel's ground IFOV, MODIS's BRDF processing strategy and an empirical test for this alternate interpretation is developed.

6.4.1   Geo-location accuracy

MODIS NIR and Red bands used in derivation of NDVI have a nominal spatial resolution of 250-m. As the sensor is not stationary over each ground point when a pixel is sampled, a triangular weighting function is applied to the reflectance response such that 25% of the response will relate to an area outside of the nominal 250-m area (Nishihama et al., 1997). The MODIS earth location algorithm uses earth ellipsoid and terrain surface information in conjunction with spacecraft ephemeris and attitude data, and knowledge of the MODIS instrument and Earth Observing System (EOS) satellite geometry to compute geodetic position for each nominal 1-km nadir resolution ground field of view. A set of parametric equations and a table of sub-pixel corrections for each detector in each wavelength band is included in the geo-location data product to capture the effects of detector-to-detector offsets and permit calculation of the locations of the centres of the 250-m and 500-m picture elements. An error of 0.1 of a

pixel (100-m) at nadir for the 1-km resolution pixels has been estimated with geo-location. (Masuoka et al., 1998).

Geo-location inaccuracies are likely to be random and the effects on MODIS BRDF modelling and the derived height-to-width ratio are therefore also likely to be random, e.g. appearing as noise within the results. Figure 6.9 shows the derived height-to-width ratio for the study area for four consecutive epochs. The variations in the derived height-to-width ratio in Figure 6.9 do not appear spatially or temporally random, i.e. they appear spatially consistent in relation to surface feature boundaries and temporally consistent between epochs. Therefore, whilst geo-location inaccuracies may be a contributing factor, the spatial and temporal consistency of larger height-to-width ratio suggests that geo-location inaccuracies are not the prime cause of the observed variations in the height-to-width ratio.

18th Feb 2005

26th Feb 2005

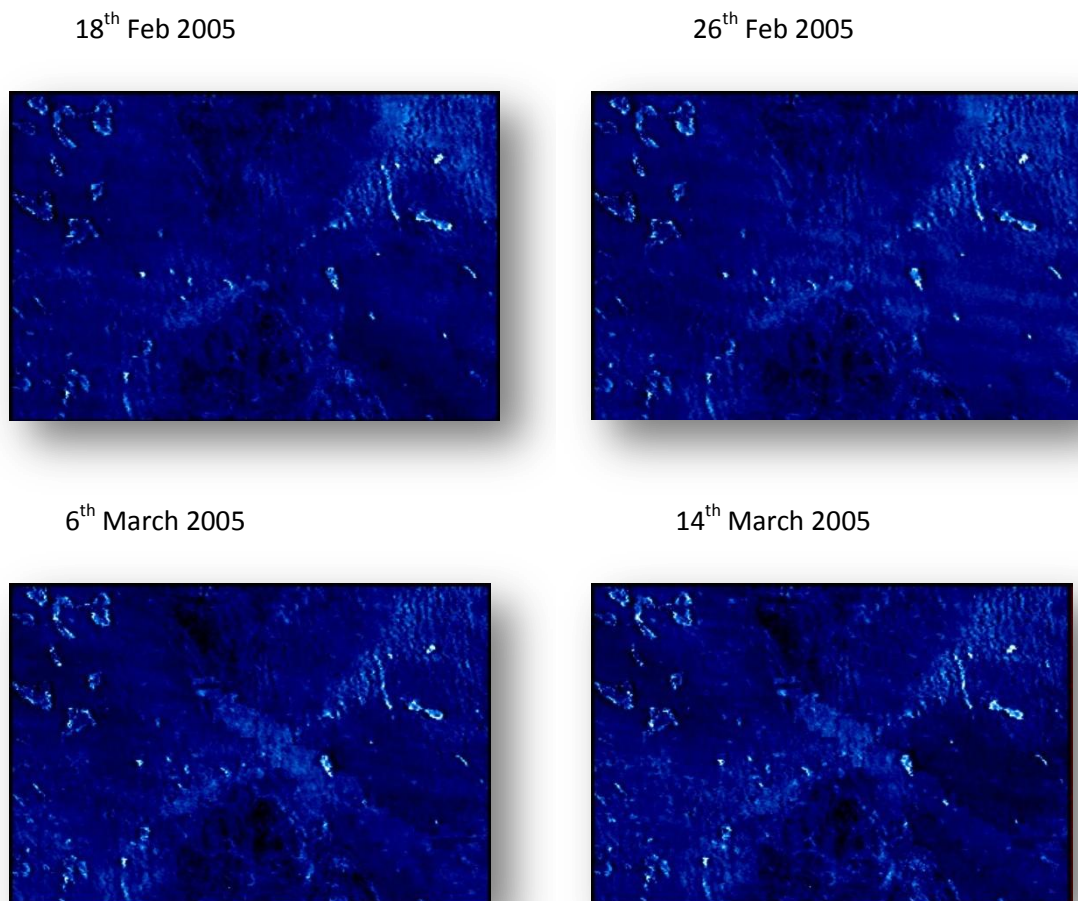6th March 2005

14th March 2005

Figure 6.9 – Derived height-to-width ratio for four consecutive epochs across the study area

6.4.2 Enlargement of pixels' ground IFOV

The footprint size on the ground (i.e. ground instantaneous field of view (IFOV)) of a pixel increases at the edge of the swath. "At nadir, a nominal 1-km pixel has dimensions of 1 x 1-km, but as the scan angle increases from nadir, the pixel dimension grows until at either end of the scan a pixel is approximately 4.8-km cross track x 2-km along track (the 500-m and 250-m nominal pixels increase proportionally to 2.4-km x 1-km and 1.2-km x 0.5-km cross and along track)" (Masuoka et al., 1998) (page 1317). Because pixel size increases with swath angle, a single swath covers 10-km along track at nadir but expands to cover 20-km along track at the end of the scan. The area on the ground overlaps the swath above and below it and means that the same feature on the earth may appear in several scan lines of a MODIS scene if it occurs in a region seen near the edge of the MODIS swath (Masuoka et al., 1998). Individual observations cover several adjacent grid cells at high view zenith angles because the grid cell size of MODIS images are fixed at the same dimensions as the observation dimensions at nadir. The difference between observations and the grid cells increase as the view zenith angle increases because the size of the observation increases while the size of the grid cell remains unchanged (Tan et al., 2006).

Whilst geo-location variations are likely to be random, increases in the ground IFOV are not random and are associated with pixels acquired at the edge of the swath, i.e. when acquired with a larger zenith view angle. Both the height-to-width ratio (derived from MODIS BRDF modelling) and a larger ground IFOV are related to view zenith angles. This common association with the view zenith angle is indicative that the larger ground IFOV may be a causal effect to the height-to-width ratio as described above.

6.4.3 MODIS BRDF processing strategy

A critical assumption in compositing processes (e.g. MODIS BRDF modelling being based on a compositing process) is that the repeated satellite observations cover the same ground area. This assumption is compromised by gridding artefacts that undermine the correspondence between observations and grid cells. Few studies have investigated the bias in biophysical parameters resulting in compositing data (Tan et al., 2006).

Consideration of increases in pixel's ground IFOV have been identified as a possible source of error in MODIS BRDF algorithm although the effects have not been well explored nor are they considered by the MODIS BRDF algorithm (Lucht et al., 2000). The MODIS Science Team at Boston University responsible for the BRDF algorithm are aware of enlargement of pixel's IFOV when acquired at the edge of the swath and the impact that this may have on BRDF inversions and the processing strategy is summarised here. *The V005 MODIS BRDF/Albedo Product MCD43A1 algorithm uses all cloud-free, high quality directional surface reflectances (MO/YD09) L2G (L2Glie) available from both Terra and Aqua over a 16 day period. If, firstly, eight observations (7 or greater) are available and, secondly, the data are not so noisy so that the Ross-Thick-Li-Sparse-Reciprocal BRDF kernel model cannot be fit to the data with a strong RMSE, and, thirdly, if the observations available also sufficiently sample the BRDF view/illumination hemisphere (as determined by the weights of determination (WOD)), then (and only then) can a high full inversion be accomplished.* (The WOD quantifies the adequacy of angular sampling used in the BRDF inversion (Lucht and Lewis, 2000))*. Furthermore the MCD43 algorithm also checks to see if there is an obvious outlier in the data and removes it and then attempts a full retrieval again – if the RMSE and WoD are better with one outlier removed, then that rendition of the model retrieval is used instead. This outlier detection strategy was implemented to primarily remove undetected or sub-pixel clouds or snow. However, it can also come into play whenever one observation is distinctly different from the rest. Note also that we (Boston University) also understand the bowtie effect and the actual observation coverage (obscov) of each gridbox and this can play into the weighting (along with weighting by quality) that each observation receives before the model fit is attempted. While we need sufficient sampling of the view geometry (and therefore need some bigger edge of scan observations) to achieve a full inversion we also attempt to weight these looks to compensate for their size and if they are too obviously unrepresentative then the can cause the retrieval to fail* (personal communication with author 2012).

The selected epochs from which the height-to-width ratio has been derived are for summer 2005. Winter epochs show poorer quality inversions, which were also observed for the spatial transect in this area. For this reason, only epochs with 'best quality inversion' have been considered here. For these epochs, both the near infrared and red band BRDF quality flags specify 'best quality inversions', i.e. indicating that the BRDF inversion includes appropriate angular sampling, cloud contamination is not an issue and that 8 observations have been included in the inversion. This can also be

interpreted as meaning that no outlier observations have been removed or that whilst some observations have been identified as outliers and removed, there still remain 8 or more observations in the BRDF inversion. For example, combining observations from both MODIS sensors on the Terra and Aqua EOS may enable more than 8 observations to be available for inversion of the BRDF model. The specific criteria for updating the quality inversion flags is not known or published to distinguish between these interpretations of the band quality flag when indicating 'best quality inversion'. However, if appropriate observations had been removed from the inversion and the quality flags still indicate 'best quality inversion', then the observed effects around the rim of the dried salt lakes should no longer be apparent. If the described effect remains evident, this suggests that more observations will need to be removed from BRDF inversion processing to fully eliminate this artefact in MODIS BRDF modelling. Growth in pixels' ground IFOV due to non nadir view zenith angles will be gradual and thus the associated variations in reflectance will also be smooth but still exist for all non nadir view angles; albeit reflectance variations will tend to be much smaller for smaller view zenith angles. Whilst consideration of pixels with band quality flags indicating 'best quality inversions' supports greater validity of the results, the appearance of this effect is an issue irrespective of status of the band quality flag. For example, it will equally be problematic if this effect were apparent in the fall back archetypical database of BRDF that is used when insufficient observations are available to perform a BRDF inversion.

It is a design characteristic of the MODIS sensors that all pixels are recorded at their nadir spatial resolution (i.e. 250-m, 500-m and 1-km), even though the ground footprint of pixels are known to increase in size when acquired with non nadir view angles (Tan et al., 2006, Masuoka et al., 1998). An alternative design of the MODIS sensor may have been to vary the spatial resolution of pixels in relation to the view angle at which the pixel was acquired, but this will likely introduce an alternate set of issues, for example creating mosaics from mixed pixel sizes will be problematic. Considering this design characteristic of the MODIS sensors, there are two effects associated with viewing a surface at an oblique angle. It brings the vertical profile of any 3-D shapes on the surface into view and it increases the footprint area on the ground represented by a pixel. If considered at an individual pixel level, variations in surface reflectance could equally and validly be attributed to either of these two effects. There is no means of distinguishing either of these two effects as the source of variations in surface reflectance for a pixel viewed at a non nadir view angle. Based upon variations in view angle only, it is arbitrary as to which of these two effects the changes in reflectance are

attributed. In choosing to measure one effect, the influence of the other effect is assumed negligible or zero. The MODIS BRDF algorithm attributes all reflectance variations to BRDF effects, i.e. directional scattering of reflected light theoretically derived from 3-D surface protrusions and assumes that reflectance variations from pixel footprint growth are negligible or zero. A similar modelling approach may have been developed to measure and correct reflectance variations due to pixel footprint growth, where the BRDF effects may be assumed to be negligible or zero. The results of MODIS BRDF modelling must therefore be a combination of the effects associated with directional scattering of reflected light and reflectance variations from pixel footprint growth.

Separation of directional scattering effects based on sub pixel 3-D surface objects and effects of the larger ground IFOV is not possible at a pixel level without new additional information; that is there are too many degrees of freedom - two effects to be quantified based on observations associated with one variable; the view angle.

In summary, the MODIS BRDF processing strategy does not specifically consider effects associated with the enlargement of pixel's ground IFOV when acquired at the edge of the swath, but seeks to treat observations where this may be an issue as 'outliers' and remove them from BRDF inversion processing.

6.4.4   Testing the pixel growth hypothesis

The hypothesis is that the larger ground IFOV associated with pixels acquired at the edge of the swath is responsible for the height-to-width ratio effects observed around the rims of dried salt lakes as shown in Figures 6.6 and 6.7. To test this hypothesis, NDVI for pixels with a larger ground IFOV can be approximated by calculating the mean NDVI for a pixel and its neighbouring pixels. A 500-m MODIS pixel increases its ground IFOV to 2.4-km x 1-km at the edge of the swath. This can be approximated using MODIS pixels as; 5 x (500-m) pixels cross the track and 3 x (500-m) pixels along the track. As MODIS is onboard a polar orbiting satellites, cross the track is in an East – West direction (i.e. longitude) and along the track in North – South direction (i.e. latitude). Diagrammatically this is shown in Figure 6.10. MODIS bands 1 and 2 used to derived NDVI and are acquired at a nominal spatial resolution of 250-m and aggregated to 500-m nominal spatial resolution for derivation of MODIS BRDF. Therefore this approach to

estimating the effects of a larger ground IFOV is considered a best approximation for 500-m nominal resolution reflective bands and represents the largest possible effect for bands acquired at a 250-m nominal spatial resolution that are aggregated to 500-m nominal spatial resolution, i.e. the spatial resolution of all MODIS pixel's considered in this thesis.
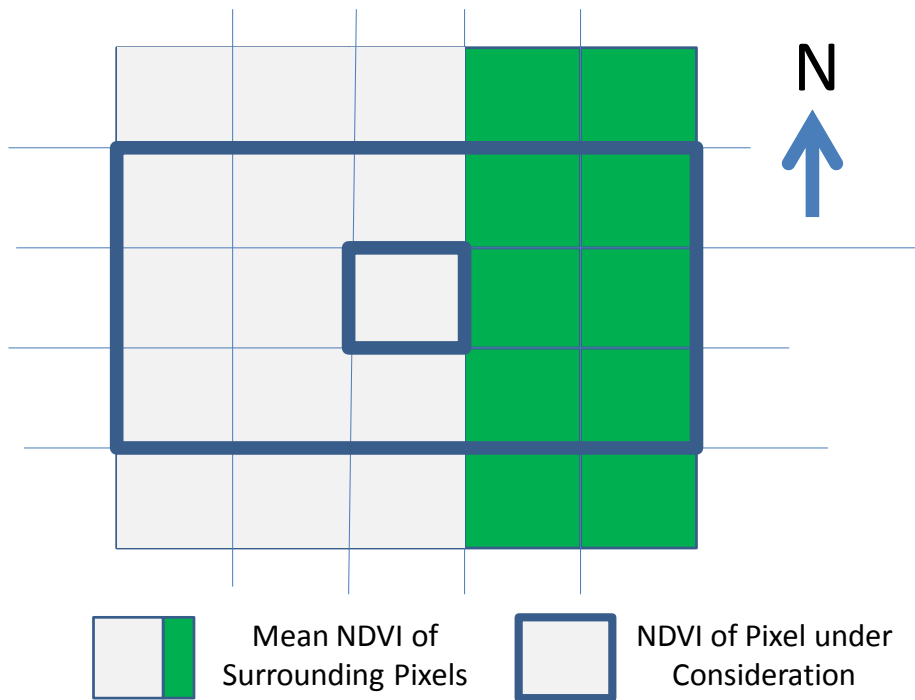
Figure 6.10 – Depicts a pixel under consideration on the inside edge of the dried salt lake when acquired at nadir and the same pixel with a larger ground IFOV when acquired at the edge of the swath and approximated by the mean NDVI response from surrounding pixels.

The mean NDVI response from surrounding pixels provides an approximation for the NDVI response associated with the larger ground IFOV. By taking the difference between the NDVI response from surrounding pixels and the pixel under consideration (i.e. the pixel at the centre), and then dividing by the NDVI response from the pixel under consideration, a unitless ratio results. This has been termed the 'NDVI-ground-footprint ratio' and is mathematically expressed by equation 28. NDVI-ground-footprint ratio approximates the difference in the NDVI response between a pixel acquired at nadir and when the pixel is acquired at the edge of the swath and expresses the

difference as a unitless ratio of the pixel's nadir response. Being expressed as a unitless ratio it can then be directly compared to height-to-width ratio, which is also a unitless ratio.

$$NDVI\ ground\ footprint\ ratio = \frac{NDVI\ Mean - NDVI\ (0°)}{NDVI(0°)} \qquad (28)$$

Where NDVI (0°) is NDVI as observed from a 0° view angle, 0° illumination and 0° relative azimuth for the pixel under consideration and is evaluated from MCD43A1 product as the normalised difference of the NIR and Red weights of the isotropic kernel, and

NDVI Mean is the arithmetic mean NDVI response from the 15 surrounding pixels when observed from a 0° view angle, 0° illumination and 0° relative azimuth, evaluated from MCD43A1 product as the normalised difference of the NIR and Red weights of the isotropic kernel.

The NDVI-ground-footprint ratio may be derived from different datasets, as the focus of consideration is on the relative difference in the NDVI response between a MODIS sized pixel if acquired at nadir compared to the larger ground footprint of the pixel had it been acquired at the edge of the swath. For example, NBAR, MOD09, Landsat ETM+ or any other sensor's data with appropriately rescaled pixels could be used, although alternative sensors may introduce additional sources of variability. The use of the normalised difference between near infrared (MODIS Band 2) and red (MODIS Band 1) isotropic parameters weights (used here in equation 28) is convenient, but also represents reflectance values that are independent of angular effects and therefore most representative of a nominal 500-m pixel spatial ground resolution.

Considering the form of equation 28 some comments can be made. For surfaces that exhibit a homogeneous NDVI response over the larger ground IFOV, the NDVI-ground-footprint ratio will equal zero, i.e. *NDVI Mean = NDVI (0°)*. If the NDVI response from surrounding pixels is greater than the NDVI response of the pixel under consideration at the centre, the NDVI-ground-footprint ratio will be positive, e.g. a pixel of bare soil surrounded by vegetation. Conversely, if the NDVI response from surrounding pixels is

less than the NDVI response of the pixel under consideration at the centre, the NDVI-ground-footprint ratio will be negative, e.g. a pixel containing vegetation surrounded by bare soil. Because the NDVI-ground-footprint ratio is the result of dividing by the NDVI response of the pixel under consideration, if this value is low (e.g. bare soil) then the magnitude of the NDVI-ground-footprint ratio will tend to be larger. If the pixel under consideration has a high NDVI response, (e.g. dense vegetation) then the magnitude of the NDVI-ground-footprint ratio will tend to be smaller.

As per equation 28, the NDVI-ground-footprint ratio has been derived for pixels within the surface study area. This reduces the size of the surface study area by four pixels in the East – West (longitude direction) and two pixels in the North – South (latitude direction). The results are shown in Figure 6.11 and an enlargement of the area at the top left corner of the surface study area is shown in the left image of Figure 6.12.
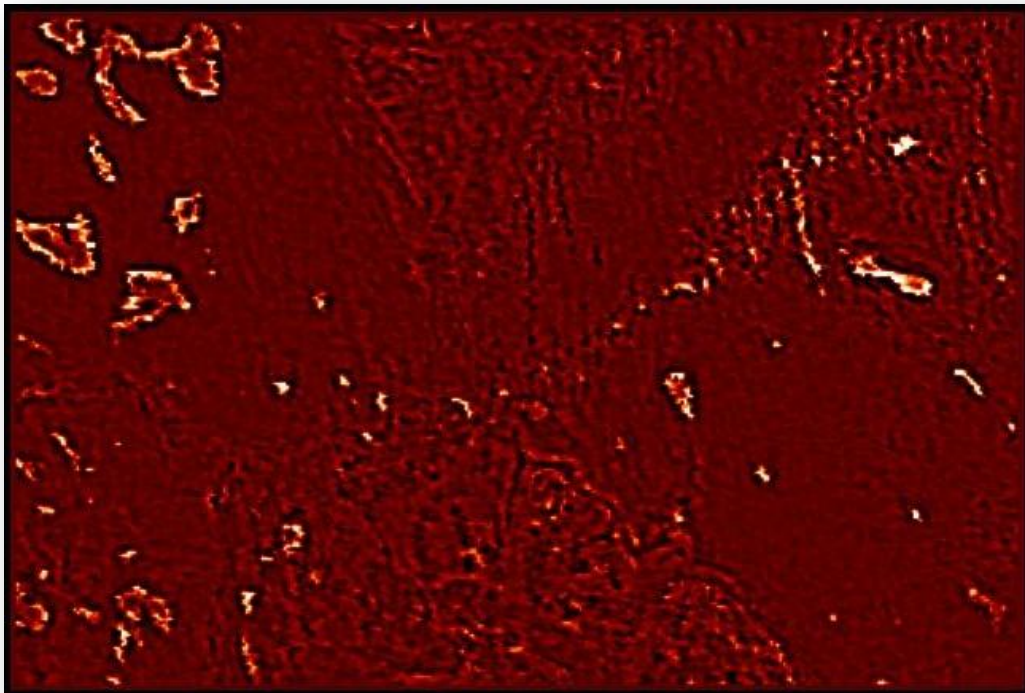

Figure 6.11 – Derived NDVI-ground-footprint ratio for the study area
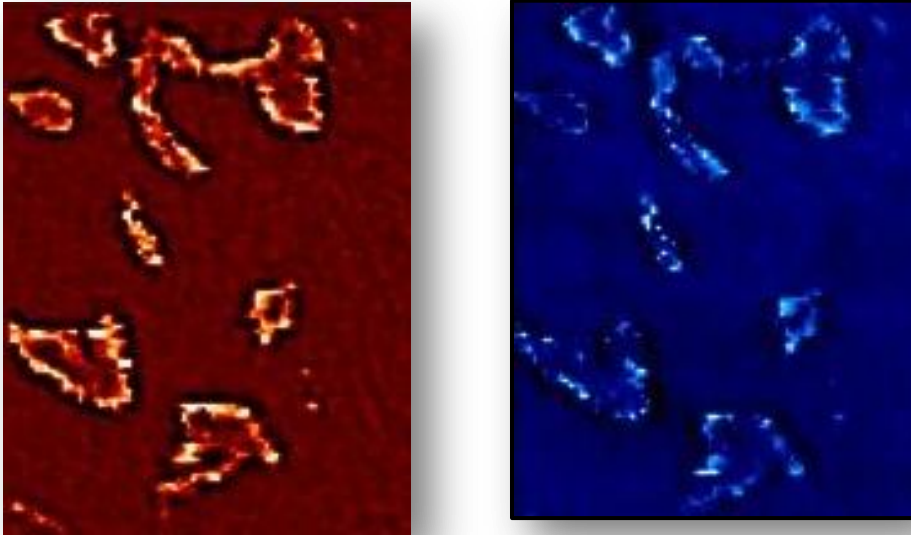
Figure 6.12 – Derived NDVI-ground-footprint ratio, showing an enlargement of the region in the top left corner of study area (left/red) and the derived height-to-width ratio for the same area (right/blue), i.e. being the same as figure 6.7.

The NDVI-ground-footprint ratio and the height-to-width ratio are shown side-by-side for the same ground surface area in Figures 6.12. Clearly, both these images exhibit similar spatial patterns, i.e. higher values on the inside rim of the dried salt lakes and lower values immediately outside. There is no valid reason why the height-to-width ratio should be related to the NDVI-ground-footprint ratio, i.e. the height-to-width ratio is derived independently for pixels and the NDVI-ground-footprint ratio is derived from NDVI differences between neighbouring pixels.

The height-to-width ratio and the NDVI-ground-footprint ratio may be considered as abstract quantities. However, a geometric interpretation can also be considered and may assist to further explain the cause of the relationship between height-to-width ratio and the NDVI-ground-footprint ratio. Just as NDVI may be considered to represent the horizontal surface area within a pixel covered by vegetation, the height-to-width ratio and the NDVI-ground-footprint ratio may also be considered to be areas of vegetation cover, expressed as a ratio of the horizontal vegetation cover within the pixel when viewed at nadir. The height-to-width ratio describes a vertical surface area if upright prisms of vegetation are considered and made visible by a larger zenith view angle and the NDVI-ground-footprint ratio describes a horizontally flat surface area of vegetation in surrounding grid cells made apparent by the larger ground IFOV when pixels are acquired with a larger zenith view angle.

112

The height-to-width ratio and NDVI-ground-footprint ratio express the change in NDVI as unitless ratios of the NDVI response from the pixel derived at a nadir observation. The NDVI-ground-footprint ratio approximates variations in NDVI response associated with the larger ground IFOV where the height-to-width ratio considers pixels to be of a fixed size (as per MODIS BRDF modelling) and attributes all observed variations in NDVI to vertical structure.

As discussed in chapter 4, modelling is equivalent for pixels containing one large vegetation prism or a large number of smaller vegetation prisms, as would be realistically expected, as only the surface area of the vegetation prisms and not the volume that the vegetation prisms occupy in 3-D space is being considered. Similarly, for changes in the NDVI response due to the larger ground IFOV, it is inconsequential where within the larger footprint the vegetation occurs, i.e. clumped together in one neighbouring grid cells or distributed across several neighbouring grid cells as may realistically be expected. Diagrammatically, Figure 6.13 depicts a single prism of vegetation and a single clump of vegetation as being responsible for height-to-width ratio and the NDVI-ground-footprint ratio respectively. MODIS BRDF modelling (from which the height-to-width ratio is derived) does not consider enlargement of a pixel's ground IFOV and therefore all variations in NDVI resulting from the larger ground IFOV are attributed as sub pixel vertical structure, i.e. MODIS BRDF modelling interprets variations in the left image of Figure 6.13 as if it were the right image of Figure 6.13.
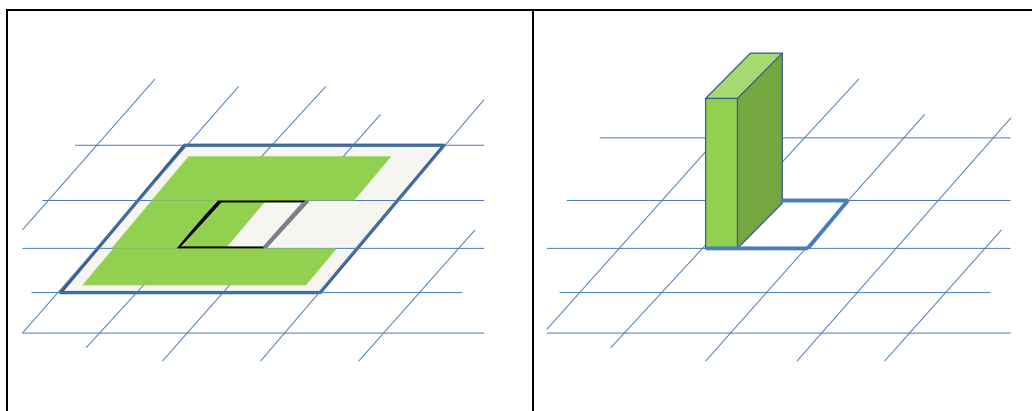
Figure 6.13 – Depiction of the increase in the area of vegetation cover associated with a larger ground IFOV (left) and the increase in the area of vegetation associated with the exposure of the vertical surface (right), both made apparent with increased view zenith angles

Figure 6.14 is a scatter plot of the height-to-width ratio against the NDVI-ground-footprint ratio. For the plotting of points and their inclusion within Figure 6.14, if the correlation (between the model and NDVI derived from MODIS BRDF across the same range of view angles) is less than 0.99 or the RMSE is greater than 0.005, then the mean height-to-width ratio and mean of the NDVI-ground-footprint ratio have been substituted in the plot. This seeks to remove a small number of values where the model did not provide a good fit with MODIS BRDF modelling. As shown in Figure 6.5, when the model described in this thesis does not a provide a good re-expression of MODIS BRDF modelling (i.e. low correlations and high RMSE) then the derived values for the height-to-width ratio generally tend to be zero.

As discussed above, both the height-to-width ratio and the NDVI-ground-footprint ratio can be considered to represent the additional vertical and horizontal areas respectively of vegetation relative to the vegetation cover within the pixel. Therefore, if the larger ground IFOV is responsible for the observed variations in the height-to-width ratio, the relationship between the height-to-width ratio and the NDVI-ground-footprint ratio should be linear as both parameters can be considered measures of the surface areas of vegetation cover.

Figure 6.14 - Derived height-to-width ratio (y-axis) against NDVI-ground-footprint ratio (x-axis). The cardinal axis and a line of best fit have been included in the plot. Y-intercept = 0.024 and slope = 0.644

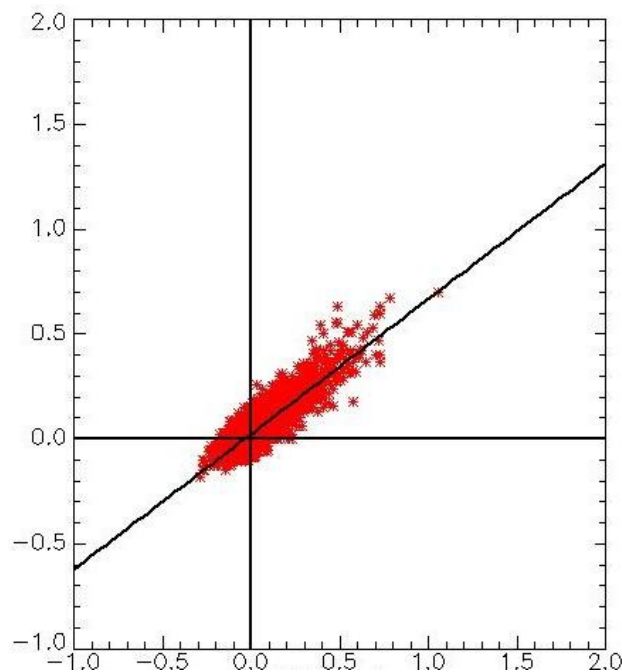Figure 6.14 shows a linear relationship between the height-to-width ratio and the NDVI-ground-footprint ratio with a correlation of 0.7. The line of best fit passes (nearly) through the origin, indicating that if the NDVI-ground-footprint ratio is zero (i.e. a homogeneous surface over the area of the larger ground IFOV) then the height-to-width ratio will also tend to zero. A zero height-to-width ratio implies a 3-D flat surface where the surface is invariant to view angle, i.e. an isotropic surface where no BRDF effects are apparent. This suggests that the variations in NDVI associated with a larger ground IFOV are the predominant cause of variations in the height-to-width ratio.

It may be expected that surface features with particular characteristics and spatial scales may more prominently highlight this effect, i.e. features that have sharp well defined boundaries within an area of the larger ground IFOV footprint (i.e. 2.4km x 1km) and where the NDVI difference between the feature and surrounds is greatest. Very large scale features that have a fuzzy boundary, such as the gradual transition between grassland and forest will appear homogenous at the larger ground IFOV scale and therefore will not generate significant NDVI-ground-footprint ratio or height-to-width ratio effects. Surfaces dominated by sub-pixel sized features (e.g. individual trees) will also tend not to provide recognisable spatial patterns and the variations in NDVI associated with sub pixel distribution of these features will appear as random noise in derived height-to-width ratio maps. The dried salt lakes in the study area just happen to be features that most prominently highlight this artefact in MODIS BRDF modelling and can also be readily associated with identifiable surface features. However, the continuous distribution of plot points in Figure 6.14 suggests that this effect exists uniformly across the whole study area, even if not necessarily identifiable with well defined surface features in Figures 6.6 and 6.7.

In summary, section 6.4 described an alternate interpretation for observed variations in the derived height-to-width ratio, i.e. variations in the height-to-width ratio are highlighting an artefact in the MODIS BRDF modelling. This is due to variations in the NDVI response associated with a larger ground IFOV when pixels are acquired at the edge of the swath. This is a well understood characteristic of the MODIS sensor but is not specifically considered by the MODIS BRDF algorithm. Finally, an empirical test has been developed which shows a strong relationship between the height-to-width ratio and variations in NDVI associated with a larger ground IFOV. It is difficult to identify any reason why a relationship between these variables should exist, other that the

explanation suggested here. This combines to provide good evidence in support of this alternate interpretation of the results.

6.5   Consideration of other surface areas

One reason for selecting the study area in north east South Australia was that it was sparsely vegetated. Issues associated with mutual obscuration of vegetation, which is not considered by the model are therefore minimised. If however, the derived height-to-width ratio is primarily associated with variations in NDVI from surrounding pixels then this constraint on the selection of a study area no longer needs to be observed. Providing the MODIS BRDF band quality flags indicate 'best quality inversion' a broader range of study areas may be examined and should produce the same relationship between the height-to-width ratio (derived from MODIS BRDF modelling) and the NDVI-ground-footprint ratio (derived from variations in NDVI associated with the larger ground IFOV). Furthermore, the study area in north east South Australia is an extreme (arid, low NDVI) environment and this may have impacted results.

Three additional surface areas have been selected along the transect line between Melbourne – Darwin (chapter 5). Areas of 1 ½ ° longitude by 1° latitude have been selected and at temporal periods where the MODIS BRDF band quality flags indicate 'best quality inversions'. Each of these additional study areas is approximately 18,000 km^2 with their location indicated within the image of the Australian continent (Figure 6.15) and table 6.16.

Figure 6.15 – The Australian continent showing the location of the additional study

surface area indicated by the white, yellow and green boxes (Source : Google Earth)

Table 6.16 – Location and selected epoch for additional study surface areas

Study Area	Location (lower left to upper right corner)	Epoch
Victoria (Green)	37° Lat, 143° Long To 36° Lat, 144° 30' Long	18th Feb 2005
T Simpson Desert (Yellow)	26° Lat 35° Long To 25° Lat, 36° 30' Long	18th Feb 2005
Northern Territory (White)	14° 30' Lat, 131° Long To 13° 30' Lat 132° 30' Long	4th July 2005

The height-to-width ratio and the NDVI-ground-footprint ratio have been derived as

previously described. As with the previous study area, the model (with best fit height-

to-width ratio substituted) provides a good fit with NDVI derived from MODIS BRDF modelling over the same range of view angles. Scatter plots of the derived height-to-width ratio against the NDVI-ground-footprint ratio for the three areas are shown in Figures 6.17, 6.18 and 6.19. For the plotting of points and their inclusion in Figure 6.17 – 6.19, the mean height-to-width ratio and mean NDVI-ground-footprint ratio have been substituted for values where the correlation is less than 0.99 or where the RMSE is greater than 0.005 or where MODIS BRDF band quality flags indicate other than 'best quality inversion'. This seeks to remove a small number of values where the model did not provide a good fit with MODIS BRDF modelling or where there were MODIS BRDF inversions issues, e.g. water bodies. The cardinal axis and lines of best fit have also been included in the plots.
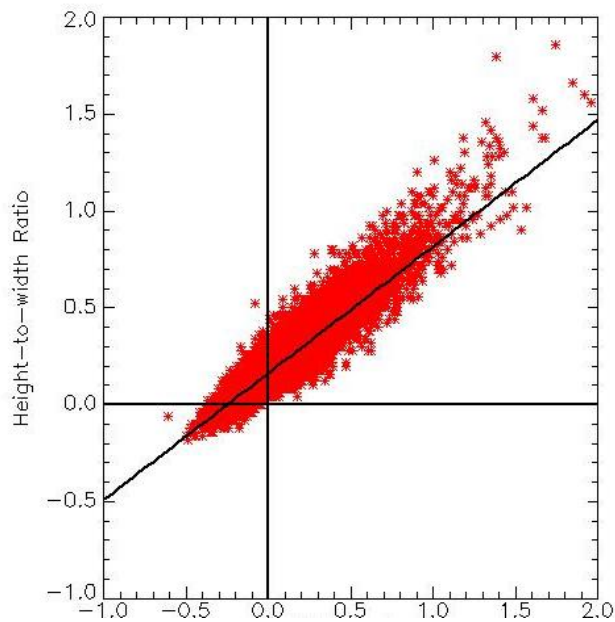

Figure 6.17 – Derived height-to-width ratio (y-axis) against NDVI-ground-footprint ratio (x-axis) for the Victorian study area
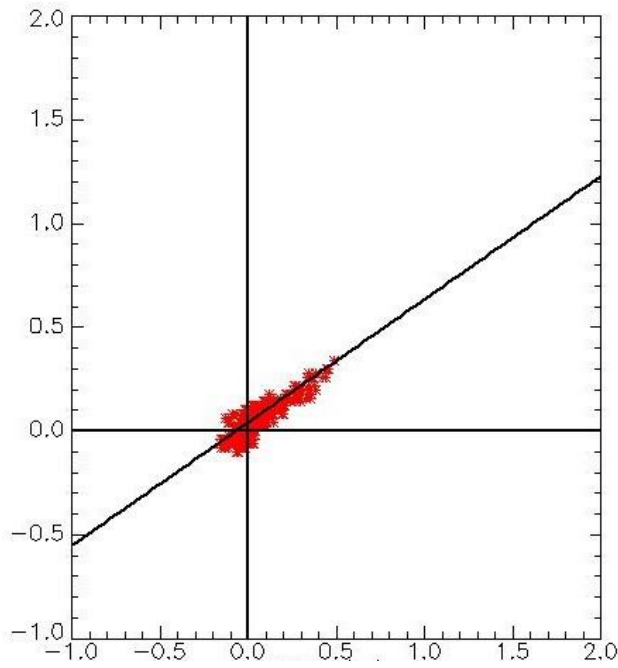
Figure 6.18 – Derived height-to-width ratio (y-axis) against NDVI-ground-footprint ratio (x-axis) for the Simpson Desert study area
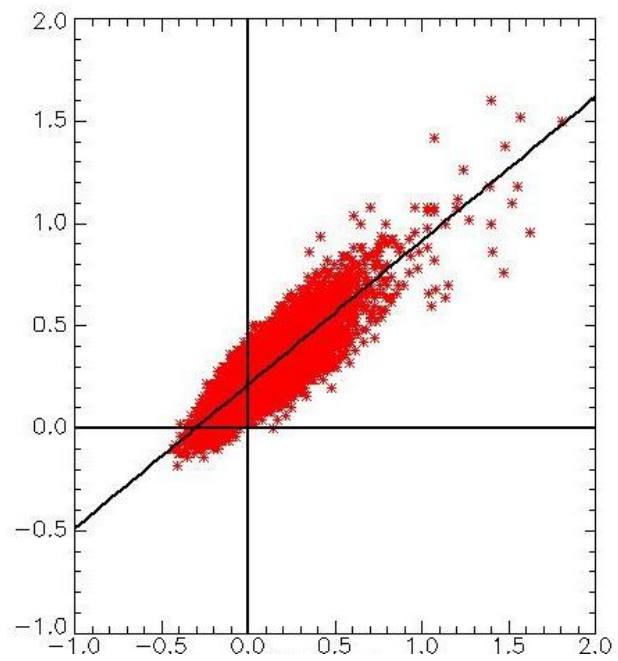

Figure 6.19 – Derived height-to-width ratio (y-axis) against NDVI-ground-footprint ratio (x-axis) for Northern Territory study area

All four surface study areas demonstrate the same relationship between the NDVI-ground-footprint ratio and the height-to-width ratio, i.e. a strong linear relationship with the same gradient. The Simpson Desert showed lower magnitude values, reflecting the homogeneous nature of the area and also displayed a lower correlation (0.5) which is consistent with values being more clumped about the origin.

One significant difference between the four study areas is the y-axis intercept, i.e. the gradient of the line of best fit remains the same but plot points appear shifted by a constant. The two desert regions have a near zero intercept. The Northern Territory and Victorian intercepts are both positive. The Northern Territory intercept is higher than Victoria's. This is consistent with the spatial transect between Melbourne and Darwin where the derived height-to-width ratio was generally observed to be lower across central Australia and tending to be larger in the Northern than in Southern areas of Australia. An explanation, in the context of the spatial transect was unclear, although latitude or solar angle were suggested in chapter 5 as possible factors. An examination (refer Appendix 1) of these areas taken at different epochs (i.e. realising different solar angles) suggests that neither the latitude nor the solar angle are prime factors associated with different intercept points and this difference remains unexplained.

6.6   Reinterpretation of results from the temporal and spatial transects

With the understanding that the height-to-width ratio is very significantly associated with an artefact in MODIS's BRDF modelling, can the results from the temporal transect (chapter 4) and spatial transect (chapter 5) be reinterpreted? In particular, can the results that were difficult to explain in chapter 4 be now explained?

For the temporal transect (chapter 4), single species cropped fields were selected, that were greater than $1km^2$ in area, in order that random pixel geo-location inaccuracies could be effectively ignored, i.e. whilst the ground location of a pixel notionally vary up to +/- 250m, the pixels will always fall within the area of the designated field. The larger ground IFOV for pixels acquired at the edge of the swath would indicate that fields approaching $4km^2$ in area would need to be found for this criteria to be fully valid. Therefore, the results from the single species cropped fields used in chapter 4 are likely to have been influenced by vegetation cover from surrounding areas outside of the

cropped field being studied. This is depicted in Figure 6.20 which shows ground footprint of a MODIS 500-m pixel (acquired at nadir) and the same pixel if acquired at the edge of the swath for Cubbie Station field 2.

Figure 6.20 – Depicts a nominal 500-m MODIS pixel and a MODIS pixel with a larger ground IFOV when acquired at the edge of the swath at Cubbie Station

(Source: Google Earth)

As discussed in chapter 5, larger derived height-to-width ratios were observed for bare soil on fields at Cubbie Station than for pixels taken from the Simpson Desert, although both exhibited very similar (low) NDVI responses. The larger height-to-width ratio for bare soil on fields at Cubbie Station is well explained by the influence of vegetation cover from the surrounds or from neighbouring fields. Similar variations are unlikely to exist for pixels taken from the Simpson Desert where larger homogenous areas tend to be present and therefore the NDVI-ground-footprint ratio will be close to zero and the derived height-to-width ratio will also be near zero, i.e. more isotropic reflectance. With similar considerations, differences in the derived height-to-width ratio between cotton/wheat at Cubbie Station and sugar cane at Davco Farming can also be explained. Figure 5.1 shows that for NBAR NDVI responses in the range of 0.3 – 0.5, the derived height-to-width ratio for cotton/wheat grown at Cubbie Station is less than the derived height-to-width ratio for sugar cane grown at Davco Farming. The cotton/wheat fields at Cubbie Station are approximately 50% larger in area than the sugar cane fields at Davco Farming and furthermore neighbouring fields at Cubbie Station tend to have the same cropping cycle, i.e. when a field is fallow the neighbouring fields also tend to be

fallow. This means that the study areas at Cubbie Station tend to be more homogeneous over an area represented by the larger ground IFOV. This greater homogeneity within an area the size of the larger ground IFOV results in smaller angular variability in MODIS BRDF modelling and smaller height-to-width ratios as per the modelling described within the thesis.

For the single species cropped fields, the effects associated with the larger ground IFOV also explain the end-member profiles, i.e. a rising profile of NDVI with larger view angles for bare soil and a falling profile of NDVI with larger view angles for mature crop canopies. Refer to Figure 4.21. For epochs when NDVI is lowest (i.e. bare soil), any enlargement of the ground IFOV will generally tend to increase the NDVI response which is at the lowest possible value and lower values are unlikely to be observed. Therefore a larger ground IFOV will tend to produce larger NDVI responses and a rising NDVI profile with larger view zenith angles for bare soil end-members. The opposite applies to epochs when NDVI is largest (i.e. mature crop canopy). Any enlargement of the ground IFOV will generally tend to decrease the NDVI response which is at the highest possible value and higher values are unlikely to be observed. Therefore a larger ground IFOV will tend to produce lower NDVI responses and a falling NDVI profile with larger view zenith angles for mature crop canopy end-members.

It was suggested in chapters 4 and 5 that the height-to-width ratio may be able to detect low densities of vegetation that are only apparent when viewed obliquely. In a manner this can still be said to be true, however the detection of vegetation is not related to vegetation within the pixel but rather from surrounding vegetation that is made apparent by the larger ground IFOV when a pixel is acquired at higher view zenith angles and used in MODIS BRDF modelling. Where there are large differences in NDVI response from neighbouring pixels, these effects will tend to be largest. For example, the 'spikes' in the derived height-to-width ratio along the spatial transect are likely to be the inside rims of dried salt lakes (or similar features) that have a low NDVI response but are surrounded by areas with a higher NDVI response.

In chapter 4, three aspects of the result were identified as inconsistent or difficult to explain. Firstly the negative values for the derived height-to-width ratio can now be explained as being due to the NDVI response of a pixel being higher than the NDVI response from surrounding areas, e.g. a pixel of vegetation surrounded by bare soil. The two other effects that were difficult to explain were the magnitude of derived height-to-width ratio and its insensitivity to crop row orientations. Both these aspects are very

specific to sub pixel vegetation structure. If MODIS BRDF modelling was detecting sub pixel structure (as theoretically considered by the modelling) then results should be sensitive to these effects. That the derived height-to-width ratio appears insensitive to these considerations can be taken as further evidence that the dominant influence in the derived height-to-width ratio is variation in NDVI from surround pixels and not vertical vegetation structure at the sub pixel level.

In summary, all the observed results for the temporal and spatial transects are consistent and support the interpretation that the height-to-width ratio is the result of NDVI variations between a pixel and it's surrounds rather than the directional scattering of reflected EMR caused by vertical structures within the pixel as theoretically considered by BRDF modelling.

6.7   Partitioning the derived height-to-width ratio

6.7.1   Introduction

Whilst the derived height-to-width ratio appears dominated by the effects of reflectance variations associated with the larger ground IFOV, the derived height-to-width ratio may still contain some information about the vertical structure of vegetation within the pixel. For example, for surfaces that are homogeneous across an area equal to the larger ground IFOV, the NDVI-ground-footprint ratio will be zero and therefore any non-zero values for the derived height-to-width ratio can be considered fully attributable to the vertical structure of vegetation within the pixel. Finding surfaces that are homogeneous at a 500-m and 4km^2 scales (being the area of the larger ground IFOV) may be difficult and will tend to be extreme arid desert regions effectively devoid of vegetation, e.g. the Simpson Desert. The original objective of this thesis may still be achieved if the derived height-to-width ratio can be partitioned and effects attributable to variations in NDVI associated with the larger ground IFOV removed, i.e. answering research question 4 that sought to use MODIS BRDF effects to identify the vertical structure of vegetation at the pixel level.

6.7.2 Development of process for partitioning effects

In certain circumstances the derived height-to-width ratio can be separated into the contribution attributable to reflectance variations associated with the larger ground IFOV and a contribution attributable to the vertical vegetation structure within the pixel (i.e. directional scattering of reflected EMR). For temporally invariant surfaces, BRDF effects associated with the vertical structure of vegetation present in the pixel may be considered constant over a (short) period of time and therefore all temporal variations in the derived height-to-width ratio over the same time interval may be attributed to effects associated with enlargement of pixels' ground IFOV. Furthermore, the derived height-to-width ratio can be considered to include these two components in a linear combination as evident in Figure 6.14. Considering the derived height-to-width ratio of a pixel from a temporally invariant surface over several consecutive epochs will enable a 'best fit' separation of these two effects; i.e. a 'constant' associated with the vertical vegetation structure within the pixel and a 'multiple' associated with variations in NDVI between the pixel and its surrounds made apparent by the larger ground IFOV. With this consideration, surfaces that are not spatially homogeneous over an area the size of the larger ground IFOV may be examined and vertical vegetation structure within the derived height-to-width ratio isolated. These considerations are mathematically expressed by equation 29.

$$H_{(x, y, t)} = C_{(x, y)} + M_{(x, y)} \times N_{(x, y, t)} \qquad\qquad (29)$$

Where: $H_{(x, y, t)}$ is the height-to-width ratio (derived as per equation 27) for a pixel with grid positions (x, y) at epoch t,

$C_{(x, y)}$ is a constant representing the component of the height-to-width ratio attributable to the vertical structure of vegetation within the pixel with grid positions (x, y),

$M_{(x, y)}$ is a linear multiple of the NDVI-ground-footprint ratio for a pixel with grid positions (x, y), and

$N_{(x, y, t)}$ is the NDVI-ground-footprint ratio (derived as per equation 28), for a pixel with grid positions (x, y) at epoch t.

The study area previously considered in north east South Australia may be considered temporally invariant during summer months. The height-to-width ratio and NDVI-ground-footprint ratio have been derived for five consecutive epochs as per the methods discuss in previous chapters. Values for the parameters $C_{(x, y)}$ and $M_{(x, y)}$ are derived independently for each pixel that yield a best fit over five consecutive epochs. Schematically this is depicted in Figure 6.20.
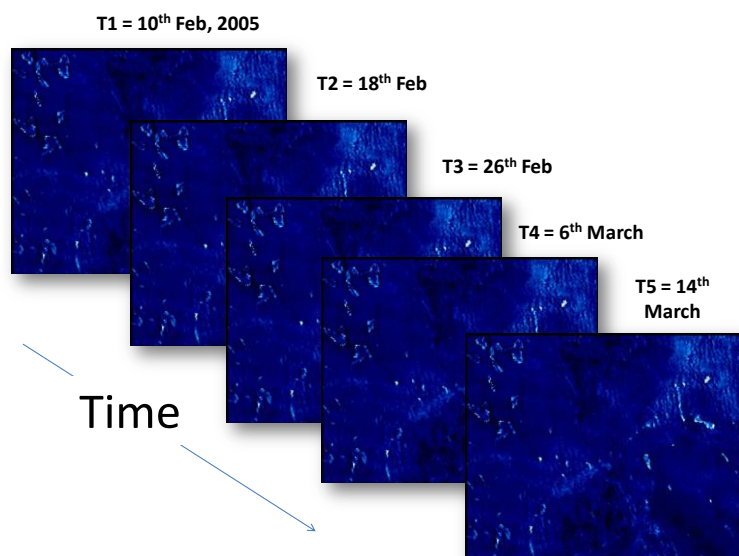
Figure 6.20 – Derived height-to-width ratio from sequential epochs

It is a necessary assumption that the surface is invariant across the 5 (observation) epochs, i.e. 10th Feb to 14th March. The inclusion of a larger number of epochs will provide greater redundancy in deriving the two component parameters (i.e. $C_{(x, y)}$ and $M_{(x, y)}$) but necessitates extending the assumption of temporal invariance for a longer period of time. Deriving two parameters from 5 observations (epochs) is considered appropriate and may be compared with MODIS BRDF modelling which seeks to derive 3 parameters from 8 observations, although observations used in MODIS BRDF modelling are over a much shorter time window, i.e. MODIS BRDF modelling uses daily observations rather than the 8 day interval data used here to separate the derived height-to-width ratio.

6.7.3 Results

The results are displayed as two intensity maps for the study area. Figure 6.21 shows the component of the height-to-width ratio attributable to the vertical structure of vegetation within the pixel, i.e. the constant $C_{(x,y)}$ and Figure 6.22 shows the multiple attributable to variations in NDVI associated with enlargement of the ground IFOV, i.e. $M_{(x,y)}$. For the study area of approximately 68,000 pixels, the mean of $C_{(x,y)}$ is 0.026 and mean of $M_{(x,y)}$ is 0.603. These values are comparable and consistent to the y-intercept and slope of height-to-width ratio when plotted against the NDVI-ground-footprint ratio in Figure 6.14 and Figures 6.17 – 6.19 which represent a single epoch only. This means that whether considered temporally or spatially, variations in NDVI associated with the larger ground IFOV contribute similarly to the derived height-to-width ratio.

To assist visualisation, both Figures 6.21 and 6.22 have floor values defined as their mean less three standard deviations and ceiling values defined as their mean plus three standard deviations. The images in Figures 6.21 and 6.22 have had brightness values scaled within these respective ranges. White/lighter coloured areas indicate higher values and darker areas indicate lower/negative values.
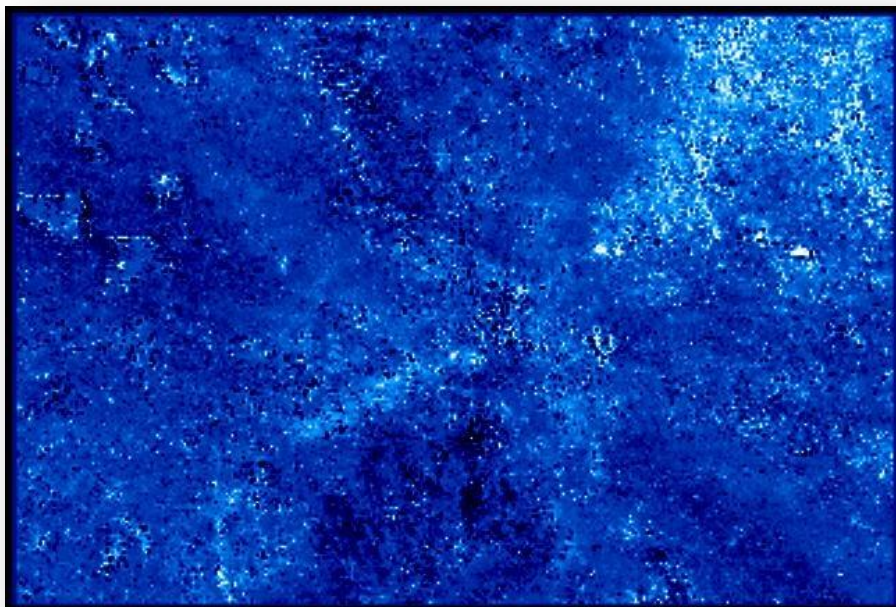
Figure 6.21 – The derived 'constant' of the height-to-width ratio attributable to the vertical structure of vegetation within the pixel, i.e. $C_{(x,y)}$
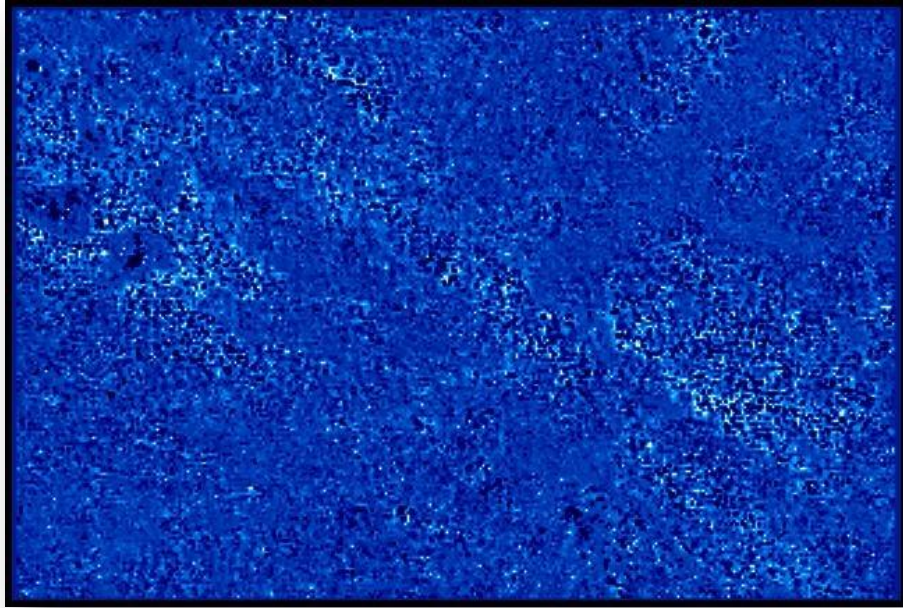
Figure 6.22 - The derived component of the height-to-width ratio attributable to variations in NDVI that are associated with enlargement of the ground IFOV, i.e. the linear 'multiple' of the NDVI-ground-footprint ratio $M_{(x, y)}$

The derived coefficients ($M_{(x, y)}$) attributable to the NDVI-ground-footprint ratio do not appear associated with any particular surface features, i.e. Figure 6.22 appears almost uniform and featureless with no apparent spatial pattern with known surface features. This indicates that variations in NDVI associated with enlargement of the ground IFOV are consistent and uniform across the study area.

In Figure 6.21, the magnitude of derived values for the "constant" component is small and close to zero, i.e. mean value is 0.026. Variability around the rims of the dried salt lakes has diminished, but larger values are still apparent in the top right of the image which surround Cooper Creek. Other than to say that the constant component of the height-to-width ratio appears to exhibit more spatial information and variability compared to the derived coefficient associated with the NDVI-ground-footprint ratio, it is difficult and speculative to make an interpretation of Figure 6.21.

This approach to partitioning the derived height-to-width ratio into components is similar in principal to that used by MODIS BRDF modelling, where by the surface is considered temporally invariant during the period when observations are acquired and

all reflectance variations are attributable to angular effects. The procedure described here assumes that the height-to-with ratio is temporally invariant during the period when observations are acquired and all variations are attributable to larger ground IFOV effects. The procedure is analogous to adding an additional parameter (and kernel) to the RossThick-LiSparse representation used for MODIS BRDF modelling. The additional (fourth) parameter represents reflectance variations associated with enlargement of the pixel's ground IFOV and would free the isotropic, volumetric and geometric parameters to model the directional scattering of reflected light as intended. The procedure described here is retrospective in its approach to removing effects associated with enlargement of a pixel's ground IFOV from MODIS BRDF modelling. The approach described here is indicative and is not suggested as being a robust solution. For example, the approach is derived using 8 day interval data, requires the surface to be temporally invariant over a two month period and is based upon variations in NDVI rather than individual reflectance bands. Further research is required if information about the (vertical) structure of vegetation is to be derived from MODIS BRDF modelling or MODIS BRDF modelling were to be enhanced to address pixel enlargement issues.

6.8 Summary of results exploring the spatial relationship of BRDF effects

In chapter 6, the model previously described for interpreting MODIS BRDF effects was applied to a surface area. This allows the derived height-to-width ratio to be displayed in a map format and the spatial pattern for derived values was explored. An arid area in central Australia, through which the spatial transect line passed indicating variability in the height-to-width ratio associated with water features and was selected as the principal surface study area. The model (with best fit height-to-width ratio substituted) provided good correlations to NDVI derived from MODIS BRDF modelling and had low RMSE. This supports the model and derived height-to-width ratio as a valid re-expression of MODIF BRDF modelling.

Larger height-to-width ratios appear evident on the inside rim of dried salt lakes with corresponding low values immediately outside the dried salt lakes. Rather than a sub-pixel structural characteristics of vegetation being the cause of this effect, an alternative explanation is that this effect is highlighting an artefact in MODIS BRDF modelling

associated with the larger ground IFOV of pixels, when observations used in deriving MODIS BRDF parameters, have been acquired towards the edge of the swath.

Section 6.4 summarised the argument for this alternative explanation by identifying:

- Enlargement of pixels' ground IFOV is a well understood characteristic of the MODIS sensor.
- Enlargement of pixels' ground IFOV is not specifically considered in the MODIS BRDF algorithm.
- The height-to-width ratio is derived independently for each pixel, as is MODIS BRDF modelling for which the height-to-width ratio seeks to re-express. However, positive and negative values for the derived height-to-width ratios appear spatially (inversely) related which suggests they are not derived independently for each pixel.
- A metric approximating the change in NDVI associated with enlargement of a pixel's ground IFOV (i.e. NDVI-ground-footprint ratio) provides a strong linear relationship (as theoretically expected) with the height-to-width ratio. Other than the hypothesis put forward here, there is no reason why these two variables should be related.

Sections 6.5 to 6.7 provide additional support for this explanation:

- A selection of other study sites across Australia all yield consistent results.
- The results of the temporal (chapter 4) and spatial transects (chapter 5) are all well explained by this alternate understanding.
- A retrospective approach to remove the contribution attributable to larger ground IFOV effects from the derived height-to-width ratio provides a consistent result in support of this alternate explanation.

These results combine to provide strong evidence in support of the alternate explanation for variations in the height-to-width ratio proposed within this thesis, i.e. variations in the derived height-to-width ratio are primarily attributable to variation in reflectance associated with enlargement of pixel's ground IFOV when acquired at the edge of the swath rather than the directional scattering of reflected EMR caused by sub pixel vertical vegetation structure as theoretically considered by BRDF modelling.

7 Conclusion

7.1 Introduction

This concluding chapter is separated into three sections. The first section summarises the key finding of this thesis. However, rather than repeating verbatim the summaries from earlier chapters, this section seeks to summarise the findings with a retrospective understanding. The second section considers corollaries and implications of this finding to MODIS BRDF modelling in general. The final section suggests further research opportunities that directly follow from the findings within this thesis.

7.2 Summary of results from previous chapters

The motivation for this thesis was to explore how multi-angular satellite data could assist with the characterisation of vegetation. More specifically, by viewing vegetation from nadir to progressively oblique angles, some measure of the height of vegetation may be determined, i.e. research question 4. For example, it may be expected that tall thin vegetation will appear to increase in its abundance when viewed at increasingly oblique angles compared with low flat vegetation. This effect may be observed directly by acquiring multi angular images from an EOS sensor and modelling changes in the appearance of vegetation cover. However directly acquiring and modelling suitable multi-angular views of appropriate surfaces is difficult and the processing required would be essentially the same as deriving parameters for a BRDF representation.

It is common in remote sensing analysis to standardise data to a common viewing geometry to enable a more valid comparison of surface features; the default being to bring surface reflectance data to a nadir viewing geometry. For the MODIS sensor, a standard product exists to achieve this where the product parameters have been derived and are available at a pixel level for individual reflectance bands, i.e. the MCD43 product. The MCD43 product is based on MODIS observations and models the Bidirectional Reflectance Distribution Function (BRDF) of reflected EMR from surfaces theoretically based upon a sub pixel 3-D surface structure. An alternative use of this

130

product is to forward model or generate 'observations' of how the appearance of vegetation varies based on viewing vegetated surfaces at progressively oblique angles. For example, using the MCD43 BRDF product parameters for the near infrared and red bands, a representation of how NDVI changes with view angle can be derived. A simple geometric model was developed to assist in interpreting the changes in NDVI (as derived from the MODIS MCD43 BRDF product) when considered at increasingly oblique view angles. This approach replaces the need to directly observe vegetated surfaces at oblique viewing geometries in order to quantify and model changes in the appearance of vegetation. This approach may also be considered a re-expression of the MODIS MCD43 BRDF product into an alternate parameter set, namely NDVI and a parameter defined here as a the height-to-width ratio.

This model was applied to well defined surfaces (i.e. single species cropped fields considered in chapter 4) in order to derive a measure of the height-to-width ratio of vegetation components present within a single MODIS pixel. The re-expression of MODIS BRDF modelling described by equations 21 – 23 provides a very good fit (with substituted derived values) to MODIS's BRDF modelling, i.e. correlations close to 1 and low RMSE. Therefore this modelling can be considered a valid re-expression of MODIS BRDF. However, noise appeared to be a major issue in the derived values, particularly for the height-to-width ratio and an explanation of results unclear. Given the nature and selection of the study surfaces, better results may have been expected. If the MODIS MCD43 BRDF product appears noisy for such well defined homogeneous surfaces, what impact will noise have on large scale, heterogeneous poorly understood surfaces? Excessive noise may be an inevitable problematic effect within the MODIS MCD43 BRDF product or it may be indicating the presence of additional factors influencing results.

The same modelling approach, with broadened applicability was considered for a spatial transect between Melbourne and Darwin (chapter 5) and for a surface area of approximately 68,000 MODIS pixels in central Australia (chapter 6). From this modelling, the derived height-to-width ratio can be considered a single numeric value that quantifies the relationship between NDVI and view angle.

Application of the model for a surface area enabled the derived height-to-width ratio to be displayed in a map format and the spatial pattern between surface features considered. The MODIS MCD43 product is derived independently for each pixel and the height-to-width ratio which seeks to interpret this product is therefore also derived

independently for each pixel. It was observed that the height-to-width ratio was correlated with the NDVI response from surrounding pixels. It is a well know effect associated with wide field of view sensors such as MODIS, that enlargement of the ground IFOV occurs when pixels are acquired towards the edge of the swath. MODIS BRDF modelling does not specifically consider enlargement of the ground IFOV and this provides a plausible explanation of the observed relationship between a pixel's height-to-width ratio and variations in NDVI associated with enlargement of pixels' ground IFOV.

It is a design characteristic of MODIS processing that all pixels are considered at their nadir spatial resolution (i.e. 250-m, 500-m and 1km), even though the ground footprint of pixels is known to increase in size when acquired with non nadir view angles (Masuoka et al., 1998). Considering this characteristic of the MODIS sensors, there are two effects associated with viewing a surface at an oblique angle. It brings the vertical profile of any 3-D shapes on the surface into view which is the theoretical basis for MODIS BRDF modelling, and it also increases the footprint area on the ground represented by a pixel. If considered at an individual pixel level, variations in surface reflectance could equally and validly be attributed to either of these two effects as there is no means of distinguishing the source of surface reflectance variations based only on variations in view angle. In choosing to measure one effect, the influence of the other effect is assumed negligible or zero. The MODIS MCD43 algorithm does not specifically consider enlargement of the ground IFOV when pixels are acquired at larger view angles. The MODIS MCD43 product attributes all reflectance variations to the directional scattering of reflected EMR theoretically derived from 3-D surface protrusions and assumes that reflectance variations from pixel footprint growth are negligible or zero. Implicitly the effects associated with directional scattering and reflectance variations associated with enlargement of pixels' ground IFOV are included within the MODIS BRDF product.

To test the hypothesis that MODIS BRDF modelling is significantly impacted by variations in the ground IFOV, an approximation of the variations in NDVI between pixels acquired at nadir and when acquired at the edge of the swath was developed for direct comparison with the height-to-width ratio (i.e. the NDVI-ground-footprint ratio). A strong linear relationship between the height-to-width ratio and the NDVI ground-foot-print ratio was observed. This relationship was consistent for multiple study surfaces selected. Other than the explanation provided, there is no reason conceived as to why

the height-to-width ratio, derived from the MCD43 BRDF product independently for each pixel, should be related to NDVI variations from surrounding pixels. Considering derived values of height-to-width ratio plotted against the NDVI-ground-footprint ratio for the central Australian study area (refer Figure 6.14) the line of best fit passes through the origin, indicating that the variations in NDVI associated with a larger ground IFOV are the predominant cause of variations in the height-to-width ratio. This suggests that homogeneous surfaces across an area the size of the larger ground IFOV will tend to have an NDVI-ground-footprint ratio approaching zero, and therefore the height-to-width ratio will also tend to zero, which is consistent with isotropic reflectance.

The finding that variations in the height-to-width ratio are primarily associated with horizontal structure between a pixel and neighbouring pixels due to enlargement of the ground IFOV when pixels used in the MODIS BRDF inversion are acquired towards the edge of the swath has two implications. Firstly, it explains the results from chapters 4 and 5. That is, for the temporal transect the thesis findings explain noise in the derived parameters, the shape of the bare soil and closed crop canopy end-members, negative values for the derived height-to-width ratio, and for the spatial transect; spikes in the derived height-to-width ratio can be explained with the understanding that MODIS BRDF modelling is significantly impacted by size variations in pixels' ground IFOV. Secondly, whilst these results specifically relate to a model describing the relationship between NDVI and view angle, the result is likely to be applicable to MODIS BRDF modelling more generally. Enlargement of a pixel's ground IFOV when acquired at the edge of the swath is a well known effect applicable to all MODIS bands. It may therefore be necessary to reconsider the validity, interpretation and application of all MODIS BRDF related products in light of this finding, e.g. Nadir BRDF Adjusted Reflectance (NBAR) and broadband surface albedo products. Furthermore, the MODIS BRDF product is used as the basis for atmospheric and BRDF corrections of Landsat images for Australia (Li et al., 2010) and the MODIS BRDF product is also used in the development of the foliage clumping indices (He et al., 2012). Downstream products and applications based on MODIS BRDF modelling may also require reassessment based on the findings contained in this thesis. Full understanding of the implications from this finding for products derived directly or indirectly from MODIS BRDF modelling is unclear and requires further research.

Even though effects associated with larger ground IFOV appear the dominant factor in MODIS BRDF modelling, directional scattering based upon sub pixel 3-D vertical

structure may still be present in MODIS BRDF modelling. For temporally invariant surfaces, the directional scattering effects may be considered constant over a (short) period of time and within this same time interval all temporal variations in the derived height-to-width ratio can be associated with variations in the ground IFOV. The derived height-to-width ratio can be considered to comprise a constant component, representing directional scattering effects associated with a temporally invariant surface, and a multiple of the NDVI-ground-footprint ratio representing larger ground IFOV effects. Considering a temporally invariant surface over several consecutive epochs, a 'best fit' separation of these two components contained in the derived height-to-width ratio has been performed and the results of this procedure further supports the dominance of larger ground IFOV effects in MODIS BRDF modelling. Whilst some information related to directional scattering effects may remain to assist in the characterisation of vegetation, the results appear weak (refer Figure 6.21) and an interpretation of the directional scattering component is unclear (refer Appendix 1).

MODIS BRDF modelling is theoretically derived with consideration of sub pixel structure, e.g. individual vegetation components that scatter EMR within their canopies, and canopies that cast shadows and obscure other features that result in non isotropic reflectance. However, MODIS BRDF inversions are realised from observations that are at a much coarser spatial scale than individual vegetation components, i.e. 500-m to more than 1 km^2 for pixels acquired at the edge of the swath. The finding within this thesis that MODIS BRDF is dominated by reflectance variation associated with enlargement of pixels' ground IFOV and not sub pixel vertical structure suggests that modelling based on considerations at one scale are not necessarily valid at different scales. As discussed in the literature review, features that are significant at one scale may be insignificant when observed at another scale.

The finding of this artefact within the MODIS BRDF product means that the original research questions were not able to be addressed using MODIS BRDF data. However and perhaps more importantly, the identification of this artefact raises significant issues for the validity, use and interpretation of all land surface products based directly or indirectly on MODIS BRDF modelling.

7.3   Implications for MODIS BRDF modelling

7.3.1   Extension of these findings to MODIS BRDF modelling in general

The modelling undertaken within this thesis is focused on investigating how reflectance changes with view angle and quantifying this relationship with a metric termed the height-to-width ratio. In doing such, it was found that the height-to-width ratio (derived from MODIS BRDF modelling) is related to the NDVI-ground-footprint ratio (which approximates effects associated with the larger ground IFOV for pixels acquired at the edge of the swath). Can these findings be extended to MODIS BRDF modelling in general, i.e. can it be inferred that MODIS BRDF modelling for all bands, all illumination/viewing geometries and all surfaces are equally impacted by the effects associated with the larger ground IFOV?

The height-to-width ratio is derived from BRDF modelling and the model described in this thesis (with best fitting height-to-width ratio substituted) provides strong correlations with NDVI derived from MODIS BRDF modelled across the same range of view angles. This suggests that the model and derived height-to-width ratio are a valid re-expression of NDVI changes associated with view angle from MODIS BRDF modelling.

The RossThick-LiSparse BRDF representation used in MODIS modelling is reciprocal, i.e. the view and solar angles are interchangeable and the direction of light's travel can be reversed to yield the same result. It can be inferred that the result presented in this thesis can also be achieved considering variations in NDVI associated with changes in the solar zenith angle as derived from MODIS BRDF modelling. However, only variations in view angle result in enlargement of a pixel's ground IFOV. Using the RossThick-LiSparse-Reciprical model, reflectance variations associated with enlargement of a pixel's ground footprint will therefore be distributed between illumination and view angles effects. Furthermore, MODIS BRDF is derived from observations from both Terra and Aqua satellites, which due to their ascending and descending orbits will realise different solar illumination angles. An exact knowledge of all individual observations utilised in the derivation of MODIS BRDF parameters for each pixel is necessary to fully quantify the effects that the large ground IFOV has on individual MODIS pixels.

The effects associated with larger ground IFOV on BRDF modelling are the consequence of the specific characteristics of the MODIS sensors. These effects are not specific to the

BRDF model used. Whilst MODIS BRDF uses the RossThick-LiSparse-Reciprocal model, pixel enlargement issues will be equally problematic should any other BRDF model be used with MODIS observations.

MODIS modelling does not derive the BRDF parameters for NDVI directly, but rather they are derived separately for the near infrared band, red band and for five other bands. Combining BRDF effects between bands into a metric associated with NDVI serves to highlight the variability that might not otherwise be apparent in examining the BRDF effects associated with individual reflectance bands. That is, combining BRDF effects between two bands does not create anything that is not present in respective individual bands. Enlargement of the ground IFOV of pixels acquired at the edge of the swath (i.e. at a high view angle) is not specific to red or near infrared bands and is an effect applicable to all MODIS bands. There is no reason to suspect that these effects are limited to red and near infrared bands.

Whilst the results specifically only relate to variations in NDVI associated with view angle, it is reasonable to infer that the effects of larger ground IFOV are broadly applicable to all MODIS BRDF modelling in general, although empirically testing for all bands and possible geometries may be difficult.

7.3.2   Implication for MODIS BRDF products

The results presented in this thesis do not suggest that directional scattering of reflected EMR or BRDF effects are not evident in remotely sensing data, only that BRDF effects derived in the MODIS BRDF product are dominated by effects associated with the larger ground IFOV. Whilst detailed and specific impacts of these findings on MODIS BRDF related products are beyond this thesis, the findings suggest a need to reconsider the validity and interpretations placed on all products derived from MODIS BRDF modelling.

One specific aspect of MODIS BRDF modelling that the findings in this thesis may allow further comment on is the use of MODIS BRDF effects to assist with the characterisation of vegetation. The tendency for a pixel to exhibit a "bell shaped", "bowl shaped" or isotropic BRDF effect associated with NDVI may indicate something about the spatial distribution, homogeneity, clumping of vegetation and may be described as the textural properties of the landscape which are important attributes in describing vegetated surfaces. The relationship between BRDF effects and vegetation clumping has

previously been identified and investigated (He et al., 2012, Hill et al., 2008) and the findings within this thesis may significantly explain the cause of this association between BRDF effects and clumping indices.

Based upon the finding within this thesis, isotropic BRDF effects will be associated with zero height-to-width ratios and zero NDVI-ground-footprint ratios, i.e. homogeneous surfaces when considering the distribution of vegetation across an area of 4km^2 which equates to pixel's larger ground IFOV. The homogeneity of a surface is independent of the vegetation cover, e.g. a surface can be homogeneous bare soil or homogeneous green vegetation.

For a given pixel, a "bowl shaped" NDVI BRDF profile will occur when there is a positive NDVI-ground-footprint ratio and positive height-to-width ratio. This occurs for a pixel with a lower NDVI response surrounded by pixels with a higher NDVI response, i.e. a bare soil pixel surrounded by vegetation. When considered with respect to changes in view angle in the principle plane, the BRDF profile will appear as an upward sloping curve as shown in Figures 4.18 and 4.21. For a given pixel, a "bell shaped" NDVI BRDF profile will occur when there is a negative NDVI-ground-footprint ratio and negative height-to-width ratio. This occurs for a pixel with a higher NDVI response surrounded by pixels with a lower NDVI response, i.e. a pixel containing vegetation surrounded by bare soil. Again, when considered with respect to changes in view angle in the principle plane, the BRDF profile will appear as a downward sloping curve as shown in Figures 4.18 and 4.21. The magnitude of the NDVI-ground-footprint ratio and height-to-width ratio (positive or negative) will be greatest when the NDVI differential between a pixel and its surrounds is greatest, i.e. less homogeneous surfaces over an area of the larger ground IFOV.

For a surface area represented by a large number of pixels, it may be expected that there will be an equal number of pixels exhibiting a "bowl shaped" NDVI BRDF profile and a "bell shaped" NDVI BRDF profile. A greater number of pixels exhibiting a "bowl shaped" NDVI BRDF profile will occur if, within areas the size of the larger ground IFOV, there are fewer high NDVI pixels compared to lower NDVI pixels, e.g. a tendency for vegetation to be clumped. A greater number of pixels exhibiting a "bell shaped" NDVI BRDF profile will occur if, within areas the size of the larger ground IFOV, there are fewer low NDVI pixels compared to higher NDVI pixels, e.g. pockets of bare soil in an otherwise vegetated area. Therefore within a sufficiently large region, a greater number of pixels with positive or negative BRDF profiles associated with NDVI (i.e. positive or

negative height-to-width ratios) may be useful in describing the spatial distribution and clumping of vegetation at a particular spatial scale. In this context the height-width ratio may be describing textural properties of the landscape.

7.4   Recommendations for further research

The MODIS BRDF product has been operational for 12 years and the MCD43 product is widely used. The MODIS MCD43 science team have been advised of these results and the implications drawn in this thesis. The findings in this thesis are recognised as being contentious and potentially difficult for the broader remote sensing scientific community to accept without further and independent validation. Therefore these results need to be independently validated across the widest possible range of surfaces types, locations and temporal periods. Whilst any logic errors can be identified by examination of the processes described in this thesis, possible computational errors in the processes described here or with pre-processing of data (e.g. in the re-projection and mosaic processes) may only be identified by repeating the experiment. All further research in this area is contingent on firstly reconfirming the principal finding in this thesis.

It is reasonable to suggest that the effects of larger ground IFOV will be applicable broadly to all MODIS BRDF modelling and related products, e.g. NBAR, broadband albedo and any products that include MODIS BRDF modelling in their derivation. For example the MODIS BRDF product is used as the basis for atmospheric and BRDF corrections of Landsat images for Australia (Li et al., 2010) and the MODIS BRDF product is also used in the development of the foliage clumping indices (He et al., 2012). Downstream products and applications based on MODIS BRDF modelling may also require reassessment based on the findings contained in this thesis. The effects on these products needs to quantified and understood in order that interpretation of these products is appropriate.

In plots of the derived height-to-width ratio against NDVI-ground-footprint ratio, consistent slopes were observed, however the y-intercept values varied for differing surfaces. For example, larger y-intercepts were observed for regions in northern Australia compared to southern Australia. Refer to Appendix 1. Similarly, in section 6.7, there may be some vegetation structural information remaining the in height-to-width

ratio after removing the effects associated with larger ground IFOV; this is equivalent to the y-intercept of the height-to-width ratio when plotted against the NDVI-ground-footprint for pixels of an area taken at a single epoch. Further research is needed to understand these results and their significance. For example, consideration of these results in relation to vegetation "clumping" or other vegetation structural characteristics.

The method in section 6.7 to partition the derived height-to-with ratio into components attributable to direction scattering based on sub pixel 3-D surface structure and larger ground IFOV effects was more theoretical than operationally applicable due to the constraints imposed. Assuming the MODIS BRDF product is a mix of these two effects, developing an operational means of partitioning directional scatter of reflectance and ground IFOV effects from the 12 year history of this dataset will be significant progress.

Finally, as these results are the consequence of specific characteristics of the MODIS sensor, is there an alternative approach for deriving BRDF effects from space borne sensors, including future sensors where effects associated with enlargement of pixel's ground IFOV can be considered within processing?

8 Appendix 1

In addition to the study areas along the transect line between Melbourne and Darwin, a further area in central Queensland has been examined, refer Figure 8.1. The area in central Queensland represents 1 ½ ° Longitude and 1° Latitude (i.e. SW corner being 24° South, 149° East to the NE corner 23° South, 150° 30' East). The Tropic of Capricorn runs approximately East/West through the middle of this area, therefore in summer the solar noon angle will be 0° and in winter approximately 45°. This provides a surface study area that is not as extreme or arid as the NE area in South Australia or the Simpson Desert, and is also mid latitude between the Northern Territory and Victorian study areas. Two epochs for the central Queensland study area are considered in addition to four consecutive winter epochs from the previously considered NT study area, four consecutive summer epochs from the previously considered NE South Australian study area, and one each from the previously considered Victorian and Simpson Desert study areas. This provides a total for twelve study areas/epochs from which height-to-width ratio and the NDVI-ground-footprint ratio can be derived and plotted against one another to determine (through approx 68,000 plot points/pixels for each study area/epoch) the y-intercept and gradient of the line of best fit.
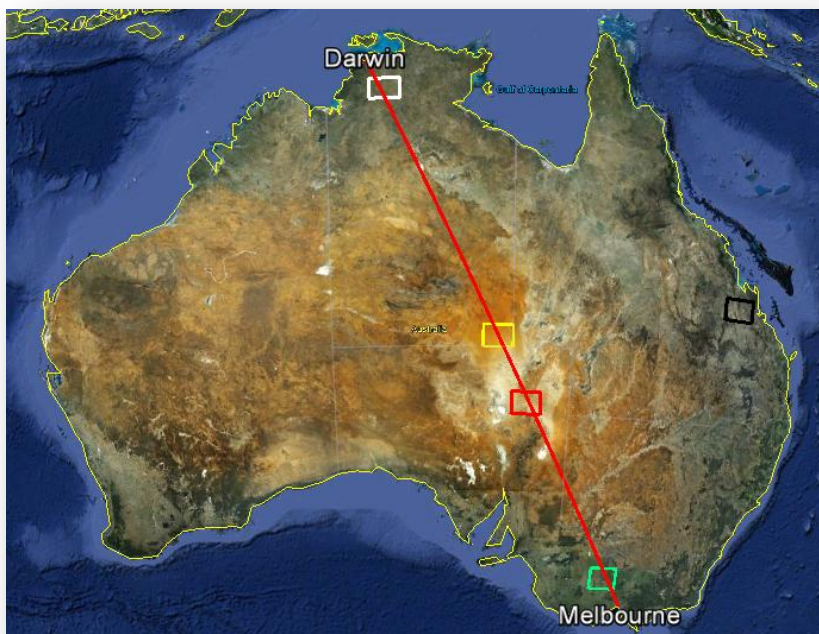

Figure 8.1 – The Australian continent showing the location of the additional study surface area in Queensland indicated by the black box (Source : Google Earth)

140

These twelve study areas/epochs enable variations in latitude and the solar angle to be considered with regards to the observed differences in the y-axis intercept of the line of best fit as discussed in section 6.5. As in chapter 6, if the correlation was less than 0.99 or the RMSE greater than 0.005 or MODIS BRDF band quality flags indicated less than the 'best quality inversion', the mean height-to-width ratio and 'NDVI ground-footprint-ratio' values were substituted in the plot in determination of the line of best fit.

Four plots are shown in Figures 8.2 – 8.5 based upon the line of best fit between the height-to-width ratios when plotted against NDVI-ground-footprint ratios. The four plots show; the y-intercept against the mean solar angle, the y-intercept against latitude, the gradient against the mean solar angle and the gradient against latitude.
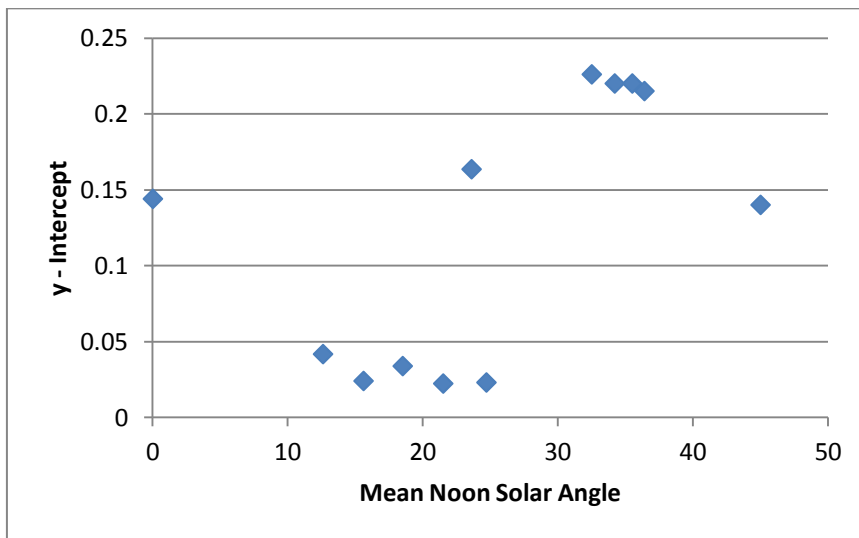

Figure 8.2 -Y -intercept against the mean solar angle
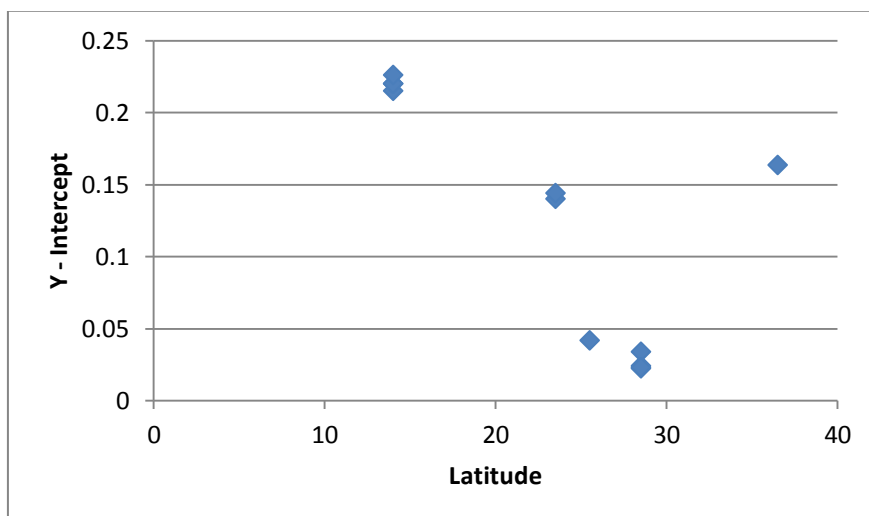

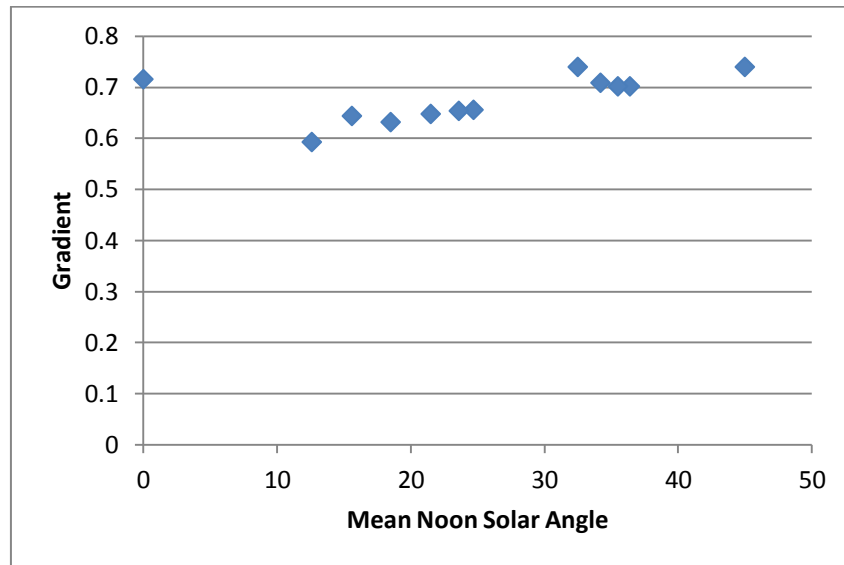Figure 8.3 - Y -intercept against Latitude

Figure 8.4 -gradient against the mean solar angle
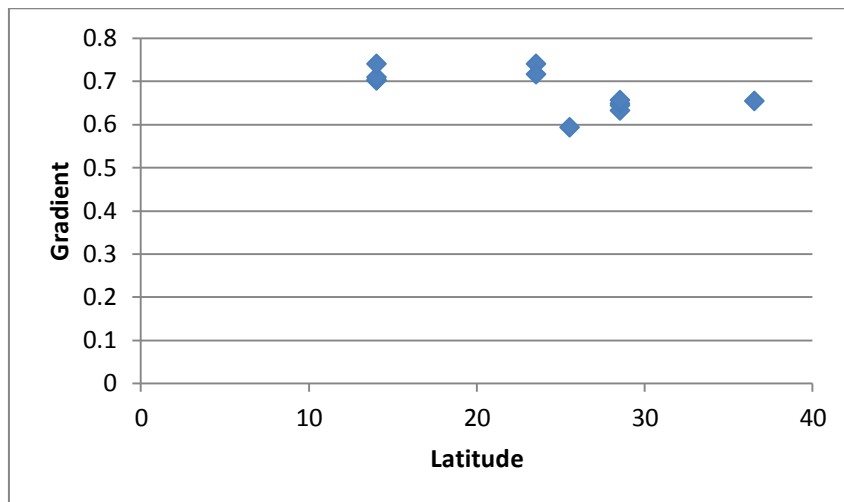
Figure 8.5 -gradient against Latitude

The gradient (ranging between 0.6 to 0.75) for the line of best fit between the height-to-width and NDVI-ground-footprint ratio appears consistent for all study areas and epochs, and therefore appears independent of latitude, the mean noon solar angle or vegetation cover. The y-Intercept is more variable. However, it is difficult to see a clear relationship between the y-intercept and either the mean noon solar angle or latitude of study areas. Furthermore, the y-intercept appears to have a consistent value for a given study area, e.g. the area in central Queensland has the same y-intercept for both the summer and winter epochs examined. It may be expected that there exist differences in the vegetation cover between summer and winter epochs for the central Queensland

study area. Therefore, the same y-intercept for both epochs suggests that the y-intercept is also not related to vegetation cover. An interpretation of variability in the y-intercept remains unclear.

9 Publications and Conference Papers

Currently in review

McCamley, G., Grant, I., Jones, S., Bellman, C. The Impact of Size Variations in the Ground Instantaneous Field of View on MODIS BRDF Modelling, submission to Remote Sensing of Environment is currently in review (January 2014).

Reviewed Conference Papers

McCamley, G., Grant, I., Jones, S., Bellman, C. Characterising Heterogeneous Vegetated Surfaces Using Multi-angular Satellite Data, Surveying and Spatial Sciences (SSSC), Wellington, 2011

McCamley, G., Grant, I., Jones, S., Bellman, C. Characterising Heterogeneous Vegetated Surfaces Using Multi-angular Satellite Data, RMIT University, School of Mathematics and geospatial Science (SMGS), Geospatial Science Research (GSR 1) Conference, Melbourne 2011

McCamley, G., Grant, I., Jones, S., Bellman, C. Characterising Heterogeneous Vegetated Surfaces Using Multi-angular Satellite Data, 22nd Congress of the International Society for Photogrammetry and Remote Sensing (ISPRS) 2012 Conference, Melbourne

Unreviewed Conference Papers

McCamley, G., Grant, I., Jones, S., Bellman, C. Characterising Heterogeneous Vegetated Surfaces Using Multi-angular Satellite Data, 34th Internationals Symposium on Remote Sensing of Environment (ISRSE), Sydney, 2011

10 References

Cotton Australia Education Kit [Online]. Available: http://cottonaustralia.com.au/ [Accessed 2012].

ARMSTON, J. D., SCARTH, P. F., PHINN, S. R. & DANAHER, T. J. 2006. Analysis of multi-data MISR measurements for forest and woodland communities, Queensland, Australia. *Remote Sensing of Environment*, 287 - 298.

ASNER, G. P., BRASWELL, B. H., SCHIMEL, D. S. & WESSMAN, C. A. 1998. Ecological Research Needs for Multiangular Remote Sensed Data. *Remote Sensing of Environment*, 155 - 165.

AUSLIG 1990. AUSLIG, 1990, Atlas of Australian Resources. 1990 ed.: Australian Surveying and Land Information Group Department of Administrative Services.

BANNARI, A., MORIN, D., BONN, F. & HUETE, A. 1995. A Review of Vegetation Indices. *Remote Sensing Reviews,* 13, 95 - 120.

BARNSLEY, M. J., STRAHLER, A. H., MORRIS, K. P. & MULLER, J.-P. 1994. Sampling the Surface Bidirectional Reflectance Distribution Function (BRDF): 1. Evaluation of Current an Future Satellite Sensors. *Remote Sensing Reviews,* 8, 271-311.

BREON, F.-M., MAIGNAN, F., LEROY, M. & GRANT, I. 2002. Analysis of hot spot directional sigatures measured from space. *Journal of Geophysical Research,* 107.

CHEN, J. M. & CIHLAR, J. 1997. A hotspot function in a simple bidirectional reflectance model for satellite applications. *Journal of Geophysical Research D: Atmospheres,* 102, 25,907-25,913.

CHEN, J. M., MENGES, C. H. & LEBLANC, S. G. 2005. Global mapping of foliage clumping index using multi-angular satellite data. *Remote Sensing of Environment,* 97, 447-457.

CHENG, J.-L., SHI, Z. & LI, H.-Y. 2008. Observation and simulation of bi-directional spectral reflectance on different type of soil. *Guang Pu Xue Yu Guang Pu Fen Xi/Spectroscopy and Spectral Analysis,* 28, 1007-1011.

CHOPPING, M. J. 2006. Progress in Retrieving Canopy Structure Parameters from NASA Multi-Angle Remote Sensing. *IEEE Transactions on Geoscience and Remote Sensing Symposium (IGARSS),* Article Number 4241217, 256-259.

COX, C. & MUNK, W. 1954. Measurement of the roughtness of the sea surface from photographs of the sun's glitter. *Journal of Optical Society of America,* 44, 838-850.

DICKINSON, R. E., PINTY, B. & VERSTRAETE, M. M. 1990. Reflecting surface albedos in GCM to remotely sensed data. *Agricultural and Forest Meteorology,* 52**,** 109-131.

DINER, D. J., ASNER, G. P., DAVIES, R., KNYAZIKHIN, Y., MULLER, J.-P., NOLIN, A. W., PINTY, B., SCHAAF, C. B. & STOEVE, J. 1999. New Directions in Earth Observing: Scientific Applications of Multiangle Remote Sensing. *Bulletin of the American Meteorological Society,* 80.

DYMOND, J. R. & QI, J. 1998. Reflection of visible light from a dense vegetation canopy - a physical model. *Agricultural and Forest Meteorology*.

FARMER, E., REINKE, K. J. & JONES, S. D. 2011. A current perspective on Australian woody vegetation maps and implications for small remnant patches. *Journal of Spatial Science,* 56**,** 223-240.

FURBY, S. L., CACCETTA, P. A., WALLACE, J. F., LEHMANN, E. A. & ZDUNIC, K. 2009. Recent development in vegetation monitoring products from Australia'a National Carbon Accounting System. *Geoscience and Remote Sensing Symposium, 2009 IEEE International, IGARSS 2009,* 4**,** 276 - 279.

GAO, F., SCHAAF, C. B., STRAHLER, A. H., JIN, Y. & LI, X. 2003. Detecting vegetation structure using kernel based BRDF model. *Remote Sensing of Environment,* 86**,** 198 - 205.

GRANT, I. F. 2000. Investigation of the Variability of the Directional Reflectance of Australian Land Cover Types. *Remote Sensing Reviews,* 19**,** 243 - 258.

GRANT, I. F., BREON, F.-M. & LEROY, M. M. 2003. First observation of the hot spot from space at sub-degree angular resolution using POLDER data. *International Journal of Remote Sensing,* 24**,** 1103-1110.

HAPKE, B. W. 1981. Bidirectional reflectance spectroscopy. 3. Correcton for macroscopic roughness. *Icarus,* 59**,** 41-59.

HE, L., CHEN, J. M., PISEK, J., SCHAAF, C. B. & STRALHER, A. H. 2012. Global clumping index map derived from MODIS BRDF product. *Remote Sensing of Environment,* 119**,** 118-130.

HILL, J. M., AVERILL, C., JIAO, Z., SCHAAF, C. B. & ARMSTON, J. D. 2008. Relationship of MISR RPV parameters and MODIS BRDF shape indicators to surface vegetation patterns in an Australian tropical savanna. *Canadian Journal of Remote Sensing,* 34**,** S247 - S267.

HUETE, A. 1987. Soil and Sun angle interactions on partial conopy spectra. *International Journal of Remote Sensing,* 8**,** 1307 - 1317.

HUTLEY, L. B., BERINGER, J., ISAAC, P. R., HACKER, J. M. & CERNUSAK, L. A. 2011. A sub-continential scale living laboratory: Spatial patterns of savanna vegetation over a rainfall gradient in northern Australia. *Agricultural and Forest Meteorology,* 151**,** 1417-1428.

JACQUEMOUD, S., BARET, F. & HANOCQ, J. F. 1992. Modeling spectral and bidirectional soil reflectance. *Remote Sensing of Environment,* 41**,** 123-132.

JENSEN, J. R. 2007. *Remote Sensing of the Environment - An Earth Resource Perspective*, Pearson Prentise-Hall, New Jersey.

JUPP, D. 1998. A compendium of kernel & other (semi-) empirical BRDF Models.

JUSTICE, C. O., VERMOTE, E., TOWNSHEND, J., R.G., DEFRIES, R., ROY, D., HALL, D. K., SALOMONSON, V. V., PRIVETTE, J. L., RIGGS, G., STRAHLER, A. H., LUCHT, W., MYNENI, R., B., KNYAZIKHIN, Y., RUNNING, S. W., NEMANI, R. R., WAN, Z., HUETE, A., LEEUWEN, W. V., WOLFE, R. E., GIGLIO, L., MULLER, J.-P., LEWIS, P. & BARNSLEY, M. J. 1998. The Moderate Resolution Imaging Spectroradiometer (MODIS): Land Remote Sensing for Global Change Research. *IEEE Transactions on Geoscience and Remote Sensing,* 36**,** 1228 - 1249.

LACAZE, R. & ROUJEAN, J.-L. 2000. G-function and HOt SpoT (GHOST) reflectance model Application to multi-scale airbourne POLDER measurements. *Remote Sensing of Environment,* 76**,** 67 - 80.

LI, F., JUPP, D., REDDY, S., LYMBURNER, L., MUELLER, N., TAN, P. & ISLAM, A. 2010. An Evaluation of the Use of Atmospheric and BRDF Correction to Standardise Landsat Data. *IEEE Journal of Selected Topics in Applied Earth Observations and Remote Sensing,* 3**,** 257 - 270.

LIANG, S., FANG, H., CHEN, M., SHUEY, C. J., WALTHALL, C., DAUGHTRY, C., MORISETTE, J., SCHAAF, C. B. & STRAHLER, A. H. 2002. Validating MODIS land surface reflectance an albedo products: methods and preliminary results. *Remote Sensing of Environment,* 83**,** 149 - 162.

LIU, J., SCHAAF, C. B., STRAHLER, A. H., JIAO, Z., SHUAI, Y., ZHANG, Q., ROMAN, M. O., AUGUSTINE, J. A. & DUTTON, E. G. 2009. Validation of Moderate Resolution Imaging Spectroradiometer (MODIS) albedo retrieval algorithm: Dependence of albedo on solar zenith angle. *Journal of Geophysical Research,* 114.

LOVELL, J. L. & GRAETZ, R. D. 2001. Analysis of POLDER-ADEOS data for the Australian continent: the relationship between BRDF and vegetation structure. *International Journal of Remote Sensing,* 23**,** 2767 - 2796.

LUCHT, W. & LEWIS, P. 2000. Theoretical noise sensitivity of BRDF and albedo retrieval from the EOS-MODIS and MISR sensors with respect to angular sampling. *International Journal of Remote Sensing,* 21**,** 81-98.

LUCHT, W., SCHAAF, C. B. & STRAHLER, A. H. 2000. Algorithm for the Retrieval of Albedo from Space Using Semiempirical BRDF Models. *IEEE Transactions on Geoscience and Remote Sensing,* 38**,** 977 - 998.

MASUOKA, E., FLEIG, A., WOLFE, R. E. & PATT, F. 1998. Key Characteristics of MODIS Data Products. *IEEE Transactions on Geoscience and Remote Sensing,* 36**,** 1313 - 1323.

MINNAERT, M. 1941. The reciprocity principle in lunar photometry. *Journal of Astrophysics,* 93**,** 403-410.

MISR. 2013. *Multiangle Imaging Spectro Radiometer* [Online]. Available: http://www-misr.jpl.nasa.gov/ [Accessed 2012].

NICODEMUS, F. E., RICHMOND, J. C., HSIA, J. J., GINSGERG, I. W. & LIMPERIS, T. 1977. Geometric Considerations and Nonmenclature for Reflectance. *In:* (US), N. B. O. S. (ed.).

NISHIHAMA, M., WOLFE, R. E., SOLOMON, D., PRATT, F., BLANCHETTE, J., FLEIG, A. & MASUOKA, E. 1997. MODIS Level 1A Earth Location: algorithm Theoritical Basis Document Version 3.0. Available: http://eospso.gsfc.nasa.gov/atbd//modistables.html [Accessed August 1997].

OTTERMAN, J. & WEISS, G. H. 1984. Reflections from a field of randomly located vertical protrusions. *Applied Optics,* 23**,** 1931-1936.

PAGET, M. & KING, E. 2008. *MODIS Land Products for Australia CSIRO Marine and Atmpospheric Research Internal Report No. 004, CSIRO Marine and Atmospheric Research Canberra, Australia. ISBN 978192142342 (pdf)* [Online]. Available: https://rs.nci.org.au/lpdaac/ [Accessed].

PICKUP, G., BASTIN, G. N., CHEWINGS, V. H. & PEARCE, G. Year. Correction and classification procedures for assessing rangeland vegetation cover with airbourne video data. *In:* 15th Biennial Workshop on Color Photograpghy and Video Graphy in Resource Assessment, 2-3 May 1995 1995a USA.

PICKUP, G., CHEWINGS, V. H. & PEARCE, G. 1995b. Procedures for correction high resolution high resolution airbourne video imergery. *International Journal of Remote Sensing,* 16**,** 1647-1662.

PINTY, B., VERSTRAETE, M. M. & DICKINSON, R. E. 1989. A physical model for predicting bidirectional reflectances over bare soil. *Remote Sensing of Environment,* 27**,** 273-288.

POLDER. 2013. *Polarisation and Directionality of Earth's Reflectance* [Online]. Available: http://smsc.cnes.fr/POLDER/ [Accessed 2012].

QUAIFE, T. & LEWIS, P. 2010. Temporal Constraints on Linear BRDF Model Parameters. *IEEE Transactions on Geoscience and Remote Sensing,* 48**,** 2445 - 2450.

RAHMAN, H., PINTY, B. & VERSTRAETE, M. M. 1993. Coupled surface-atmosphere reflectance (CSAR) model 2. Semiempirical surface model usable with NOAA advanced very high resolution radiometer data. *Journal of Geophysical Research,* 98**,** 20,791 - 20,801.

ROMAN, M. O., GATEBE, C. K., SCHAAF, C. B., POUDYAL, R., WANG, Z. & KING, M. D. 2011. Variability in surface BRDF at different spatial scales (30m-500m) over a mixed agricultural landscape as retrieved from airborne and satellite spectral measurments. *Remote Sensing of Environment,* 115**,** 2184-2203.

ROUJEAN, J.-L., LEROY, M. & DESCHAMPS, P.-Y. 1992. A Bidirectional Reflectance Model of the Earth's Surface for the Correction of Remote Sensing Data. *Journal of Geophysical Research,* 97**,** 20,455 - 20,468.

SABINS, F. F. 1997. *Remote Sensing Principles and Interpretation,* New York, W.H. Freeman and Company.

SAMAIN, O., ROUJEAN, J.-L. & GEIGER, B. 2007. Use of a Kalman filter for the retrieval of surface BRDF coefficients with a time-evolving model based on the ECOCLIMAP land cover classification. *Remote Sensing of Environment,* 112**,** 1337-1346.

SANDMEIER, S., MULLER, C., HOSGOOD, B. & ANDREOLI, G. 1998. Physical Mechanisms in Hyperspectral BRDF Data of Grass and Watercress. *Remote Sensing of Environment,* 66**,** 222 - 233.

SCHAAF, C. B. 2012. MODIS BRDF/Albedo Product (MCD43) User Guide. Available: http://www-modis.bu.edu/brdf/userguide/intro.html [Accessed 6/5/2012].

SCHAAF, C. B., GAO, F., STRAHLER, A. H., LUCHT, W., LI, X., TSANG, T., STRUGNELL, N. C., ZHANG, X., JIN, Y., MULLER, J.-P., LEWIS, P., BARNSLEY, M., HOBSON, P., DISNEY, M., ROBERTS, G., DUNDERDALE, M., DOLL, C., D'ENTREMONT, R. P., HU, B., LIANG, S., PRIVETTE, J. L. & ROY, D. 2002. First operational BRDF, albedo nadir reflectance products from MODIS. *Remote Sensing of Environment,* 83**,** 135-148.

SCHAEPMAN-STRUB, G., SCHAEPMAN, M. E., PAINTER, T. H., DANGEL, S. & MARTONCHIL, J. V. 2006. Reflectance quantities in optical remote sensing - definitions and case studies. *Remote Sensing of Environment,* 103**,** 27 - 42.

SCHAEPMAN, M. E. 2006. Spectrodirectional remote sensing: From pixels to processes. *International Journal of Applied Earth Observations and Geoinformation,* 9**,** 204 - 223.

SHIBAYAMA, M. & WEIGAND, C. L. 1985. View azimuth and zenith, and solar angle effects using spectral albedo-based vegetation indices. *Remote Sensing of Environment,* 52**,** 207-217.

STAYLOR, W. F. & SUTTLES, J. T. 1986. Reflection and emmission models for deserts derived from Mimbus-7 ERB scanner measurments. *Journal of Climate and Applied Meteorology,* 25**,** 196-202.

SU, L., HUANG, Y., CHOPPING, M. J. & RANGO, A. 2011. Variations in reflectance with seasonality and viewing geometry: implications for semi-arid vegetation mapping with MISR data. *International Journal of Remote Sensing,* 32:23**,** 8183-8193.

SU, L., YUXIA, H., CHOPPING, M. J., RANGO, A. & MARTONCHIK, J. V. 2009. An empirical study on the utility of BRDF model parameters and topographic parameters for mapping vegetation in semi-arid region with MISR imagery. *International Journal of Remote Sensing,* 30**,** 3463-3483.

TAN, B., WOODCOCK, C. E., HU, J., ZHANG, P., OZDOGAN, M., HUANG, D., YANG, W., KNYAZIKHIN, Y. & MYNENI, R. B. 2006. The impact of gridding artifacts on the local spatial properties of MODIS data: Implications for validataion, compositing, and band-to-band registration across resolutions. *Remote Sensing of Environment,* 105**,** 98-114.

TIAN, Y., ROMANOV, P., YU, Y., XU, H. & TARPLEY, D. 2010. Analysis of Vegetation Index NDVI anisotropy to Improve the Accuracy of the GOES-R Green Vegetation Fraction Product. *2010 30th International Geoscience and Remote Sensing Symposium (IGARSS).* Honolulu.

TUCKER, C. J. 1979. Red and Photographic Infrared Linear Combinations for Monitoring Vegetation. *Remote Sensing of Environment,* 8**,** 127 - 150.

WALTHALL, C. L., NORMAN, J. M., WELLES, J. M., CAMPBELL, G. & BLAD, B. L. 1985. Simple equation to approximate the bidirectional reflectance from vegetation canopies and bare soil surfaces. *Applied Optics,* 24**,** 383-387.

WANG, Z., SCHAAF, C. B., KNYAZIKHIN, Y., SCHULL, M. A., STRAHLER, A. H., MYNENI, R. B., CHOPPING, M. J. & LEWIS, P. Year. Canopy vertical structure using modis

bidirection refelctance data. *In:* 2nd Workshop on Hyperspectral Image and Signal Processing: Evolution in Remote Sensing, WHISPERS 2010 Workshop Program, art. no. 5594952, 14-16th June 2010 2010 Reykjavik, Iceland.

WANNER, W., LI, X. & STRALHER, A. H. 1995. On the derivation of kernels for kernel-driven models of bidirectional reflectance. *Journal of Geophysical Research,* 100**,** 21,077-21,089.

WANNER, W., STRAHLER, A. H., HU, B., LEWIS, P., MULLER, J.-P., X, L., BARKER SCHAAF, C. L. & BARNSLEY, M. 1997. Global retrieval of birdirectional reflectance and albedo over land from EOS MODIS and MISR data: Theory and algorithm. *Journal of Geophysical Research,* 102**,** 17,143 - 17,161.

WU, H. & LI, Z.-L. 2009. Scale Issues in Remote Sensing: A Review on Analysis, Processing and Modeling. *Sensors,* 9**,** 1768-1793.

ZEGE, E. P., KATSEV, I. L., MALINKA, A. V., PRIKHACH, A. S., HEYGSTER, G. & WIEBE, H. 2011. Algorithm for retrieval of the effective snow grain size and pollution amount from satellite measurments. *Remote Sensing of Environment,* 115**,** 2674-2685.

ZHU, G., JU, W., CHEN, J. M., GONG, P., XING, B. & ZHU, J. 2012. Foliage Clumping Index Over China's Landmass Retrieved From the MODIS BRDF Parmeters Product. *IEEE Transactions on Geoscience and Remote Sensing,* 50**,** 2122-2137.